Acta Universitatis Agriculturae Sueciae

Doctoral Thesis No. 2024:97
Faculty of Forest Sciences

Pushing the envelope

Empirical Growth Models for Forests at Change

Carl Vigren

Pushing the envelope

Empirical Growth Models for Forests at Change

Carl Vigren
Faculty of Forest Sciences
Department of Forest Resource Management
Umeå

SLU
SWEDISH UNIVERSITY
OF AGRICULTURAL
SCIENCES

DOCTORAL THESIS
Umeå 2024

Acta Universitatis Agriculturae Sueciae
2024:97

Cover: Wreath of forest herbs enclosing a forested morning landscape.

ISSN 1652-6880
ISBN (print version) 978-91-8046-424-6
ISBN (electronic version) 978-91-8046-432-1
https://doi.org/10.54612/a.7qt3hgmn6k

Swedish University of Agricultural Sciences, Department of Forest Resource Management, Umeå, Sweden

Print: SLU Grafisk service, Uppsala 2024

Pushing the envelope: Empirical Growth Models for Forests at Change.

Abstract

Global climatic change has local impacts. By extending the empirical forest growth model for single trees *PrognAus* with a climate-sensitive module for basal area increment we forecast single-layered stands of Scots Pine (*Pinus sylvestris* L.), Oak (*Quercus spp.*), and their mixture to show latitudinally ordered decreases in standing volume in the year 2100 (paper I). The forecast decreases were more severe for Scots Pine stand types than for Oak stand types; more severe between the historical reference and RCP 4.5 than the additional stress imposed by the RCP 8.5 scenario for the Oak stand type, whilst Scots Pine experienced a decrease of the same magnitude as between the historical reference and RCP 4.5; and more severe at lower latitudes than for higher latitudes. To investigate high-resolution spatiotemporal trends, we trained a static reduced model (SRM) on the forecast stands and their climatic data (paper II). We simulated the period 2018-2100 at 30-arcsecond resolution across Europe for all stand types to compare to the period 1923-2005. The Scots Pine stand type was predicted to experience substantial decreases in gross volume production relative to the historical scenario under the future scenarios RCP 4.5 and RCP 8.5. The gross volume production of the Oak stand type was predicted to decrease in northern Europe but increase in some regions of central and southern Europe. In contrast, paper III develops a proxy for the site productivity of mixed coniferous forests based on repeat airborne laser scanning which is compared to derived values for soil moisture. Our proxy for site productivity showed a weak decline with increasing soil moisture, although variation was large. In paper IV, we present preliminary results of the potential in using high-density repeated airborne laser scanning for short-term predictions of volume increment in individual trees of Norway Spruce (*Picea abies* (L.) H. Karst).

Keywords: climate change, growth, Norway Spruce, Scots Pine, Oak, productivity, remote sensing, LiDAR, site index

Att tänja gränserna: Empiriska Tillväxtmodeller för Skogar i Förändring

Abstract

Globala klimatförändringar har lokal påverkan. Genom att utöka den empiriska skogsproduktionsmodellen *PrognAus* med en klimatanpassad modul för träds grundytetillväxt kunde vi framskrida enskiktade bestånd av tall (*Pinus sylvestris* L.), ek (*Quercus spp.*) samt deras blandning och visa latitudinellt ordnade nedgångar i den förväntade stående volymen år 2100 (artikel I). Förutsedda minskningar var allvarligare i tallbestånd än i ekbestånd; för ekbestånden allvarligare i steget mellan den historiska referensen och framtidsscenariot RCP 4.5 än för steget mellan RCP 4.5 och RCP 8.5, alltjämt som tallbestånden predikterades uppleva en minskning av samma storleksordning under båda stegen; samt allvarligare minskningar på lägre breddgrader än på högre latituder. För att vidare undersöka högupplösta rum- och tidsmässiga trender passade vi en statisk reducerad modell (SRM) på de framskridna bestånden och tillhörande klimatdata (artikel II). Vi simulerade årsvis de olika beståndstyperna för perioden 2018-2100 med 30-bågsekunders upplösning för stora delar av Europa, för att sedan jämföra utvecklingen med den historiska referensperioden 1923-2005. Tallbestånd förväntades uppleva betydande minskningar i deras bruttovolymproduktion under de framtida klimatscenarierna RCP 4.5 och RCP 8.5 jämfört med den historiska referensen. Ekbeståndens bruttovolymproduktion väntades minska i norra Europa men öka i vissa regioner i centrala och södra Europa. Artikel III utforskar istället hur en bonitetsindikator såsom skattad från upprepade luftburna laserskanningar hör samman med markfuktigheten såsom skattad av Ågren *et al.* (2021). En svag nedåtgående trend återfanns, även om variationen var stor. I artikel IV presenterar vi preliminära resultat angående möjligheten att nyttja upprepad laserskanning för att uppdatera eller prediktera volymökningen hos enskilda granar (*Picea abies* (L.) H. Karst.).

Nyckelord: klimatförändring, tillväxt, Gran, Tall, Ek, bonitet, fjärranalys, LiDAR, ståndortsindex.

Preface

Modelling growth is shooting at a moving target

- *Professor Annika Nordin*

Dedication

To my loving parents, Anders & Else-Marie, for their unwavering support. Particularly you, Dad, for listening to my daily '*briefing*'.

Contents

List of publications

This thesis is based on the work contained in the following papers, referred to by Roman numerals in the text:

I. Vospernik S., Vigren C., Morin X., Toïgo M., Bielak K., Brazaitis G., Bravo F., Heym M., del Río M., Jansons A., Löf M., Nothdurft A., Pardos M., Pach M., Ponette Q., and Pretzsch H. (2024). Can mixing *Quercus robur* and *Quercus petraea* with *Pinus sylvestris* compensate for productivity losses due to climate change? Science of The Total Environment, 942 (173342), DOI: 10.1016/j.scitotenv.2024.173342

II. Vigren C., Vospernik S., Morin X., Toïgo M., Bielak K., Brazaitis G., Bravo F., Heym M., del Río M., Jansons A., Löf M., Nothdurft A., Pardos M., Pach M., Ponette Q., and Pretzsch H. (2024). Divergent Regional Volume Growth Responses of Scots Pine and Oak Stands to Climate Change in Europe. Manuscript (submitted).

III. Larson J., Vigren C., Wallerman J., Ågren A.M., and Mensah A.A. (2024). Tree growth potential and its relationship with soil moisture conditions across a heterogeneous boreal forest landscape. Scientific Reports, 14 (10611), DOI: 10.1038/s41598-024-61098-z

IV. Vigren C., Wallerman J., Mensah A.A., and Ståhl G. (2024). Exploring the potential of repeated LiDAR measurements for modelling the growth of individual trees. Manuscript.

All published papers are reproduced with the permission of the publisher or published open access. The contribution of Carl Vigren (CV) to the papers included in this thesis was as follows:

I. CV: Writing – review & editing, Formal analysis.

II. CV: Writing – review & editing, Writing – original draft, Visualization, Formal analysis, Methodology, Conceptualization.

III. CV: Writing - review & editing, Writing – original draft, Visualization, Formal analysis.

IV. CV: Writing – review & editing, Writing – original draft, Visualization, Formal analysis, Methodology, Data curation, Software, Conceptualization.

List of figures

1. Introduction

1.1 Background

Any good farmer worries about the weather. Will rains come and bring mould to the drying hay? Will a cold snap settle frost on the fresh sprouts? Will the drought break before the water reserves run out?

The fundamental worries of those who grow forests are no different – and with long rotation periods, the worries may extend over decades into the future. One such current worry is climatic change, which may cause effects such as drought, and storms causing damage from windbreak, perhaps incurred after heavy snowfall. Consequently, much current forest research is devoted to evaluating the likely consequences of climate change and how forestry can adapt to changing climate. For example, adaptation may imply that mixtures of coniferous and deciduous species should be used to a larger extent (Knoke *et al.*, 2008) or that shorter rotation periods should be applied (Zimová *et al.*, 2020). It may also involve different management strategies, such as avoiding heavy thinning operations late in the rotation (Wallentin & Nilsson, 2014). However, there are potential upsides of climate change as well, such as faster growth due to increasing temperatures and elevated atmospheric levels of carbon dioxide. The overall effect will depend largely on where a forest is located geographically and how it is managed.

Once planted (or naturally regenerated), trees must adapt in situ to their environment. They cannot, like animals, move to more favourable locations. With poor adaptation to changing environmental conditions, trees will be stressed because of several physiological mechanisms, which could lead to decreased resilience and growth, or even death. For example, cell stomata are used for maintaining cell temperatures in a viable range whilst avoiding hydraulic failure of the supporting tissues – an important reason for tree death due to drought (Mantova *et al.*, 2022). On the other hand, high cell temperatures may cause denaturation of proteins and release of excessive amounts of metabolic signalling agents which can induce cell death (Huang *et al.*, 2019). Waterlogging impacts plants in analogous ways – where typical responses might include nastic movements, programmed cell death in roots to facilitate gas exchange and energy-saving actions to limit respiration (Zhou *et al.*, 2020).

An important reason for research on impacts of climate change on forests and forestry is the many ecosystem services human society receives from healthy forests (Seidl *et al.*, 2016). These services range from materials for buildings and packaging to recreational and cultural values. Some of them have economic value as marketed goods, while others have non-market values which are typically more difficult to assess (Obeng & Aguilar, 2018). The economic value of marketed forest ecosystem services from the forestry sector (including the economic groups forestry & logging, solid wood products, pulp and paper products & wood furniture) was estimated at ~1.5 trillion USD in 2015 (Li *et al.* 2022). Further, these forestry sector groups employed 32.4 million people. This stands in relation to a global GDP reported by the World Bank Group (2024) of 75.36 trillion 2015 equiv. USD, i.e. the forestry sector contributes to about 2% of global total GDP.

This thesis has a focus on forests in Europe. Thus, it is worth highlighting that the European (excluding the Russian Federation) GDP from forestry in 2015 amounted to 423 billion USD, employing about 7.9 million people (Li *et al.*, 2022), i.e. the share of Europe´s GDP of the global GDP from forestry was almost 30%. This is a massively outsized contribution, as Europe sans the Russian Federation holds only about 5% of the world's forests (FAOSTAT 2020 SDG Indicators 15.1.1 Forest Area).

However, forested ecosystems on the European subcontinent encompass several different biomes, ranging from subarctic boreal forests to temperate and Mediterranean forests. They are strongly influenced by major weather

systems from the Atlantic Ocean and from Eurasian continental landmasses. Forest management is adapted to local conditions and traditions, meaning that forests in Europe are far from homogeneous. For example, whilst the peoples of the Iberian Peninsula have strong traditions of pastoral agroforestry integrating livestock production with large seed-trees such as Cork Oak (*Quercus suber* L.) or European Beech (*Fagus sylvatica* L.), grazing has mostly been separated from forests in Nordic and Central Europe, at the very latest following the introduction of managed pastures, e.g. Kardell (2016), albeit certainly recommended by silviculturists far earlier (ibid.).

Owing to the many differences between forests in Europe, it is not a trivial task to evaluate how forests in Europe are likely to be affected by climate change and what the relevant adaptation measures would be. Answering these questions is an important task for researchers, and practitioners alike, to safeguard that European forests should continue to provide vital ecosystem services.

However, whereas the difficulties to make projections of forest state increase due to climate change, so do the possibilities to make such projections due to technological developments. Traditionally, growth models for application in practical forestry have been based on data collected during repeated field inventories or experimental stands (Ekö, 1985). Typical data concern information about individual trees on sample plots, such as data collected during national forest inventories (Tomppo *et al.*, 2010). Mostly, all trees on plots are calipered for diameter, whereas height is measured only for a subsample of the trees. Site quality, stand age, etc., are typically assessed at plot level. Because field campaigns are costly, only relatively sparse samples are usually available from field inventories, or crude subjective methods are applied whereby stand averages are ocularly assigned for entire stands (e.g. basal area by angle count sampling, Bitterlich, 1984.) With recent developments in remote sensing methods, new possibilities for cost-efficient data collection have emerged.

A method of specific interest for forest inventories is Light Detection And Ranging (*LiDAR*, e.g. Peterson *et al.* 2007). With LiDAR, the height structure of forests, and the structure of the ground beneath forests, can be obtained at relatively low cost per area unit. This type of information has revolutionised forest inventories in several countries. For example, currently the second round of a national campaign for collecting LiDAR data wall-to-

wall for Swedish forests is currently being conducted (Nilsson *et al.*, 2017). High-accuracy maps for features such as biomass, volume, and height are being made available for different uses, related to both forestry and nature conservation (Bohlin *et al.*, 2021; Saarela *et al.*, 2020). Further, from detailed height reliefs of the ground beneath the trees, high-accuracy maps of soil moisture have been developed (Lidberg *et al.*, 2020). These have found broad use for making logging operations more effective, while making less negative impact on forest soils.

With this second round of LiDAR data acquisitions currently being completed in Sweden, several new possibilities are emerging. Based on forest height and height difference between consecutive measurement, maps of site quality and stand age are currently being compiled (Appiah Mensah *et al.*, 2023). Ideas are emerging that growth models for trees and stands could be improved using the same type of information.

This thesis comprises two main parts, both related to modelling the growth of trees and stands. In the first part, I focus on the likely effects of climate change on growth and discuss adaptation measures. A first article explored the effects of climate change on the growth of stands of Oak (*Quercus spp.* L), Scots Pine (*Pinus sylvestris* L.) and mixtures between the two. The stands were located at different experimental sites across Europe. In a second article, using the same data, I developed models so that geographically explicit results in terms of growth effects of climate change for the main parts of Europe could be obtained. Such results are important for assessing regional and local level consequences of climate change, as well as for discussing relevant mitigation measures.

The second part of the thesis addresses to what extent novel techniques can be used for determining site quality and improving the accuracy of growth models. Thus, in a third study, I contributed to relating site quality assessments to soil moisture data. The site quality assessments were developed wall-to-wall from repeated LiDAR acquisitions. In a fourth and final study of the thesis, I evaluated to what extent data from repeated LiDAR measurements could improve growth models based on traditional field data.

In the remaining sections of the Introduction, different areas of relevance for the thesis are reviewed. At the end of the chapter, detailed objectives for the thesis are presented.

The Past is a Foreign Country[1]; but the Future may be Stranger Still.

1.2 Growth Modelling

Modelling helps us structure what we think we know, formulate experiments for that which we do not; evaluate the impact of uncertainty; and provides us with an opportunity to extend from our constructivist assumptions to explore counter-factual statements by deductive reasoning. All models are a simplification of reality.

Modelling is a core activity in describing and predicting the growth of trees and forests, and should be tailored to provide timely, biologically plausible, robust and objective-oriented results. As a result, a broad spectrum of approaches has appeared:

Process-based modelling attempts to extend strong stoichiometric relations observed in physiological plant-studies to mimic the natural processes of growth, mortality, water and nutrient uptake, internal water flow, desiccation rates etc., and has been successfully employed to predict productivity across large scales (Coops, 1999).

Empirical modelling has a significantly longer history than the aforementioned, placing less emphasis on the causal structure of lower order processes. Empirical modelling has developed in direct relation to increased mensurational demands. Taxation is costly, and as result early research in forest mensuration was chiefly interested in finding simple and accurate means to assess core features of stands such as the standing volume and basal area. This developed into providing more-or-less sophisticated static functions, e.g. that a trees volume can be related by a power law to its diameter, e.g. Kopezky (1899), from which assessments of stand volume, assortment composition and standing valuation could be carried out based on single inventories; measurements from representative sites were rapidly combined into yield tables, later based on strong generally observed phenomena – such as *Eichhorn's rule.* Named after Eichhorn (1904), it refers to the remarkably strong relation between standing-stock and basal-area weighted mean height, regardless of age (and by proxy, site quality). It was first presented for Silver fir (*Abies alba* Mill.) and later suggested to be

[1] LP Hartley, 1953.

generalizable to other, at least coniferous species, by Gehrhardt (1923). Notable compilations of yield tables include e.g Swappach (1912) and Wiedemann and Schober (1957)

These generalisations, with varying degrees of computational processing of data, were based on considering the cross-sectional data from inventoried plots to constitute developmental trajectories. Some are still in use today, e.g. Assmann and Franz (1963, 1965)[2].

It is here suitable to dwell for a moment on the difference between *static* and *dynamic* equations, since by design what they imply is different. Static equations, relating an independent not re-measured target variable to any number of correlated features, is in essence providing the same service as did formerly tables – providing an estimate of current conditions, or projections based mainly on the assumption that the forest conditions within age classes remain stable.

Dynamic equations, on the other hand, intend to mimic the alteration of a characteristic over time – such as the 5-year *basal area increment* of a stand/stem, or site index[3] functions. Although such functions are not required by design to come from longitudinal data[4], modelling from solely cross-sectional data tends to yield biased results (Tegnhammar, 1992; Walters *et al.*, 1989; Yue *et al.*, 2023). Repeat measurements allow for a postulation of that the disturbance connected with a certain site be constant over time, such that it can be satisfactorily addressed by differencing (Furnival & Wilson, 1976). However, when the disturbance by a site is correlated with predictors, this does not properly account for the error term.

Thus, modelling forest development from longitudinal studies has today become the norm – at least where well maintained national forest inventories and long-term experiments are accessible (Fridman & Danell, 2023). However, cross-sectional studies can be the only choice for research conducted in areas with lacking experimental infrastructure.

A large number of generic models for growth modelling have been proposed and specified, such as the Lundqvist-Korf, Gompertz or Chapman-

---

[2] *pers. comm. Priv.-Doz. Dr S. Vospernik*

[3] Site Index: Index of height growth productivity, typically expressed as the expected mean height of the 100 stems with thickest diameters per hectare at a given reference age.

[4] Repeated measurements of the observed elements.

Richards model families (Bertalanffy, 1938; Gompertz, 1825; Korf, 1939; Lundqvist, 1957; Richards, 1959).

As an example, a curve fit to data for a Norway Spruce stand according to Mensah *et al.* (2022), fig. 1B demonstrates the general concepts of a moderately slow juvenile phase – the maximum periodic increment being reached as the canopy closes, and – finally – a tapering off as a stand matures cf., Assmann (German: 1961, English: 1970).

Generally speaking, the trajectory of standing volume assumes a sigmoidal-hyperbolic relation when plotted over time, or an inverse-sigmoidal/negative exponential relationship when the ratio of increase is plotted against gross production, e.g. figs. 1A, 1C. As I have mentioned before and will return to later, volume is a modelled variable, and consequently modellers have frequently preferred the sigmoidal accumulation of standing volume to be an emergent property of the system of growth equations (Vospernik *et al.*, 2015).

Note here that the culmination of periodic annual volume increment of the stand does not correspond to that of the average individual of the prevailing trees (Clark, 1990).

The nature of a potential asymptote is dependent on model objective as it is typically outside the range of underlying data and so largely subject to modeller preference. Furthermore, it is dependent on fairly characterising the effects of regular[5] and irregular[6] mortality, which is notoriously difficult (Siipilehto *et al.*, 2020).

However, as was early observed by e.g. Reineke (1933) for a number of north American tree species, there are fairly predictable species dependent density limits – the capacity to maintain a certain average individual of a given size per unit of space. As was later also found separately by Yoda *et al.* (1963), this phenomenon gives rise to the so-called 'self-thinning' line[7], alluding to that when plotted on a log-log scale, the exponential decrease in the number of survivors at an increase in the average size of the members of the population approaches a linear limit, with a slope of approximately -3/2's for a wide range of species. The self-thinning line, as the limiting border for

[5] Long-term, fairly predictable density-dependent mortality and 'background' noise such as individual wind-/snow breaks.

[6] Event-driven mortality, e.g. storm, drought, insect outbreaks with a clumped spatial distribution.

[7] Also widely known as the -3/2 slope.

the competition-density-yield effect, demonstrates that for a wide range of initial plant spacings, final yield is rather unaffected. However, the slope certainly varies even between woody species (Pretzsch & Biber, 2005; Vospernik & Sterba, 2015). It should here be noted that one can typically distinguish between the *species boundary line*, which follows from the

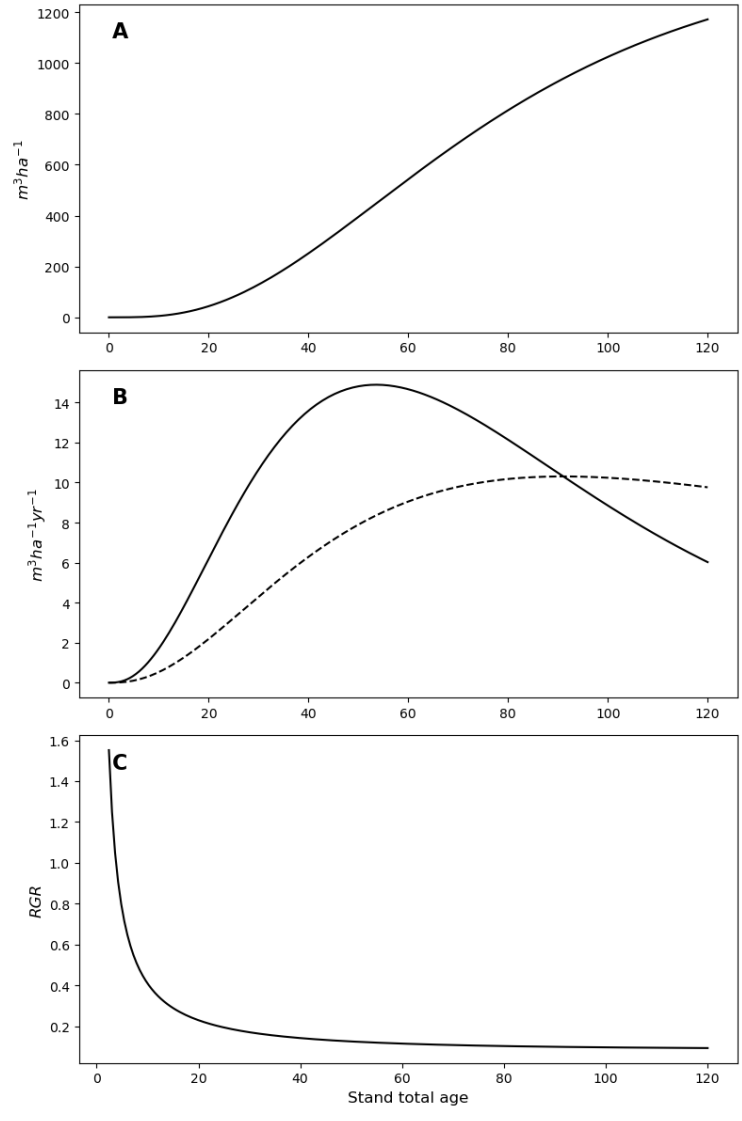

Figure 1. Principal illustration of A) Net production of a stand of Norway Spruce (H100: 30 meters), B) solid line: current annual increment (CAI), dashed line: mean annual increment (MAI), and C) Relative Growth Rate (RGR).

definition above, and the *dynamic thinning line*, the trajectory undertaken by single stands (Weller, 1990).

The formalisation of a self-thinning line as an emergent property of rules-based games has attempted to clarify whether the apparent limit is inherently expressing a property related to an allometric relation to biomass, or some proxy limiting the planar spatial extent such as crown-diameter (Westoby, 1984). It can arise even in very simple systems, such as that suggested by Slatkin & Anderson (1984), wherein points from a homogenous Poisson point process are placed on a surface and grown as circles from a common radius in discrete steps by some monotonically increasing growth function. Whenever two circles overlap, one randomly dies. An example implementation by the author is demonstrated in fig. 2[8], where the points are grown on a unit flat torus at a relative increase of the radius of 3% per growth step. Note that the first step of instantiation is not shown, where overlapping circles before the first growth period are removed. A quantile regression to the 99th percentile of the result yields an almost identical slope to the proposed -3/2 slope by Yoda & Reineke. Overall, it clearly demonstrates both the accumulation of trajectories close to the *species boundary limit* (rule of constant final yield) as well as widely varying individual trajectories. Large increases in diameter without concomitant decreases in the density demonstrate the competition-yield-density effect. Individual variations between runs clearly occur due to the suboptimal placement of the surviving points.

[8] Note inversion of axes, yielding a -2/3 relation equivalent to the proposed -3/2 slope of the boundary limit.

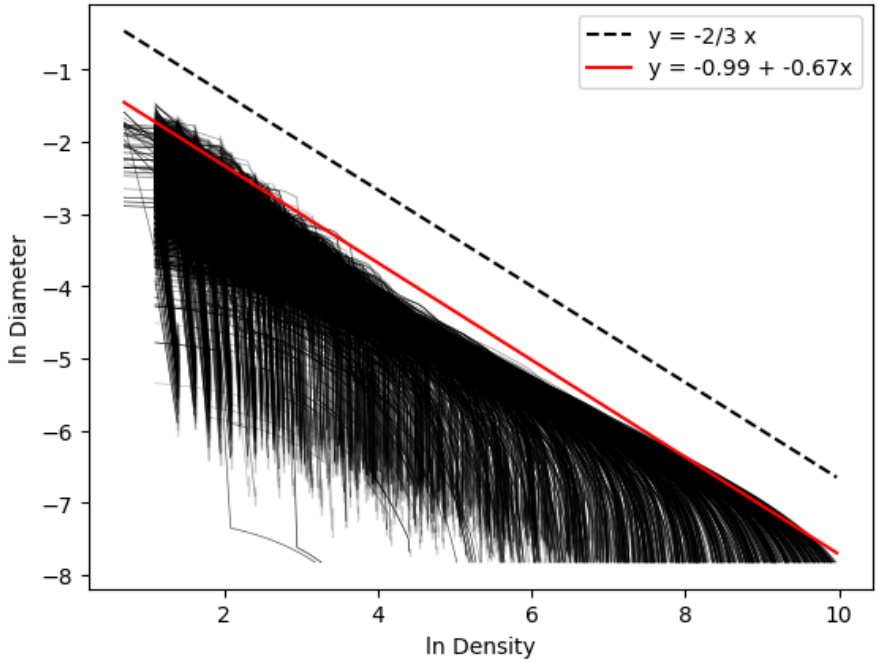

Figure 2. Results from 2'000 runs of the Slatkin & Anderson's game. A quantile regression to the 99th percentile yields a relation (solid, red line) of almost identical slope to that of the -3/2 line (dashed line).

Note that the circles in Slatkin & Anderson's game are not size-limited, and that the maximum diameter of trees at low densities would therefore taper off considerably compared to fig. 1, e.g. producing a curvilinear relation (Cao & Dean, 2015). Large variation in outcome depending on small changes in initial conditions, such as the spatial distribution and number of circles in Slatkin & Anderson's game, is typical of chaotic processes. Without any knowledge of the generative system, we might question to which degree these fluctuations in outcome are, in fact, due to undirected perturbations from external influences (random noise) or whether they are a property of an inherently chaotic single or aggregate process. We conclude that the modelling scale and structure of the model are critical to delivering operatively robust, if not informative, estimates. The fact that linear formulations have been so serendipitously applied in physics and

engineering by no means entails that the same is true for complex ecological systems[9].

1.3 Uncertainties in growth modelling

Uncertainty is inherent to studies of forest growth. A first observation in this context is that some variables of interest, such as tree or stand volume, are not directly measurable (without great effort and cost) but start- and endpoint observations must also be modelled. However, even if a growth model is based on directly observable variables, such as the diameter of trees, several sources of uncertainty exist in predictions from an estimated model.

Firstly, the specified model relationship may be incorrect (for any number of reasons), which leads to errors that can be difficult to assess. Secondly, the parameters of a model must be estimated from sample data. Thus, variability in the estimated model parameters occurs, depending on the sample data used for parametrising the model. Further, most models of biological features comprise a large intrinsic variability even under ideal circumstances. This variability is expressed as an error term, like ε in the simple model $V = f(B, H) + \varepsilon$ for determining the volume, V, of a tree, based on its basal area, B, and its height, H.

Depending on the area of application, different errors are important to consider. When predicting the growth of a single tree or stand, the variability of the error term is mostly the most influential part, whereas when predicting the average growth for a large area variability in estimated parameters is usually the larger part (Lin *et al.*, 2023). Likewise, for growth modelling under climate change, large errors may be committed if growth models based on empirical data are applied unless the data for the models did not include large environmental gradients (cf., Vospernik, 2021).

In addition to the aforementioned sources of uncertainty, measurement errors may occur among both the dependent and independent variables in a model. Examples of the magnitude of such errors are given by, e.g. Broman and Christoffersson (1999), Prodan (1965, p. 164) and Stereńczak *et al.* (2019).

[9] *Sensu R. M. May.*

An illustration of the variability in growth modelling results is given in fig. 3, where Monte Carlo simulation was applied to, based on fixed estimates for the asymptote and of starting conditions, sample new parameter values in each growth sequence. In this simple example, independence between parameters, and Gaussian distributions for all the parameters were assumed.

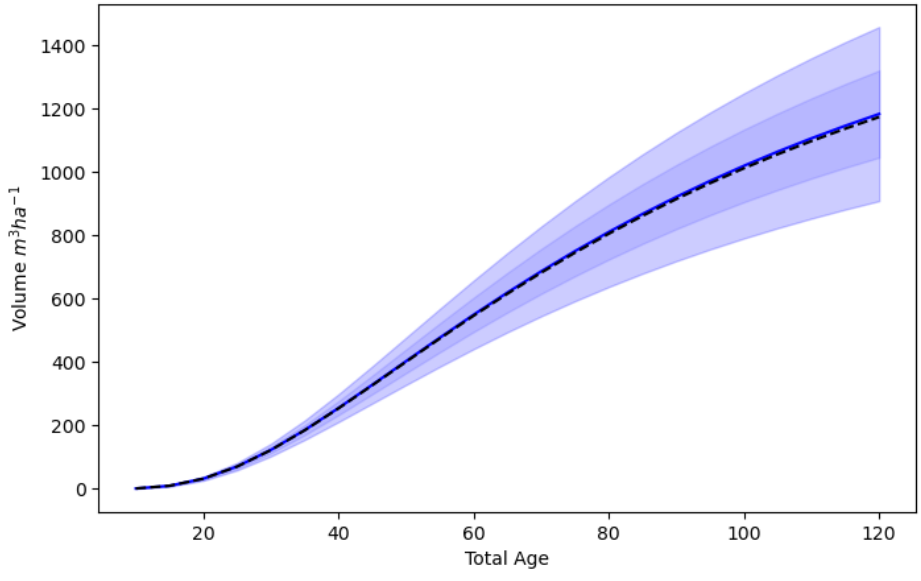

Figure 3. Results from 2'000 repeated projections of a single stand illustrating model uncertainty about the parameters in the growth model. The dashed line gives the projection using the model parameters assumed to be true. The solid line corresponds to the average of simulated projections. The deep blue, shaded area includes projections contained within one standard deviation of the mean; the light blue, shaded area includes projections contained within two standard deviations of the mean.

1.4 Site quality

The capacity of forest soils to provide yield in terms of tree volume has long been a focus in research and application. In a landmark study, Cajander (1909) suggested, based on preliminary work in southern modern-day Germany, that *forest types* seemed stable, spare *fleeting* changes following e.g. cutting, and that they might be used successfully to differentiate between

site qualities. Together with Ilvessalo (1920), yield tables were statistically formalized using statistical methods such as those championed by Cajanus (1914). These demonstrated differences in productivity between the suggested types. Later studies demonstrated that forest types ordered by productivity differed with regard to soil nutrients, where, e.g., the more productive forest types had higher concentrations of nitrogen available for plants (Aaltonen, 1929; Valmari, 1921).

Production capacity is typically expressed in terms of a quantitative estimate, such as site productivity (Skovsgaard and Vanclay, 2008). As a result of the breadth of conditions in which forests grow, and increasing focus on the spatiotemporal variation about the mean productivity beyond the stand unit, there's likely no single approach to estimating such that will suit all conditions, interest scales and use-cases (Skovsgaard and Vanclay, 2013).

The picture is further complicated by that the realisation of the potential growth is affected by both management and species-choice, whilst experimental trials are both expensive and time-consuming. This leads to a wide-variety of model-based estimates, such as the relations presented by Agestam *et al.* (1981). In fig. 4, the system developed by Mensah *et al.* (2022) was used as a basis for illustrating the relation between the estimated site productivity and its proxy, here site index.

Many systems for determining site quality are based on the relationship between top height, often expressed as the mean height of the 100 coarsest trees per hectare, and the mean age of these trees. However, since the relation between height and age is considerably confounded in many situations, site quality assessments based on geobotanical factors assumed to affect site fertility have also been developed, e.g. Lundmark (1974), Hägglund and Lundmark (1977) and Hägglund (1979). As their basis, i.e. the constancy of the underlying allometric relations, may change with climatic conditions or between regions, also these relationships have come under heightened scrutiny, e.g. Bontemps & Bouriaud (2014).

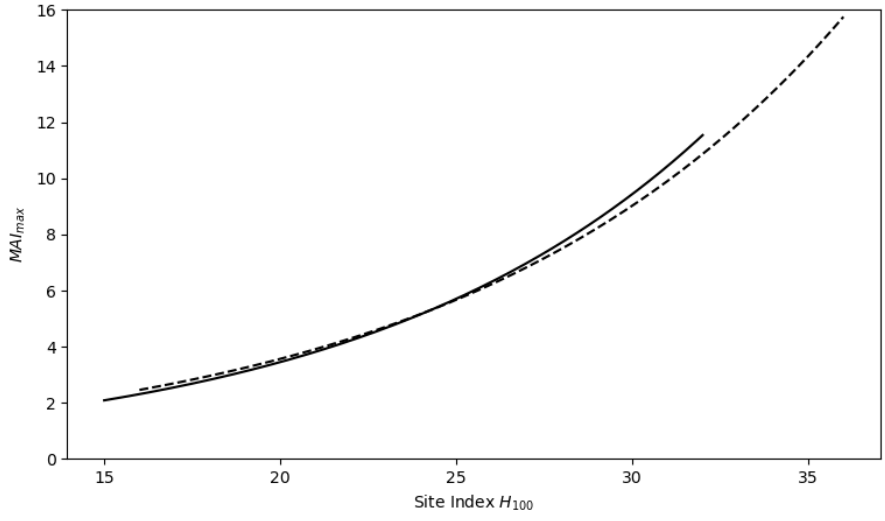

Figure 4. Yield potential, the maximum attainable MAI (in m3ha-1yr-1), for different site indexes. After Mensah et al. (2022). Solid line: Scots Pine. Dashed line: Norway Spruce.[10]

1.5 Climate Change

Fourier is generally credited as being the first to compare the insulative effect of the atmosphere to that of a greenhouse, based on the experimental work of de Saussure, who demonstrated that the amount of direct radiation from the sun increases with altitude (Fleming, 1999). Only later did Tyndall (1861) provide a mechanism by which the atmosphere could retain heat in water vapour, and proposed that such could be the case also for carbon dioxide (CO_2). This was, in turn, shown only a few years later by Arrhenius (1896). Arrhenius concluded that the rate of burning of coal could, indeed, *ceteris paribus,* over the next 3'000 years cause an increase in the concentration of atmospheric CO_2 by some 50%, with an accompanying rise

[10] N.B. Although the growth may seem similar at a given site index, this should not be taken to imply that the site index of different species be the same at a given site!

in temperature by 3.4 °C (1896a)[11]. Water vapour, despite representing some 50% of total radiative forcing, is a by-product of the mean temperature with a short atmospheric life-time, and so only works as an 'amplifier' (Lacis *et al.*, 2010).

It will have escaped no widely read person that the rate of CO_2 emissions has doubled roughly every 32 years since 1896 (Andrew & Peters, 2024; Friedlingstein *et al.*, 2023)[12]. At the same time, the global average annual concentration of atmospheric CO_2 has increased from ~294 ppm (1900) to 419 ppm in 2023, roughly corresponding to an increase of 42.5% (NOAA, 2024; Ritchie *et al.*, 2024). By comparison, the global monthly mean temperature for each month between July 2023 – June 2024 exceeded 1.5 °C increase relative to their monthly average 1850-1900 (C3S/ECMWF, 2024). The World Meteorological Organization currently estimates that it is as likely as not that the 2024-2028 mean increase will exceed 1.5 °C (WMO, 2024).

General Circulation Models (*GCM's*) include a wide range of different models, objectives and applications, but for the purposes of this thesis will refer to coupled atmospheric-oceanic general circulation models (*AOGCM's*), such as ACCESS1.3 (Bi *et al.*, 2013), CMCC-CM (Scoccimarro *et al.*, 2011); MIROC5 (Watanabe *et al.*, 2010) or CESM1-BGC (Lindsay *et al.*, 2014), which are constructed from both process-based and parameterized components. As mentioned above in a forestry context, many model parameters may be uncertain, or have only been observed within certain ranges.

In transient climate simulations[13] the key input to differing experiments include physics, model-warm up/initial conditions, and future inputs such as greenhouse gas (*GHG*) emissions scenarios (e.g., *Special Report on Emissions Scenarios,* or *SRES*), GHG concentration trajectories like the *Representative Concentration Pathways* (*RCP*s), or the *Shared Socioeconomic Pathways* (*SSP*s) in which emission scenarios have been constructed based on potential socioeconomic developments.

---

[11] Arrhenius took some comfort in that the descendants of the lecture audience might enjoy a better climate – lecture given in Stockholm 3rd of February 1896.

[12] 1896 CO_2 emissions ~1.54 Gt; 2022 CO_2 emissions ~ 37.15 Gt.

[13] In transient climate simulations, the model can be exposed to a time-series of drivers, e.g. emissions, where the global climate is modelled in discrete steps.

Both the RCP and SSP scenarios are categorized by the level of radiative forcing[14] at year 2100, e.g. RCP4.5 or SSP2-4.5 entail an end-of-century level of radiative forcing of ~4.5 Wm^{-2}. This should be compared to a radiative forcing of ca. 3.4 Wm^{-2} in 2022, representing a 49% increase in radiative forcing due to anthropogenic emissions[15] since the 1990 reference year of the Kyoto protocol (UNFCCC, 1997). Note, however, that the global mean temperature will continue to rise even under the absence of further emissions as climatic feedbacks take effect, and that the global mean reflects neither the potential change at local to regional scales, nor the potential impact.

Europe has warmed at a rate more than twice the global mean between 1980 and 2022 (Copernicus Climate Change Service (C3S), 2024). As found by Abatzoglou, Dobrowski and Parks (2020), multivariate quantities accounting for change in more than one measure could show that the observed departure from climatic references is even more rapid than for single measures, and associated with changes in means, rather than only change in variance. Abatzoglou *et al.* (ibid.) additionally warn that the adaptive capacity of ecosystems may not be aligned with the observed changes. Mahony *et al.* (2017) demonstrate for the North American continent moderate departures during RCP 4.5, with limited regions (7% of area) experiencing climate conditions meeting a fixed dissimilarity criteria during the projected 2071-2100 normal period, whereas up 40% of the terrestrial area is projected to exceed the same criteria under the RCP 8.5 scenario, with major implications for long-term forest growth projections.

In many studies, the principle of uniformitarianism (*the past is the best key to the future*) is implicitly assumed to hold – however no such guarantee can be held in multivariate departures far outside the observed range in any complex system. This is particularly the case where environmental change is both rapid and of large magnitude, pre-empting possible adaptation by gradual change in local community composition of vegetation and/or necessary biological structures. An example is given by Hinze, Albrecht and Michiels (2023, fig. 5) on the climatic comparison between current distributions of potential vegetation, *c.f.* Tüxen (1956), in Europe and that

[14] Radiative forcing is the net change in radiative flux (W/m^2) by an external driver. The total effect is roughly attributable (63% CO_2, 19% methane, 6% nitrous oxide, etc.).

[15] NOAA AGGI index.

during 2070. Under the RCP4.5, RCP 8.5 scenarios the vegetation potentials indicate a northward contraction of boreal *Picea abies* forests, being strongly exacerbated under the RCP 8.5 scenario. Likewise, north-easterly shifts in the European areas classed as *Quercus-Carpinus* forests towards the lower basin of the Baltic Sea, Baltics and the Russian Federation were observed under RCP 4.5. In RCP 8.5 such forests migrated further into Sweden and Finland. A rapid expansion across the lowlands of Western Europe was foreseen for the thermophilic *Q. pubescens,* which is currently found in southern France and Italy. It is important to note that vegetation community and respective abundances of species are indicative not of any species absolute potential, but of each species' growth rate in relation to that of its competitors (*sensu Ellenberg*[16]).

The impacts of environmental change on forest growth have been studied for some time. From the *Spruce sickness* of Saxony mentioned by Wiedemann *et al.* (1923), the *Waldsterben* and acid-rain of the 1980's (Ulrich, 1990), the increase in growth during the same period, cf. Spiecker *et al.* (1996), and currently, assessing the potential impact of climatic change, e.g. Reyer (2015), Reyer *et al.*, (2017).

[16] Heinz Ellenberg noted in 1953 that the distribution of the abundance of plants are shifted away from their physiological optimum by competition, e.g. Crawley (2007).

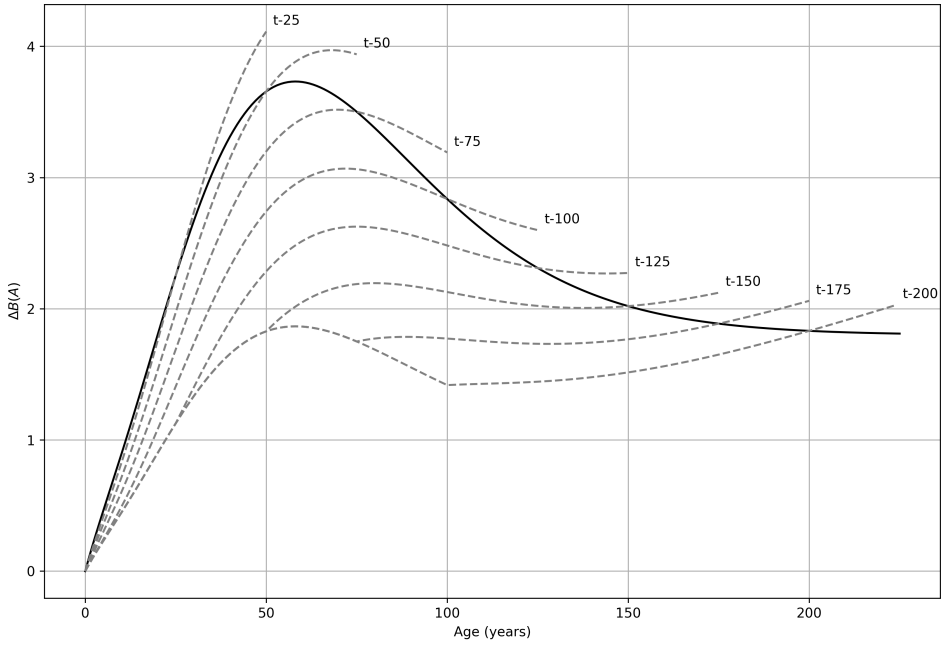

Figure 5. Conceptual effect of external forcing on biomass accumulation, after Hember et al. (2012). Solid line marks actual growth function. Dashed lines labelled by starting year (Biomass = 0.001).

Hember *et al.* (2012) demonstrated the conceptual growth impacts on a fixed ontogenic trajectory of biomass growth of a stand (fig. 5). Between 200 and 100 years before present, the stand grows ½ as well as usual. Between 100 years before present and present day, growth increases again to 100% (solid line). This improvement continues out to 25 years into the future (time *t*) – e.g. the dashed line representing the growth of a stand planted at 100 years before present is denoted t-125. However, as noted by Hember *et al.*, such a direct modulation approach failed to capture carry-on effects such as defoliation after drought, or intrinsic change (change in form of function).

Paterson's CVP Index[17] is log-linearly related to the productivity of forest stands expressed as $m^3ha^{-1}yr^{-1}$ (Paterson, 1956). By comparing the development of CVP over time Pretzsch *et al.* (2023) found that between 1975 and 2017 the climatic conditions for forest growth had declined across south-western Europe (Portugal to western Italy) whilst strongly improving across the Scandinavian peninsula.

1.6 Remotely sensed data for improved growth modelling

During recent decades, the challenges for accurate growth prediction have increased due to climate change, but so have the possibilities to increase the accuracy of growth models by making use of new techniques, facilitating the incorporation of new types of data in the models. Not least, the developments of remote sensing techniques, which have been rapid over recent decades, offer such possibilities.

Aerial photographs have been available for a long time and proved their importance for cartography, including production of maps for purposes of forest planning. Aerial photographs have also been extensively used for assessing features such a stand volume (Gingrich & Meyer, 1955). A milestone in the development of remote sensing techniques for forest inventory occurred when optical data from satellite-borne sensors were first made available for civilian applications in the 1970s through the Landsat missions (Goward *et al.*, 2017). Since then, a plethora of satellite-borne sensors have collected Earth information, with resolutions ranging from coarse to fine. Whereas the main purposes of the missions have seldom been forest inventory, data from medium and fine resolution sensors (<1 - 30 meters) have proved to be useful for forestry purposes as well: monitoring harvests, forest health, species classification, crown closure as well as related estimates of forest attributes such as volume (Fassnacht *et al.*, 2024).

In the 1990s, Light Detection And Ranging (LiDAR) technology was found to be extremely useful for purposes of forest inventory (Næsset, 1997).

[17] CVP – Climate Vegetation and Productivity

With LiDAR, detailed information about the height structure of trees and forests can be obtained from hand-carried or vehicle-mounted laser scanners. Derived features have been found to correlate strongly with aboveground biomass, growing stock volume, and forest height. Following large-area LiDAR campaigns in several countries, including Sweden (Nilsson *et al.*, 2017) forests maps of features such as volume and biomass have been produced and found many different uses.

In parallel with the development of LiDAR techniques for forestry, similar developments have been pursued using Radio Detection And Ranging (RADAR) and Synthetic Aperture RADAR (SAR). Longer time-series of spaceborne SAR measurements can estimate site index with reasonable results if both species and age of stems in the area of interest are known. However, silvicultural treatments tend to lead to an underestimation (Huuva *et al.*, 2023).

So far, LiDAR-based estimates of site index from existing equations have been based on LiDAR height estimates with ancillary age information from e.g. forest inventory (Holopainen *et al.*, 2010; Tompalski *et al.*, 2015), LANDSAT (Tompalski *et al.*, 2015) or direct estimation from bitemporal LiDAR scanning campaigns (Noordermeer *et al.*, 2020). Socha *et al.* (2017, 2020) developed new top height growth equations from repeated ALS campaigns combined with age data from stand registers. Tymińska-Czabańska *et al.* (2021) combined the aforementioned bitemporal approach with interpolated precipitation data. Recent efforts have also extended the site index concept to multitemporal ALS-data from mixed-wood stands using the growth-rate at height approach outlined by Salas-Eljatib (2020), e.g. Riofrío *et al.* (2023).

Some countries now run their second round of wall-to-wall LiDAR data acquisitions. As a result, new opportunities to assess change are emerging, including changes due to tree growth. Further, with dense LiDAR data information derived from individual trees, it is possible to assess the competition status between trees wall-to-wall as well as the height growth of single trees. Results are promising and indicate that this new type of data has a potential to increase the accuracy with which past growth, current state, and probably even future growth of forests can be modelled. In fig. 6, the principle of estimating site quality from repeat LiDAR measurements is outlined.

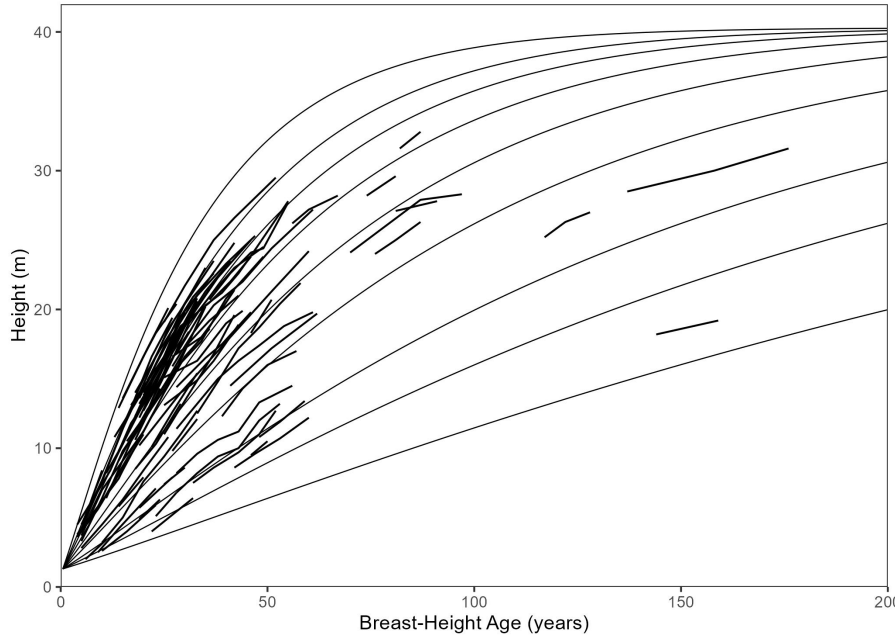

Figure 6. The Norway Spruce dataset (thick, solid black lines) underlying current site index equations for use in Sweden fitted with Salas-Eljatib's (2020) height growth rate at height equation. N.B. Actual dataset registered total age, rather than age at breast height. Thus, data subjectively shifted along abscissa to match. Sheath of curves based on initial point (0.5,1.3).

LiDAR measurements to some extent penetrate vegetation cover and can thus be used for providing detailed maps of ground topography. These types of maps can also be used as input for soil moisture mapping. For example, Ågren *et al.* (2021) and Lidberg *et al.* (2020) have produced maps of soil moisture for Sweden by combining height relief data derived from LiDAR measurements with soil moisture as assessed by the Swedish national forest inventory.

Thus, novel technologies offer new possibilities to improve growth modelling through the incorporation of new metrics which correlate strongly with growth into models.

2. Objectives

The main objective of this thesis was twofold: (i) to assess the consequences of climate change on the growth of Scots pine (*Pinus sylvestris* L.) and oak (*Quercus spp*. L.) stands at European level, and (ii) to assess how novel metrics from remote sensing could be utilised for improving the accuracy of models in determining potential future growth of forests.

The specific objectives of the included papers were:

Paper I. A climate-sensitive basal area increment model for single trees has been developed by Vospernik (2021) and used to simulate the growth of inventoried stands of *Q. spp., P. sylvestris* and their mixture on the same sites given varying climatic scenarios. We specifically hypothesized:

i) *Decreased standing volume in year 2100 expected for all stand types with increased scenario severity (Historical << RCP 4.5 << RCP 8.5).*

ii) *If hypothesis I holds, Q. spp. will buffer these decreases better than P. sylvestris.*

iii) *Mixed stands will show less of a response than the monocultures.*

iv) *Decreases will be more severe at low latitudes.*

Paper II: Given the outcomes from study sites in paper I, we further hypothesized that for species with low levels of subspeciation, such as *Q. spp.* & *P. sylvestris*, the functional relationship between annual weather patterns and volume growth may be very similar across their distribution. We trained a static reduced model from yearly outputs by *PrognAus* to look at relative differences in expected growth between 2017 and 2100 at a European level.

Paper III: In the third study, a primary objective was to investigate the relationship between some factors which are known to affect soil fertility, soil moisture from maps developed by Ågren *et al.* (2021), and a proxy of site quality as estimated from repeat LiDAR measurements across a boreal landscape.

Paper IV: In the last study of the thesis, the objective was to compare the accuracy of single-tree growth models developed based on traditional field data with the accuracy of models based solely on LiDAR data, as well as models where the two types of metrics were combined. The models concerned growth in terms of volume.

Whereas a traditional approach to assessing the likely consequences of climate change on growth is based on process-based modelling, this thesis explores how empirical growth models based on data with large environmental variation could be used for the same purpose, thus "pushing the envelope" regarding the application of empirical growth models. Further, novel metrics from remote sensing are explored for purposes of modelling growth, thus demonstrating how such modelling might be cost-effectively used in practical forestry.

3. Material and Methods

3.1 Articles I & II

3.1.1 PrognAus

Developed in the early 1990s as a response to rapidly changing management practices across Europe, *PrognAus* aimed to provide inventory projections across both even- and uneven-aged mixed forest stands (Sterba & Monserud, 1996). The growth module of *PrognAus* therefore absconds both age and site index as independent variables, since these translate poorly to uneven-aged forests (Ledermann, 2006). N.B. *PrognAus* employs a direct estimation of increment, rather than a potential growth approach, e.g. Kahn (1994), or Newnham (1964).

Initially the growth module was composed of functions for basal area increment (Monserud & Sterba, 1996), height increment (Hasenauer, 1999; Kneeling, 1994; Schieler, 1997), crown-ratio (Hasenauer & Monserud, 1996), mortality (Monserud & Sterba, 1999), and later also ingrowth (Ledermann, 2002).

PrognAus continues to be actively developed today. The latest version of the growth module of *PrognAus* includes a climate-sensitive basal area increment function (Vospernik, 2021), and an updated height increment model (Nachtmann, 2005). The climate-sensitive basal area increment function was an important basis for the studies presented in papers I and II.

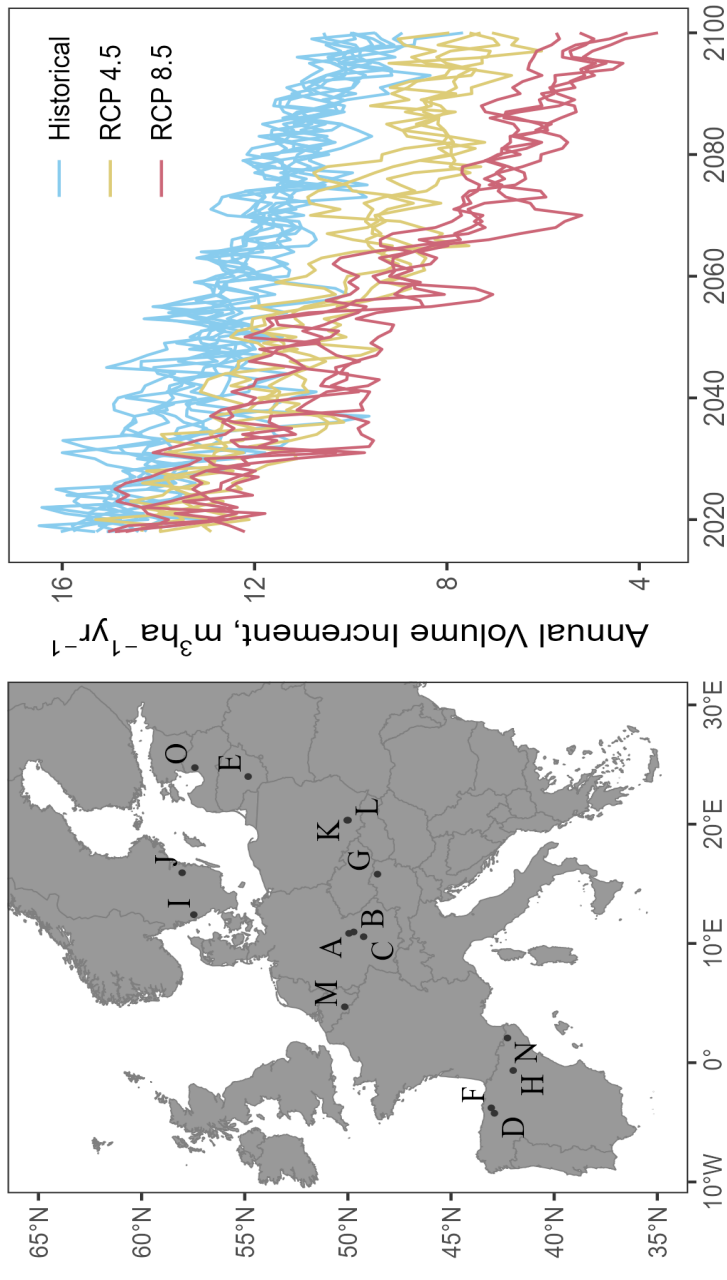

Figure 7. Left: Triplet locations used in papers I and II. Right: Example of projections of a single stand at one of the triplet locations highlighting differences between choice of climatic scenario and GCM.

3.1.2 Forecasts for Triplet Sites

In connection with the ERA-Net SUMFOREST project REFORM (*Resilience of FORest Mixtures*), a subset of inventoried triplets[18] (23/36) were chosen to be forecast under climatic conditions given by a set of historic and future scenarios. Each triplet contained three plots on similar site conditions: one plot each from monospecific stands of *P. sylvestris* and *Quercus spp.*, and one mixed species stand (fig. 7, left facet).

These triplets have previously been included in a series of studies *i.a.* exploring species mixing effects on growth (Pretzsch *et al.*, 2020), drought response (Steckel *et al.*, 2020), influence of competition and climate on annual diameter growth (Vospernik *et al.*, 2023), and impact of thinning and species mixing on productivity (Engel *et al.*, 2021).

Based on data from individual trees on the triplet sites, we then forecast the standing volume at year 2100.

3.1.3 Linear Mixed Model

In paper I, a linear mixed model was used for summarizing the results in terms of the standing volume in year 2100 from the forecasts with *PrognAus*. Predictor variables in the model were latitude and longitude, climate change scenarios, and variables describing stand conditions. By estimating the model parameters and interpreting the results, we were able compare potential outcomes in terms of confidence and prediction intervals.

[18] Triplet: group of three plots.

In generic form, a linear mixed model can be expressed as

$$\boldsymbol{y} = \boldsymbol{X\beta} + \boldsymbol{Zu} + \boldsymbol{\epsilon}$$

$$\epsilon \sim \mathcal{N}(0, \sigma_\epsilon^2)$$
$$\mathrm{u} \sim \mathcal{N}(0, {\sigma_\mathrm{u}}^2)$$

where $\boldsymbol{y}$ is a vector of observations of the dependent variable, dependent on one or more explanatory variables stored in the matrix $\mathbf{X}$ with respective coefficients $\boldsymbol{\beta}$. A vector $\boldsymbol{u}$ provides the estimated random effects, assigned along $\mathbf{X}$ by design matrix $\boldsymbol{Z}$. Finally, $\boldsymbol{\epsilon}$ is a vector of random error terms. The random effects, $\boldsymbol{u}$, were included for handling the problem that three stands were located at each site, and thus the observations were not independent. The random effects were assumed to be independent from the random error terms**.** Both the random effects and the random error terms were assumed to be normally distributed, with constant variance within each group.

To estimate the parameters and variance of the linear mixed model by Restricted Maximum Likelihood we used the package `lme4` [v. 1.1.33] by Bates *et al.* (2015).

3.1.4 Confidence and Prediction Intervals

In paper I, we discuss two types of uncertainties:

i) How certain are we about the true mean standing volume at year 2100 for stands of a certain kind, as forecast by *PrognAus*?

ii) How certain are we about the true value of the standing volume for a single stand at year 2100, as forecast by *PrognAus*?

iii) With what certainty might a single unobserved plot in the year 2100 of a species, mixture from our sample achieve at least the median volume of a second species mixture?

For case (i) we can construct a *confidence interval*, which is a stochastic interval that in a certain proportion (e.g. 95%) of repetitions of an experiment contains the true mean value. For case (ii), we can construct a *prediction*

interval, which is a stochastic interval that contains the true value of an individual stand in a certain proportion of repetitions. To further illustrate the difference, an example by Haman & Avery (2017) is rephrased below:

> To show off the breaks on your fast new car to your friends, in a daredevilish manoeuvre you drive towards a steep cliff, planning to hit the brakes at the last second. Unbeknownst to your frightened friends, you have done some calculations beforehand. You assure them – don't worry! I'm 95% certain that the average stopping distance at our speed is less than the distance to the cliff! Your friends start screaming *louder*. Realising your mistake, you quickly correct yourself – I'm 50% certain that *our* stopping distance will be shorter than the distance left to the cliff!

Returning to paper I, let us break down the statistical issue at hand. Some different sources of uncertainty exist in the model. First, there exists an uncertainty about our parameter estimates. From the sample data and regression analysis, we obtained the BLUE[19] point estimates of our fixed effect coefficients, $\hat{\beta}$. That means that for given covariates, $\boldsymbol{X_i}$, we estimate the mean outcome as

$$\hat{y}_i = \boldsymbol{X_i}\widehat{\boldsymbol{\beta}}$$

Since our model does not perfectly describe the real world – there is residual variation not explained by our feature variables which we assumed to be normally distributed $\epsilon \sim \mathcal{N}(0, \sigma_\epsilon^2)$ and shared between our different species mixtures.

By adding a random variable from this distribution, ϵ_i, we generate new responses for each data point to get a simulated values of our *n* observations, $\mathbf{Z} = \{z_i, z_{i+1}, \ldots, z_{n-1}\}$, where each $z_i = \boldsymbol{X_i}\widehat{\boldsymbol{\beta}} + \epsilon_i$. We retrieve the statistic of interest (the mean outcome) and repeat the process 10'000 times to get an approximation of the distribution of the mean of the outcome, our *confidence interval*, for which we retrieve a useful metric reflecting the range in which the mean outcome might lie with some level of certainty, e.g. 95%

[19] Best Linear Unbiased Estimates

confidence interval (2.5th and 97.5th percentiles). Since our errors are normally distributed, we get a symmetric distribution.

To get the prediction interval, we must also consider the random-effects $\boldsymbol{u}$. If we are interested in predicting an unobserved observation from our subjects, we utilise the estimated random effects. Our simulated responses then become $z_i = X_i\hat{\beta} + Z_i u_i + \epsilon_i$. For an observation from a new unobserved subject, we would increase the variability further by drawing a value from the distribution of the random effects as we did for the residual error.

In paper I, we specifically ask with what probability a new observation from one of our subjects of a certain kind (*mixture, climatic scenario, latitude, longitude, age, volume, stem density...*) would be expected to achieve a standing volume in year 2100 of *at least* the mean of a second group. This reflects the overlap of the respective empirical cumulative distribution functions and helps a forest manager understand how often we expect this would occur. For example, under the RCP 8.5 future climatic scenario at latitude 42°N we expect, based on our simulated sites, that the standing volume of a *Q. spp.* stand (as projected by *PrognAus*), would achieve at least the mean of a mixed stand of *Q. spp.* and *P. sylvestris* in 68.46% of cases.

3.1.5 Generalized Linear Mixed Model

Before we move on to the second paper, we must first introduce the generalized linear mixed model,

$$\boldsymbol{\eta} = \boldsymbol{X\beta} + \boldsymbol{Zu}$$
$$g(\mu) = \eta$$
$$y \mid u \sim Exponential\ Family(\mu, \phi)$$
$$u \sim \mathcal{N}(0, G)$$

The GLMM is an extension of the LMM by means of a link function $g(\cdot)$ relating the mean to the linear predictor η ('eta'). Our independent variable y conditioned on the random effects u follows a distribution from the

exponential family with mean μ and dispersion ϕ ('phi'). The random effects are normally distributed with covariance matrix **G**.

3.1.6 Generalised Additive Mixed Model

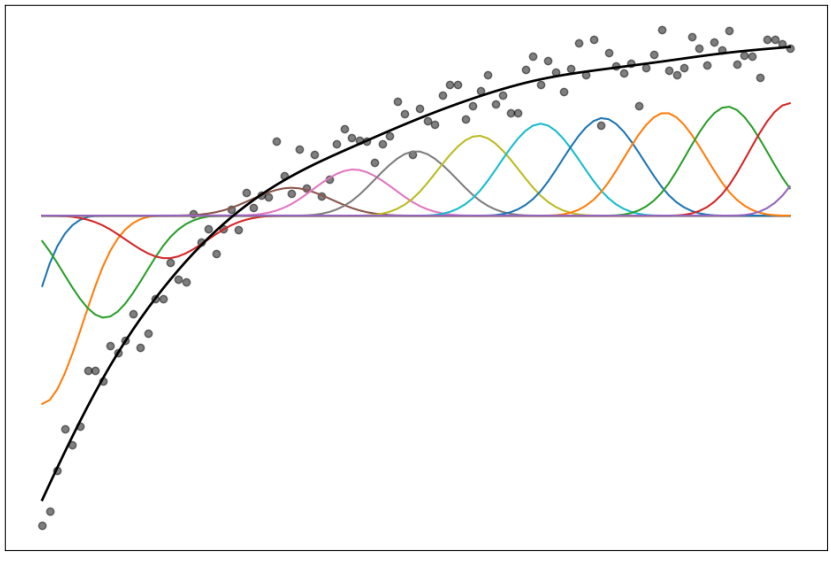

Figure 8. Penalised B-splines (solid, colored lines) about an intercept are summed to estimate a trend in data points (solid black line).

Kolmogorov-Arnolds' representation theorem allows for the representation of many useful continuous multivariate functions as the sum of a group of univariate functions (Arnold, 1957; Kolmogorov, 1956). For an intuitive conceptual image, see fig. 8.

Let's express the approximated solid black line in fig. 8 a *'smooth'* function *f(x)* we would like to approximate. The *smooth* is the sum of a number *k* of a simpler function *b(x)* such as in fig. 8, which have different placement, size or other attributes, weighted by β:

$$f_i(x) = \sum_{j \in k} \beta_{ij} \cdot b_{ij}(x)$$

Just like the GLMM, we can then state that we want to approximate the behaviour of our independent variable y by adding together groups of functions:

$$g\big(\mathrm{E}(\mathrm{Y})\big) = \alpha + \sum_{i\in 1} f_{i(X_i)} + \varepsilon,$$

$$y \mid u \sim Exponential\ Family(\mathrm{E}(\mathrm{Y}), \phi)$$
$$u \sim \mathcal{N}(0, G)$$

As is now clear, we are relating the mean of Y, μ, to the linear predictor η by our link function $g(\cdot)$

In fig. 1C, the relative growth rate of a sigmoidal trajectory drops very rapidly and then flattens out towards an asymptote (separate from zero). We thus expect that random samples of age from a uniform distribution will have a density of instantaneous relative growth rates of gross volume which is strongly right skewed and strictly positive. Among the family of exponential distributions, one suitable distribution for modelling such data is the *Gamma* distribution.

$$if: X \sim \mathbf{\Gamma}(\alpha, \beta)$$
$$\text{where: } \forall x \in X, x > 0$$

then the probability density function of observing x is:

$$f(x) = \frac{\beta^{\alpha}}{\Gamma(\alpha)} \mathrm{x}^{\alpha-1} e^{-\beta x}$$

where the gamma function, $\Gamma(\cdot)$, is Johann Bernoulli's analytic continuation of the factorial function.

It is important to consider that the skew of the gamma distribution now causes the variance of our response to scale with the square of the expected value:

$$Var(Y) = \frac{\mu^2}{\alpha}$$

In paper II, we express the annual growth rate (*GR*) of a species-mixture as the product of a term relating the average growth rate for the given species-mixture at a given gross volume production and age, the offset from this average for a particular plot, and modification of the average by some 4-dimensional interaction between climatic variables (total precipitation and temperature of the current and previous growth periods).

We express this in terms of a GAMM, with the index m referring to species mixture, l to time point and q to plot, as:

$$ln\left(E\left(GR_{mlq}\right)\right) = \boldsymbol{Z_{mq}b} + \beta_{m0} + f_{m1}\left(\boldsymbol{\beta}_{m1}, \boldsymbol{X}_{mlq1}\right) + f_{m2}\left(\boldsymbol{\beta}_{m2}, \boldsymbol{X}_{ql}\right)$$

$$\boldsymbol{X}_{mlq1} = \left\{Volume_{mlq}, Age_{mlq}\right\},$$

$$\boldsymbol{X}_{ql} = \left\{ Prec_{ql}, Prec_{ql-1}, Temp_{ql}, Temp_{ql-1}\right\}$$

$$\boldsymbol{b} \sim \mathcal{N}(0, \psi)$$

$$GR_{mlq} \sim \boldsymbol{\Gamma}\left(E\left(GR_{mlq}\right), \phi\right)$$

Here, $ln\left(E\left(GR_{mlq}\right)\right)$ is the log-link transformation of the expected value of the growth rate. About our species-wise (m) log-averages β_{m0} is a species mixture specific intercept, $f_{m1}\left(\boldsymbol{\beta}_{m1}, \boldsymbol{X}_{mlq1}\right)$ is a smooth function involving stand conditions in terms of volume and age, $f_{m2}\left(\boldsymbol{\beta}_{m2}, \boldsymbol{X}_{ql}\right)$ a smooth function involving precipitation and temperature conditions during the years l and l-1. The random site effects, $\boldsymbol{b}$[20], were assumed to be normally distributed, with a diagonal covariance matrix ψ ('psi'). The response variable values were assumed to follow a gamma distribution, because they

[20] Note that I denote the weights '*b*' rather than '*u*', a subtle reference to that our random effects are parametric values of a spline penalised w.r.t. to the chosen variance.

cannot be negative. Our first *smooth* $f_{m1}(\boldsymbol{\beta}_{m1}, \boldsymbol{X}_{mlq1})$ is then the offset from the log-average growth rate incurred by the current combination of gross volume production and age of species *m* in period *l* and plot *q*, and our second *smooth* $f_{m2}(\boldsymbol{\beta}_{m2}, \boldsymbol{X}_{ql})$ the offset reaction by species *m* expected from our climatic variables in that plot (*q*) and year (*l*). The final model was fit by *fREML* as implemented in `*mgcv*` (Wood, 2011).

Growth has often been considered as the multiplicative product of several correlated factors (Baule, 1917; Mitscherlich, 1909)[21]. Because of the multiplicative relationship between terms in a model with a log-link, reasoning around the effects of the different components of the generalised additive mixed model is straightforward. An example is given below.

> The average growth rate of a certain species mixture is 3%. This plot grows 1.03 times as well as our plots on average. The current combination of gross volume produced at the beginning of this period and this age means we expect the years' growth rate to be thrice the species average across all studied ages. However, weather has been somewhat poorer than average, inducing a 20 percent deficit. Our expectation of the growth rate for our species and plot in the given year thus becomes 0.03 x 1.03 x 3 x 0.8 = 7.42%.

[21] Mitscherlich postulated that the returns of a fertilisation (*bone flour*) is proportional to the difference between a current and maximum level of production (law of diminishing returns).

Figure 9. Overview of the study locations and plots for papers III (Svartberget Experimental Forest) and IV (Remningstorp Estate). Solid black line in the subplots on the right correspond to LiDAR coverage from a single year. CRS in subplots corresponds to SWEREF99 TM.

3.2 Articles III & IV

3.2.1 Data from the Krycklan Catchment

During the fall and spring 2014-2015 and 2019-2020 10-meter radius survey plots distributed across Svartberget Experimental Forest (fig. 9, top-right facet) along a 350-m square grid were (re-)inventoried by field workers. Using a Haglöf POSTEX™ DPII system coordinates were recovered by ultrasound multilateration for each tree with a diameter larger than 4 cm. Height measurements from a laser rangefinder, e.g. with the Haglöf VERTEX™ series, were carried out for a subjective sample of trees reflecting the diameter distribution for each plot.

In connection with the field inventories, airborne laser scanning (ALS) campaigns were conducted with fixed-wing aircraft from an altitude of 1'000 meters with Optech Titan X (2015) and Riegl VQ-1560i-DW (2019) instruments. This resulted in an average point density of 20 points/m^2 for both campaigns, from which the data were aggregated into 10x10 m raster cells.

The height for each tree was imputed from its diameter using plot, species-level models fit to the sampled heights. The height data were used to calculate *Lorey's mean height* (h_L), i.e. the basal area weighted mean height, for each plot.

Forest management in early stages of stand development in the region is dominated by low-grading, which thus has limited impact on the dominant trees. Thus, when considering measurement series of Lorey's mean height '*false growth'* may occur as a result of thinning , wherein the basal-area weighted mean height is increased as a result of thinning (Eide & Langsaeter, 1941; Wiedemann, 1937). However, the practical impact of such false growth was assessed to be of limited importance in this study. In total, 337 sample plots were retained after filtering due to inappropriate grid placement,

e.g. plots being located outside forested areas, or due to decreasing Lorey's mean height between consecutive measurements.

At this point, h_L was preferable to dominant height as internal testing with our dataset showed a stronger correlation between h_L and our point cloud metrics (not published). To relate the laser point cloud metrics to Lorey's mean height, a simple stepwise multiple linear regression using the available LiDAR metrics was performed separately for each campaign. Final models for both the 2015 and 2019 campaigns included the 95th height percentile (P95) of the returns, the standard deviation of the height metric of the returns, and interactions between the aforementioned. The coefficient of determination R^2 for both models was about 95%.

3.2.2 Site index estimation

Site Index is typically defined as the expected mean height of the one hundred coarsest stems at breast height per hectare at a reference age, e.g. 100 years total age. Note that it does not (!) refer to the development of any single stem. Development of any individual stem can vary significantly, e.g. figure 10.

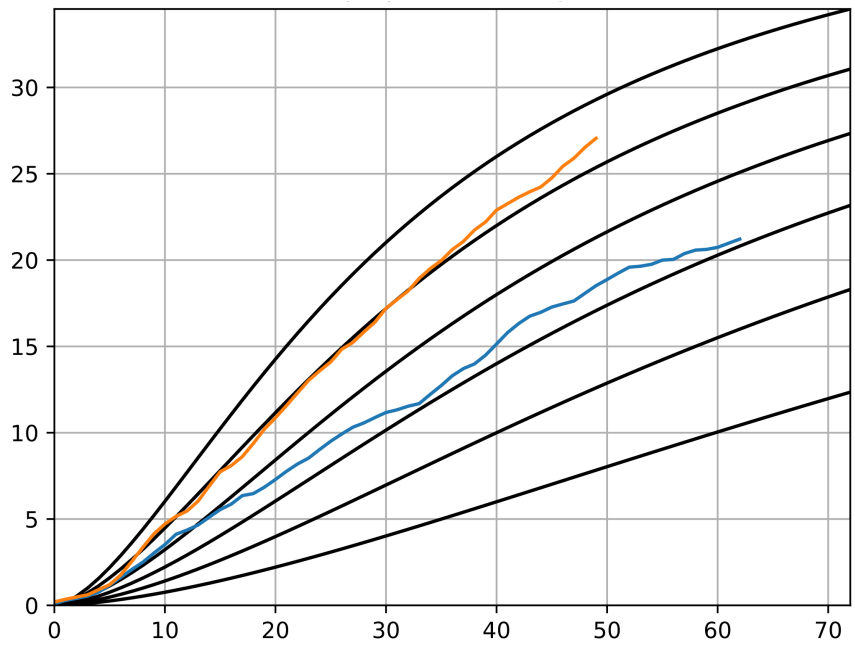

Figure 10. Development in height (meters) over total age of two stem-sectioned Norway Spruce from Oslo municipal forests (orange, blue solid lines) contrasted against dominant height trajectories in Norway Spruce plantations from Elfving (2003).

Following Elfving & Kiviste (1997), true growth functions should fulfil the following criteria:

i) have a zero-point
ii) be increasing
iii) have an asymptote parallel to the abscissa
iv) have a single point of inflection.

From growth functions fulfilling these criteria, we can retrieve systems of yield curves which are either anamorphic (scaled variants) or polymorphic[22] (curves which are not a simple rescaling of each other).

[22] Polymorphic curves, since they are not a simple re-scaling of each other, can be disjoint (non-overlapping) or non-disjoint (overlapping). Non-disjoint systems may be typically treated as resulting from covering several underlying physiographic regions.

A favourable sigmoidal equation passing through the origin is given by the Chapman-Richards yield curve, where $Y>0$ is the variable which we are specifically interested in (e.g. volume or height)

$$Y = A\left(1 - e^{-kt}\right)^{\frac{1}{1-m}}$$

where $t>0$ is age, and A, k and m are parameters. It can be noted that $\lim_{t\to\infty} Y(t) = A$, and thus A is the asymptote. Further, it can be shown that $k>0$ is the rate of growth at the inflection point, and $m>0$ governs the position of the inflection point. m is by some authors (following v. Bertalanffy 1938) preferred to approximate 2/3, but this is variable and dependent on the models' raison d'être (Zeide, 1993). Overall, no single value may fit all use-cases (Renner-Martin *et al.*, 2018).

The yield form can be solved for t, whereby an age-independent difference equation is established, e.g. Tomé *et al.* (2006):

$$Y_{i+a} = A\left(1 - e^{-ka}\left[1 - \left(\frac{Y_i}{A}\right)^{1-m}\right]\right)^{\frac{1}{1-m}}$$

In this equation, a is the interval between measurements at time points i and $i+a$.

In determining site productivity, large differences between sites are likely to be found in terms of A, i.e. this parameter may provide a useful proxy for site productivity, and it should thus be strongly related to site index, e.g. Nord-Larsen & Johannsen (2007).

For an anamorphic system where the parameters k and m are not dependent on A, we can express k as:

$$k = \frac{-1}{a} ln\left(\frac{1 - \left(\frac{Y_{i+a}}{A}\right)^{m}}{1 - \left(\frac{Y_i}{A}\right)^{m}}\right)$$

This is a complex relationship, relating the attained fractions of the maximum to the observed growth for a time units at an average growth rate

e^{ka}. The hyperbolic expression passes through (1, 0) when $\frac{Y_{i+a}}{Y_i} = 1$ and rapidly flattens out for quotients > 1. To estimate *A* for different sites without resorting to optimisation routines, we can approximate *k*, which as independent of *A,* is proportional to the observed rate of growth e.g.: $k = b\left(\frac{Y_{i+a}}{Y_i}\right)$ [sic!][23] as utilised in paper III, yielding a coefficient of b = 0.021 (strongly unresponsive to change).

Having estimated a relationship for *k* where we directly parametrised for a global *b* (0.021)*, A* (26.99) and *m* (0.57), assuming that *b* and *m* are invariant of *A* and of time, we can solve for *A* (denoted A_o when estimated thus) whenever a repeat observation is available, i.e.

$$A_o = \left(\frac{Y_{i+a}^m - e^{-ka}Y_i^m}{1 - e^{-ka}}\right)^{\frac{1}{m}}$$

The local asymptote A_o for each 10x10 meter pixel across the 68 km^2 Krycklan catchment area was estimated based on laser data for the two time points. The site productivity measure was based on Lorey's height, as initial assessments had shown that this measure could be assessed with less variability compared to top height.

The relationship between A_o and other metrics could thus be assessed, such as depth-to-water (Beven & Kirkby, 1979), terrain-wetness-index (Murphy *et al.*, 2008), down slope index (Hjerdt *et al.*, 2004), slope or elevation. Specifically in this study, the relationship between A_o and estimates from the SLU soil wetness map (Ågren *et al.*, 2021) was evaluated. This map provides the probability, for each map unit in a landscape, of the soil being classified as "wet" according to the system used in the Swedish National Forest Inventory. It was initially intended to distinguish between 5 soil moisture classes ('*Dry', 'Mesic', 'Mesic-Moist', 'Moist', 'Wet'*) used by the Swedish NFI, but a two-class binary choice (*'Dry'* or *'Wet'*) model was found to be the most accurate. Rather than classifying the site, the probability of a pixel being classified as *'Wet'* by the ensemble is presented for the Swedish forested landscape (ibid.).

[23] See discussion.

3.2.3 Remningstorp Estate Inventory

The Remningstorp Estate, situated c. 13 km north-east of the locality Skara, is owned and run by the Hildur and Sven Wingqvist[24] Foundation for the express purpose of developing a *'forest laboratory and research institute'* (Ahlberg & Kardell, 1997). The estate today encompasses an area of ~16 km^2 (including lakes), generating an estate average (1996) of 9.4 m^3 wood $ha^{-1}yr^{-1}$ (ibid.). Thus, the average site productivity is high. The forests are dominated by Norway spruce.

During 2014, 2019 and 2021 complete inventories (DBH > 4 cm) of 41 80x80 metre plots were carried out. For each tree, the position, cross-calipered diameter, and species was recorded. For each site, site index (Hägglund, 1972, 1973, 1974) was estimated from observations of vegetation type and other site properties (Hägglund & Lundmark, 1977; Lundmark, 1974). Sample trees were selected for height measurements. The basal-area weighted mean diameter of each tree was calculated from the cross-calipered diameters. A global diameter-height function (Näslund, 1936) was fit across all species.

High-density airborne LiDAR scanning campaigns were conducted in connection with the field inventories, resulting in mean pulse density per square meter of 26.3 (2014) and 59.9 (2021). From the LiDAR point clouds, metrics were calculated using the R-package *lidR (*Roussel *et al.*, 2020; Roussel & Auty, 2024). The metrics were normalized using a spatial interpolation algorithm based on Delauney triangulation (*lidR::dtm_tin*), and a digital terrain model (DTM) developed by rasterization of the same. Tree objects were identified by the *lidR* implementation of Dalponte & Coomes method (2016).

For each inferred tree, LiDAR metrics such as the 0^{th} to 100^{th} percentiles by steps of 5; the mean, standard deviation, skew, kurtosis, entropy, etc. were computed. Further, we retrieved the convex hull volume of each delineated

[24] Inventor of the multi-row self-aligning ball bearing and one of the founders of AB SKF *'Swedish Ball Bearing Factory'*.

tree object, the ground cover area of the hull, and the central positions elevation as recovered from the DTM.

3.2.4 Modelling Individual Tree Growth

Once the field-inventoried subplots for a single inventory have been properly oriented against a spatially coherent reference material (e.g. from ALS), the remaining inventories can be properly aligned against the initial reference. However, due to field-errors, analysis was considerably complicated, see appendix I.

Growth series of single trees are then established by spatially aware pairwise comparisons between adjacent inventories considering potential positioning errors remaining in the aligned data, species, and change in diameter. Trees with no successful match between adjacent inventories were iteratively compared to inventories with intermittent re-inventories to, e.g., capture trees which were overlooked during the intermediary inventory period. Obviously, a tree which has been identified in any two inventories must have been present during the interval. For the same reason, a tree of a sizeable diameter should have previous records. This may not be true for small trees which have only recently exceeded the lower limit for measurement (ingrowth). The case where trees *disappear* is more complicated. It is not obvious whether the tree has inadvertently been excluded by human error or, the tree has been cut and subsequently removed from the stand.

We are left with a *sparse* dataset, with many unobserved records.

Defining which trees have been subject to an edge-effect is equivalent to deciding at which distance from the concave hull of the inventoried stand competition, or the absence of such, from out-of-plot stems becomes negligible. This affects the amount of eligible data points when optimising the competition index function.

After creating series of diameter development from the field inventory, and corresponding crown development series from the LiDAR data, these were merged and the resulting records considered to constitute growth series of individual trees.

Since only sample trees were measured for height, we fit a simple linear model to all *P. abies* stems to adjust the 95th percentile of the return points from each tree to the field measured height, which captured about 74% of the variation about the mean:

$$Height_m = 4.22 + 0.9 \cdot ZQ_{95}$$

With diameter and height for each tree, we calculated the volume of each stem as per Brandel (1994). In total, there were 458 *P. abies* trees which increased in calculated volume between 2014 and 2021.

To explore whether LiDAR metrics could contribute to the prediction of the volume increment, we fit 3 separate models: one model with only field measures, one containing LiDAR metrics only, and one containing information from both.
We modelled this increase with a generalized linear mixed model, assuming the errors to be Gamma distributed, and enforcing predictions to be strictly positive by using a log-link to transform the mean. We included a simple random intercept per plot.

4. Results

4.1 Article I

Decreases in the mean standing volume at the end of the simulation period (year 2100) in unmanaged, single canopy stands of *Quercus spp., P. sylvestris* and mixtures between the two species are expected under both future climatic scenarios investigated (RCP 4.5, RCP 8.5) across a wide range of European latitudes (fig. 11) For all stand types, the largest losses are incurred between a moderate RCP 4.5 scenario and the historic reference. For *P. sylvestris*, the more exacerbated RCP 8.5 scenario entailed an almost doubled decrease relative that of the RCP 4.5 scenario to the historic expectation. *Quercus spp.* stands showed limited responses to the additional climatic change induced under the RCP 8.5 scenario (fig. 12).

Note that despite stronger relative losses, *P. sylvestris* is still a strong contender compared to *Quercus spp.* on the same sites. Under the RCP 8.5 scenario, the chance of drawing a new unobserved *P. sylvestris* plot, at a latitude of 42 °N from our group of plots, which achieves at least the mean of that of *Q. spp.* is 95.5%. This should not be misinterpreted as a statement that this is true for any site productivity.

At lower and median latitudes (42 °N / 50 °N), admixing *Q. spp.* stands with *P. sylvestris* becomes a less attractive alternative with increasing

scenario severity. *Dominance*[25] of *Q. spp.* against mixed stands of *Q. spp.* and *P. sylvestris* is incurred during a shift from the historic scenario to RCP 4.5 (42°: +10.26 p.p., 50°: +9.5 p.p.). Positive change in dominance is even stronger under RCP 8.5 when compared to the historical scenario (42°: +23.55 p.p., 50°: +23.21 p.p.).

At 58 °N, *Quercus spp.* even achieves a moderate dominance over *P. sylvestris* (68.10 %) under RCP 8.5, a total of +46.48 p.p. increase in dominance compared to the historical scenario. The odds of drawing an unobserved *Q. spp.* stand from our plots which achieves at least the mean of our *P. sylvestris* stands has become 7.74 times as likely:

$$\left(\frac{0.2162}{1-0.2162}\right)^{-1} \cdot \left(\frac{0.681}{1-0.681}\right) - 1 \approx 7.74$$

[25] Percentage of new observations which would achieve at least the mean of another category. Always referred to from the stronger contestant.

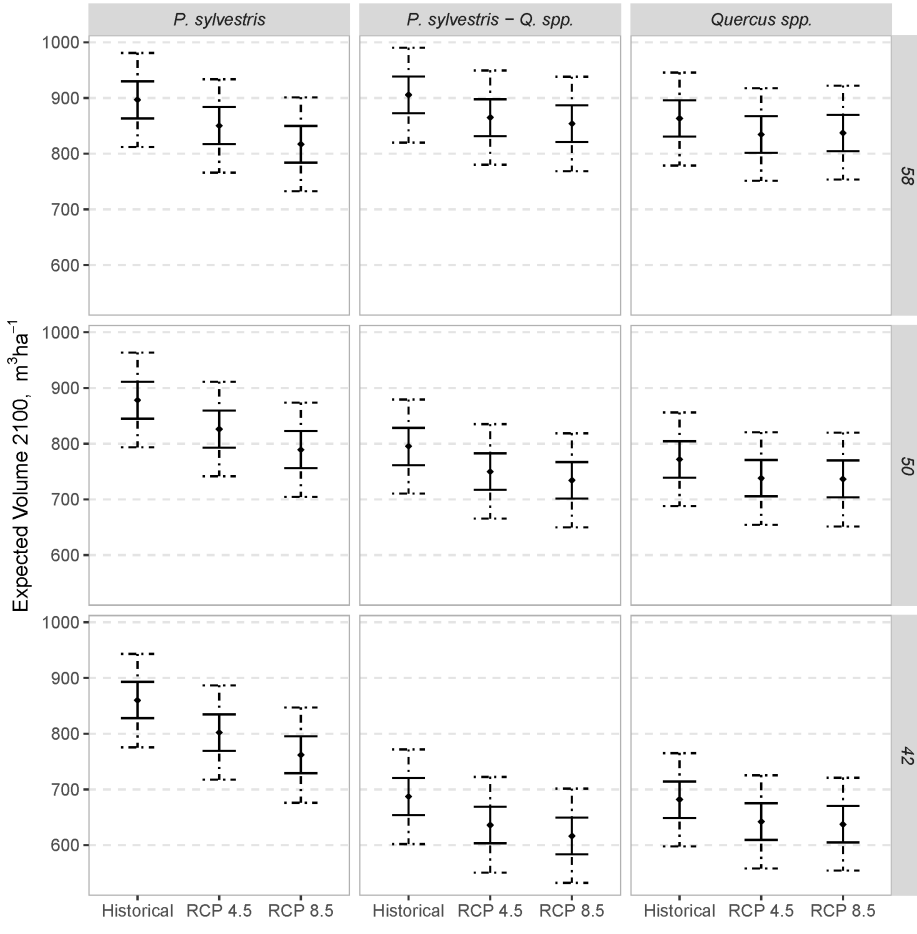

Figure 11. Expected standing volume at year 2100 by stand type, (minimum, median and maximum) latitude and climatic scenario. Solid bars: confidence interval. Dashed bars: prediction interval.

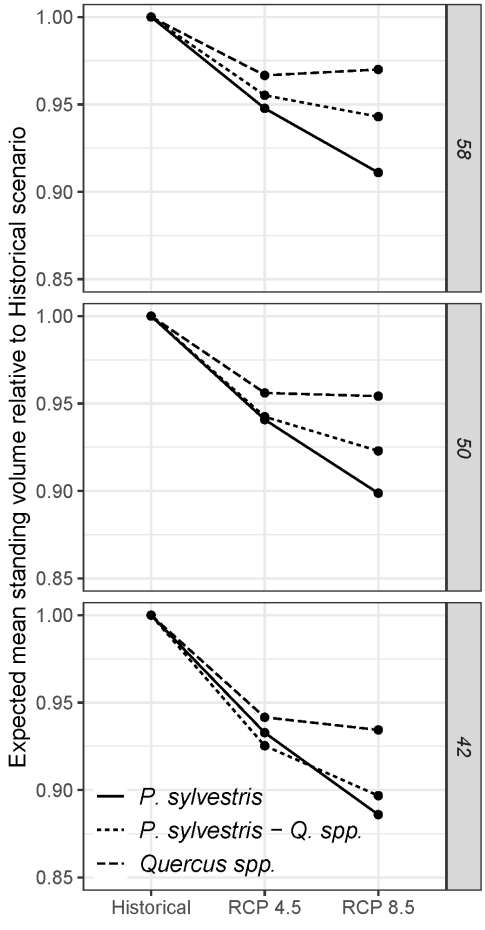

Figure 12. Resilience to scenarios of climatic change by stand type and (minimum, median and maximum) latitude.

4.2 Article II

In paper II, we used a static reduced model to present the general results from paper I in a spatially explicit context across Europe. Fig. 13 compares the ratio of end-of-period gross volume production between the future climatic scenarios (2018-2100) and their historical counterpart (1923-2005).

Note the expected increases in gross volume production of *Q. spp.* in the Mediterranean cluster (cf. fig. 14): the intermediate lowlands of Castilla & León to the south of the Cantabrian Mtn. chain, along with the coastline along the Bay of Biscay, the Danube Delta and lowland plains of southern Romania, the Pannonian plain, and regions of Italy & Greece (fig 13). This is caused by a weak (<10 percentage points) positive gain in the annual climatic response of *Q. spp.* to the average weather of the region up until about 2065 (fig. 15). In the far future beyond this point, rapid decreases are expected (c. 25-30 p.p.) for *Q. spp.* under RCP 8.5, likely associated with continued temperature increases past 15 degrees Celsius (annual mean of the monthly mean temperatures), whilst the positive gain is retained under RCP 4.5 (fig. 15).

P. sylvestris is unable to cope with this climatic change, and an ongoing decline since 1980 is continued. For RCP 8.5 the decline is -40 percentage points for 1975-2100. For RCP 4.5 it is -25 percentage points for 1975-2050. However, the volume production of the *Q. spp. – P. sylvestris* mixed stand type seems largely unaffected by the climatic change.

Declines in gross volume production by 2100 in *P. sylvestris* stands are exacerbated across continental Europe. The degree of severity is strongly latitudinally ordered. The largest declines are concentrated to land-locked lowland areas, whereas elevation can be seen to strongly alleviate declines – such as in the southern-most German states of Baden-Württemberg and Bavaria. Only limited impact to gross volume production under RCP 4.5 and RCP 8.5 is expected surrounding the southern Baltic Ocean whilst *P. sylvestris* across the northern German and Polish lowlands is more clearly negatively affected.

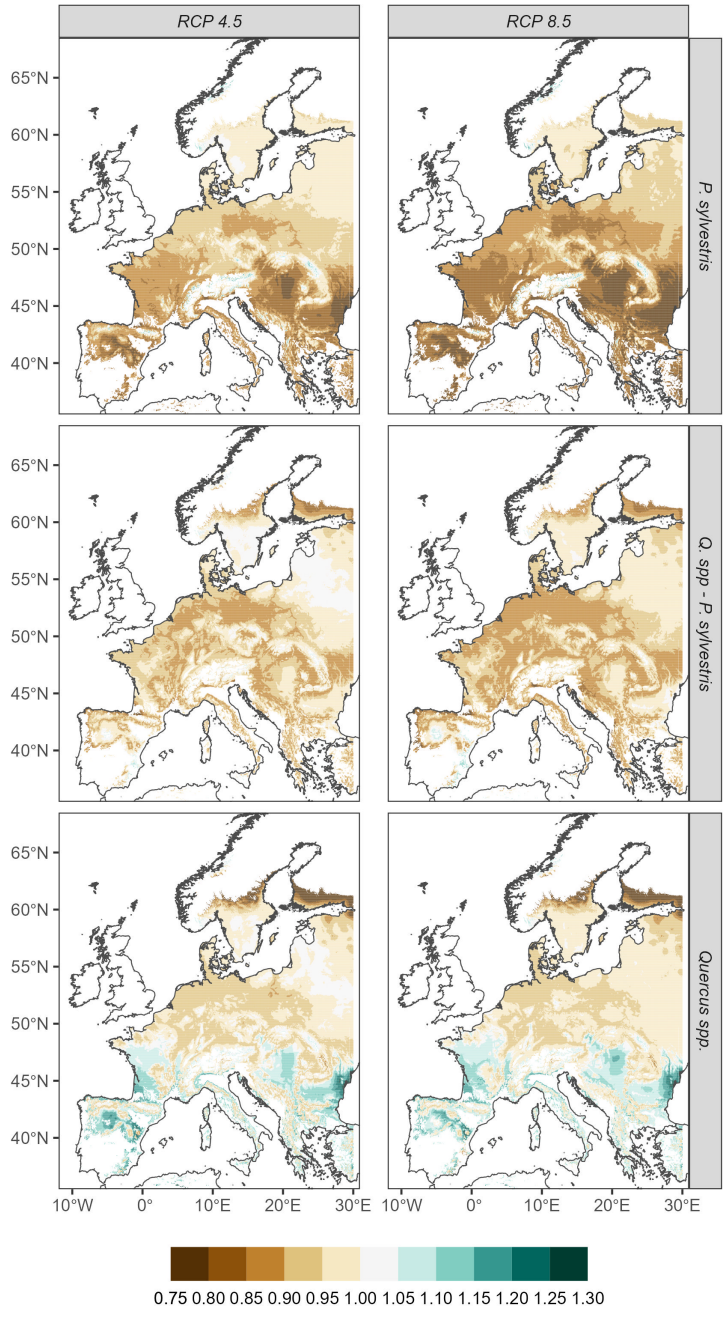

Figure 13. Ratios of end-of-period gross volume production between the two climatic scenarios for the period 2018-2100 and the historical counterpart (1923-2005)

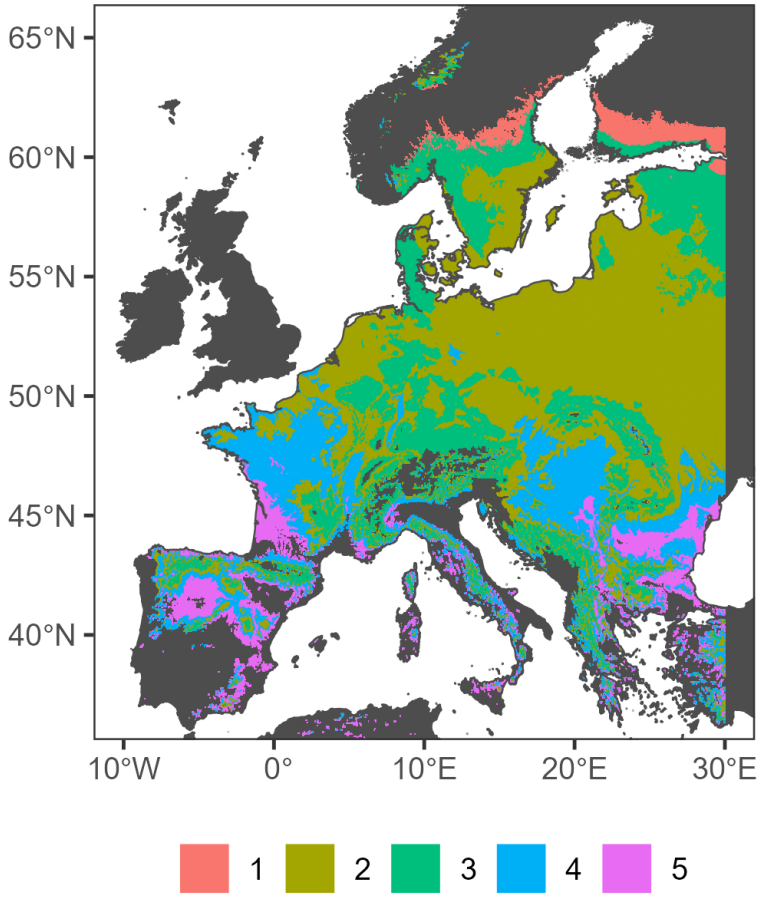

Figure 14. Clustering results from spatial predictions. 1) Boreal, 2) Continental, 3) Hemiboreal-Orotemperate, 4) Franco-Pannonian, 5) Mediterranean. Dark background for areas with climatic conditions too far from training data.

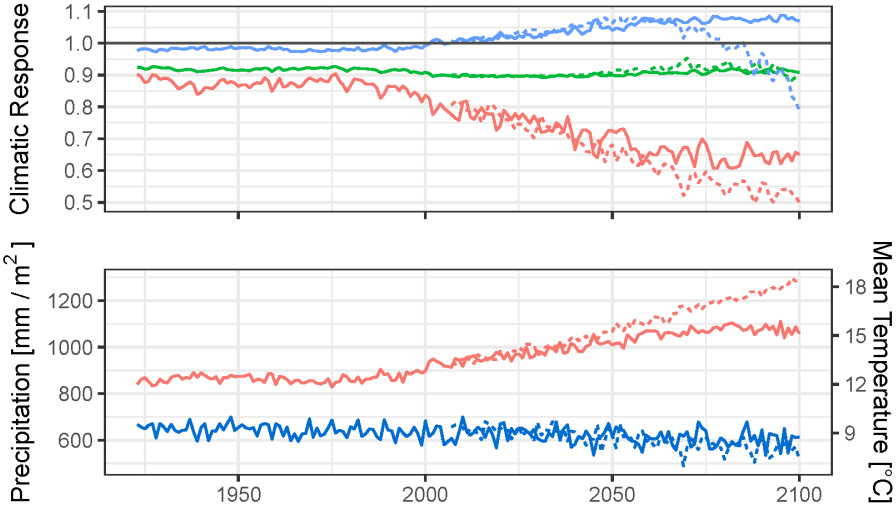

Figure 15. Mediterranean cluster. Upper facet: Climatic response term corresponding to the lower facet. P. sylvestris (red), Quercus-P. sylvestris (green), Quercus spp. (blue). Lower facet: smoothed means of the clusters mean monthly mean temperature, red (°C) and total annual precipitation, blue (mm m^{-2}). Before 2006, single solid lines show the historical development. After 2006: the solid line depicts the RCP 4.5 experiment and the dashed line the RCP 8.5 experiment.

4.3 Article III

Calculated site quality values (A_o) for each of the 337 inventoried field plots were compared with recordings of soil moisture, according to the system used by the Swedish National Forest Inventory, and soil type. Since there were large discrepancies in the representation of different classes (e.g., 251 *'Mesic'* plots and only 5 *'Wet'* plots), and non-normal within-group distributions of A_o, a Kruskal-Wallis test (Kruskal & Wallis, 1952) was conducted to identify if at least one category had a median rank different from the others. A post-hoc Dunn-Bonferroni test was applied to distinguish between sample pairs. However, judging from the wide differences in variance between groups (fig. 16) it was difficult to clearly determine whether any purported significance was indeed caused by difference in median ranks or if it was due to different variances (cf., Hart, 2001).

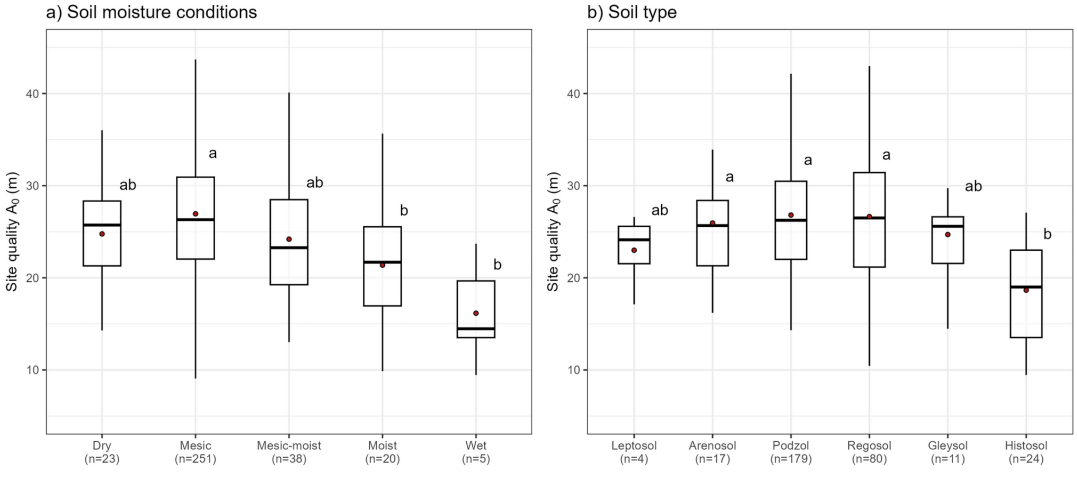

Figure 16. Box plots of calculated Ao-values for different soil moisture classes and soil types.

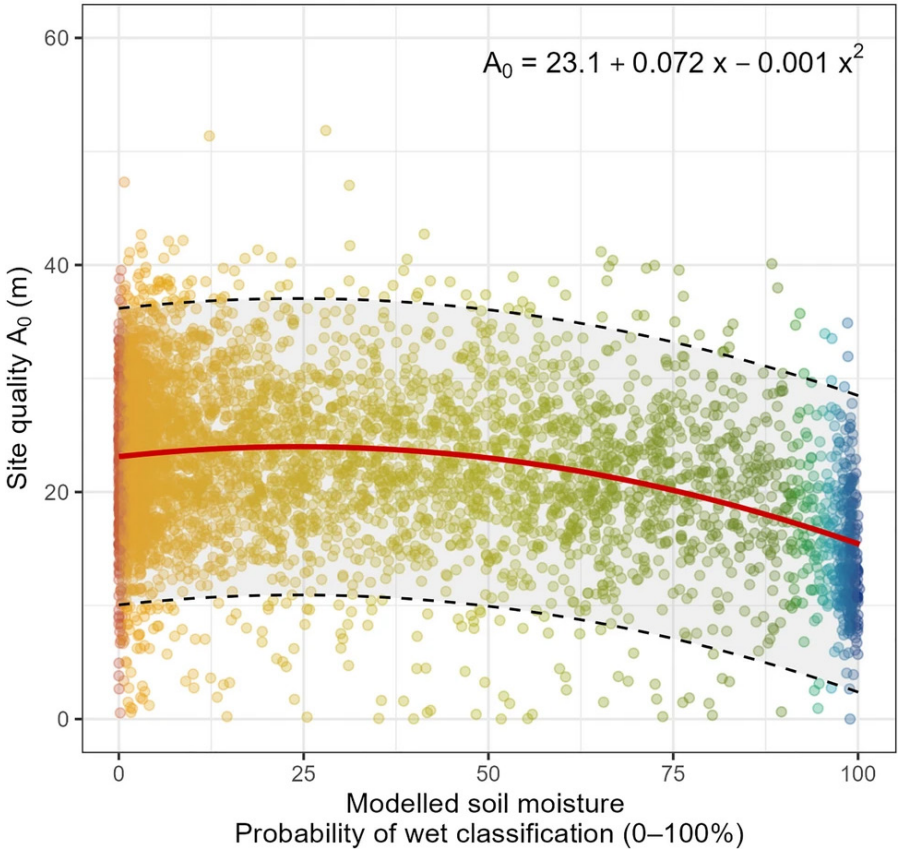

Figure 17. Ao regressed against the raw probability of a 'Wet' soil moisture classification by Ågren et al. (2021). Random subset of 5000 pixels plotted. Dashed lines denote 95% prediction intervals.

A weak quadratic trend of our estimate of site quality over modelled soil moisture was found (fig. 17), although the residual variance was very large. The probability of a *'Wet'* classification by Ågren *et al.* (2021) is not a strong predictor of site quality. A post-study example, see discussion, formulating $k = a + b*\ln(Y_2/Y_1)$ provided a 140-fold improvement in MAE, but did not lead to mentionable change in the relation shown in fig. 17 – the large variance remained; a GAM smoother demonstrated a very flat relation between the site productivity estimate out until ~90% classification confidence by Ågren *et al.* (2021), where it then drops steeply. Soil moisture conditions and soil types (fig. 16) shifted in order.

4.4 Article IV

I reiterate that article IV is still in a manuscript stage, and thus the results should be treated as preliminary. The models are as follows.
In each case, the modelled variable was $ln(Volume_{i_{2021}} - Volume_{i_{2014}})$ and the errors assumed to be gamma distributed.

Field Model:

$$\beta_0 + \beta_1 \cdot Diameter_i + \beta_2 \cdot BAL10_i + \beta_3 \cdot Diameter_i \cdot BAL10_i + \beta_4 \cdot GSI_i + \boldsymbol{Zu}$$

LiDAR Model:

$$\beta_0 + \beta_1 \cdot Height_i + \beta_2 \cdot CrownHullVolume_i + \beta_3 \cdot \Delta_{Height_i} \cdot SOL_i + \beta_4 \cdot Density_i + \boldsymbol{Zu}$$

Combined Model:

$$\beta_0 + \beta_1 \cdot Diameter_i + \beta_2 \cdot CrownHullVolume_i + \beta_3 \cdot SDR10_i + \beta_4 \cdot Height_i + \beta_5 \cdot \Delta_{Height} + \boldsymbol{Zu}$$

Here, *Diameter* is the subject trees diameter (cm) at breast height (1.3 m) in 2014, *Height* is the estimated height (m) as per the equation described in the method section from LiDAR metrics from 2014, Δ_{Height} is the difference in estimated height between 2014 and 2021, *BAL10* is Wykoff's BAL (Wykoff *et al.*, 1982), the basal area of the stems with larger diameters within 10 meters, expressed per hectare. *SOL* is the sum of the overtopping lengths of trees within 15 meters (accounting for terrain); *GSI* is the site index for *P. abies* as assessed from site factors (Hägglund, 1979); *SDR10* is Lorimer's SDR (Lorimer, 1983) within 10 meters. Density is calculated from the trees identified by LiDAR within 15 meters, expressed per hectare. The crown hull volume is the convex hull of all points in a segmented tree which are at least

2 meters above the lowest point. Finally, the random intercepts are given by vector $\boldsymbol{u}$ and assigned by design matrix $\boldsymbol{Z}$.

In the field model, only intercept and Diameter were significant variables. For the LiDAR model, intercept, Height, and Δ_{Height} were significantly different from zero. Finally, for the combined model, the same variables were significant: Diameter, Height, Δ_{Height}, and intercept.

Goodness of fit was poor for all models, which performed very similarly (RMSE ~70 dm^3).

5. Discussion

Climatic change has a wide range of impacts on forest growth and yield. The sign, magnitude and variability of the impacts are likely to depend on the investigator's timeframe for the analysis, what references are used, species choice, site type, stand composition, management regime, geographic locale, and scenario.

Throughout continental Europe, stands of *P. sylvestris* are expected to face widespread growth declines primarily because of increasing temperatures (papers I & II). Lowland sites will therefore be more likely to experience growth declines compared to sites at higher altitudes. Further, change in mean temperatures may likely be largest at high latitudes because of polar amplification (Serreze and Barry, 2011). Although not specifically investigated in this thesis, growth declines may become even more severe due to increased risks from both abiotic and biotic disturbances (Seidl *et al.*, 2017).

Throughout the southern Nordics (<60 °N), growth may be modulated by the westly influx of precipitation from the North Sea, which condenses as the result of orographic lift along the western Swedish coast and southern Norwegian coastline. As a result, the south-eastern Swedish provinces of *Smolandia, Olandia* and *Gotlandia* receive far less precipitation. In both the south-western provinces of *Hallandia, Bahusia* and *Dalia*, as well as the aforementioned easterly provinces, *P. sylvestris* may experience a decrease in annual relative growth rate of up to 20 percentage points relative the climatic baseline under RCP 8.5 – resulting in increasing difficulties in species selection as the marginal advantage of *P. sylvestris* contra *Q. spp.* is

decreased or even reversed on continental sites under the more severe future scenario.

This is in stark contrast to the Franco-Pannonian grouping, where stands of *Q. spp.* demonstrated even a moderate 10 percentage point gain in annual relative growth rate relative to the climatic baseline under both future scenarios whilst *P. sylvestris* could lose some 15 to 25 percentage points by 2100 compared to 2000.

However, also *Q. spp.* have limits to the amount of climatic stress they can tolerate. The relative growth rate for *Q. spp.* was suggested to decrease considerably during the last quarter of the century on some currently climatically advantageous sites. In some cases, even on sites where climatic preconditions for volume growth relative to the mean improved more rapidly than ditto for stands of *P. sylvestris* during the first half of the century. For example, in the lowlands of Bulgaria and the Romanian plains, the Douro River basin and foothills of the Spanish mountain chains of the central plateau, and in the Gascogne region by the Bay of Biscay.

The studies in papers I and II were conducted under the assumption that empirical growth models can be used to forecast growth under changing environmental conditions, contrary to a perception that process-based models are required for this purpose. In either approach, some admission must be made w.r.t. the genetic disposition of the studied material relative to the subject for which the model is predicting, the rate of change of soil factors, the direct impact of enhanced atm. [CO_2] or other gases such as Ozone, the level of interactions between present species, and the potential non-stationarity of these relations. As is common for forest production studies in general, all results tend to apply for stands which have been exposed to no 'acute' mortality from pests, wind- or snow-breakage - in complete disregard of what proportion of the total material is spared.

Moving on to paper III. In contrast to mainland Europe and parts of southern Sweden, precipitation has not been seen as a predominant limitation to vegetation growth in northern Sweden, including at Svartberget Research Station (Bergh *et al.*, 1999). For most of Europe, the strongest limitation to net primary production has been the amount of available solar radiation in

combination with temperature (Nemani *et al.*, 2003). However, Sprengel-v. Liebig's (Sprengel, 1828; v. Liebig, 1840) notion of a single limiting factor has been long debated, or discarded in favour of a 'law of diminishing returns' as proposed by Mitscherlich (1909) and further developed by Baule (1917).

It thus stands to reason that even though precipitation may not be the strongest limiting factor to growth in the Krycklan Catchment (the study area for paper III), nutrient mobilisation and hydrological transport by groundwater and/or run-off may have significant effects, and therefore be strongly correlated with proxy measures of site moisture, such as terrain indices. This can be exemplified by the Betsele transect (Giesler *et al.*, 1998). It is worth mentioning that whilst, for *Norway Spruce*, lateral ground water flow is positively correlated with site index, the relation is muddied by that ground water flow also increases the thickness of the eluviated soil layer – which is associated with decreasing site index (Hägglund, 1979, p. 53; Lundmark, 1974).

That article III found large variation in our proxy for site productivity both about the soil moisture conditions and the soil types is therefore hardly surprising.

Originally, we planned to use 3 field inventories (with associate ALS campaigns 2008, 2014, 2019) combined with optical satellite data. A first idea was to use a classification routine with Bayesian updating to delineate stands dominated by a single species , e.g. Axelsson *et al.* (2021). This would have been a means to develop and apply species-specific height development curves, see appendix II.

The discovery that already developed site index functions fit the data reasonably well, in combination with that H_L follows the development of the dominant height quite well over age, at least in stands of *Norway Spruce*, and particularly for lower site indices or higher ages, e.g. Assmann & Franz (1963, fig. 3), suggests that a working relationship between H_{100} and site productivity as estimated from periodic site index equations for H_L could be established, with perhaps only moderate confounding due to age.

As was also mentioned in article III (Larson *et al.*, 2024), quite a lot of variance would likely have been explainable by regressing against one of the multinomial models from Ågren *et al.* (2021), by the introduction of tree species, the application of species-separate 'site index' models, and by

translating the species-specific measures of 'site index' to some standardized expression of yield capacity e.g. MAI_{max} of *Norway Spruce* by ancillary relations presented by e.g. (Ekö *et al.*, 2008; Leijon, 1979; Mensah *et al.*, 2022).

Finally, as alluded to earlier in this thesis, the linear estimate of k will be most accurate around the average h_L growth rate (median 1.06). Other formulations could also have been used, including options such as including an intercept, relating k to $ln\left(\frac{Y_{i+a}}{Y_i}\right)$, or approximating the instantaneous growth rate $\frac{Y_2-Y_1}{a}$ and directly fitting the differential equation (Burkhart & Tomé, 2014, p. 134). Relating $k = ln\left(\frac{Y_{i+a}}{Y_i}\right)$ in a post-project investigation gave a 140-fold improvement in MAE.

However, the relationships found indicate that our approach to estimate a proxy value of site productivity from repeated LiDAR measurements is a useful method, which could be developed further by modelling the *reduction in development of an ideal* unhindered tree, i.e. by means of Bayesian hierarchical modelling such as Matsushita *et al.* (2015) or Upper Boundary Limit analysis, e.g. Tian *et al.* (2023). A height growth rate at given height approach cf. Salas-Eljatib (2020) is a promising base model which is potentially applicable to both rotation and continuous cover-type forestry, although age-trends demonstrated by Matsushita *et al.* (ibid.) may indicate that some extension of the modelled state-space is required to capture carry-on legacy effects from previous states, e.g. crown reduction.
A clear example of the potential of single-tree models developed from data derived from LiDAR campaigns is given by the competition-sensitive tree-height growth equation for *P. radiata D. Don* developed by Gavilán-Acuña *et al.* (2022) from a single ALS survey.

I further pursued the study of repeated LiDAR measurements for single trees in paper IV. In this case, the ambition was to explore the possibilities to make short-term forecasts of volume growth of single trees by incorporating LiDAR metrics in the modelling. Several metrics contributed to improving models based on field measurements only. Particularly, the introduction of a height-difference estimate, $ZQ95_{t2}$-$ZQ95_{t1,}$ between the measurements at time point 1 and 2, improved the model substantially.

It should be stressed that this study was mainly exploratory, and several issues remain to be solved before the approach might be applied in practice. Attaining a high degree of tree identification (True Positives) may likely continue to be an issue for some time, and require substantial tuning of algorithms (Dalponte & Coomes, 2016; Li *et al.*, 2012) currently implemented in *lidR* (Roussel *et al.*, 2020; Roussel & Auty, 2024) or the application of novel methods, e.g. '*SegmentAnyTree*' (Wielgosz *et al.*, 2024).

Further, we made several simplifying assumptions in the study, including that LiDAR metrics could provide height metrics for single trees close to the truth; although given the high density of returns and moderately small footprint of the utilised sensor, this may be a fair assumption (Socha *et al.*, 2020).

With ancillary repeat LiDAR data, this type of model could be utilised to update forest inventories in short-term forecasts of a kind highly demanded for tactical forest planning, and suitable for future applications in, e.g. data assimilation pipelines where new information is continuously merged with existing information (Nyström *et al.*, 2015).

Rapid and accurate information from LiDAR-based approaches is likely to continue to develop. For both scientific and operational implementations, applications of difference equations with age implicit (Tomé *et al.*, 2006) or novel methods such as that by Salas-Eljatib (2020) are likely choices. Inclusion of annual environmental variables into growth functions can be successfully conducted and are necessary to model futures under different climatic conditions.

6. Conclusion

To '*push the envelope*' means extending oneself or a system past given limits to attempt and evaluate novel ideas, even if they may appear radical. In this thesis, I have applied and evaluated two recently proposed ideas in the context of growth modelling and assessment of site productivity.

The first idea is that consequences for tree and stand growth under climate change might be explored with empirical growth models, although the traditional approach is process-based modelling. With an empirical model calibrated with data from a large climatic gradient (*PrognAus*), I evaluated the likely growth consequences of climate change for *Scots pine* and *Oak* stands across large parts of Europe. While the growth consequences were found to be mainly negative, the opposite was observed for *Oak* in some parts of south-central Europe.

The second idea is to utilise data from repeated LiDAR measurements for enhancing assessments of site productivity and growth, potentially wall-to-wall across large areas. I found that repeat LiDAR measurements were suitable for assessing site quality. In an exploratory study, I also found a promising potential for using data from repeated LiDAR measurement for improving tree-level growth models.

However, as always tends to be the case in research, further studies would be needed for assessing if the assumptions underpinning empirical modelling of growth under climate change are supported. There would also be several opportunities to further develop the proposed methods for assessing site productivity and growth based on repeated LiDAR measurements.

References

Aaltonen, V. T. (1929). Über der möhlichkeit einer bonitierung der waldstandorte mit Hilfre von Bodenuntersuchungen. *Acta Forestalia Fennica*, *34*(28), Article 28.

Abatzoglou, J. T., Dobrowski, S. Z., & Parks, S. A. (2020). Multivariate climate departures have outpaced univariate changes across global lands. *Scientific Reports*, *10*(1), 3891. https://doi.org/10.1038/s41598-020-60270-5

Agestam, E., Eriksson, H., & Hägglund, B. (1981). *En orienterande studie rörande sambandet mellan bonitet och höjdbonitet för Gran i Sverige* (3; HUGIN RAPPORT, p. 55). Royal College of Forestry.

Ågren, A. M., Larson, J., Paul, S. S., Laudon, H., & Lidberg, W. (2021). Use of multiple LIDAR-derived digital terrain indices and machine learning for high-resolution national-scale soil moisture mapping of the Swedish forest landscape. *Geoderma*, *404*, 115280. https://doi.org/10.1016/j.geoderma.2021.115280

Ahlberg, O., & Kardell, L. (1997). *Remningstorp: Från herresäte till skogslaboratorium*. Hildur och Sven Wingquists stift. för skogsvetenskaplig forskning ; Skogssällsk. [distributör].

Andrew, R. M., & Peters, G. P. (2024). *The Global Carbon Project's fossil CO2 emissions dataset* (Version 2023v43) [Dataset]. Zenodo. https://doi.org/10.5281/ZENODO.10562476

Appiah Mensah, A., Jonzén, J., Nyström, K., Wallerman, J., & Nilsson, M. (2023). Mapping site index in coniferous forests using bi-temporal airborne laser scanning data and field data from the Swedish national forest inventory. *Forest Ecology and Management*, *547*, 121395. https://doi.org/10.1016/j.foreco.2023.121395

Arnold, V. (1957). On functions of three variables. *Proceedings of the USSR Academy of Sciences*, *114*, 679–681.

Arrhenius, S. (1896a). Naturens värmehushållning. *Nordisk Tidskrift*, *14*, 121–130.

Arrhenius, S. (1896b). On the influence of carbonic acid in the air upon the temperature of the ground. *The London, Edinburgh and Dublin Philosophical Magazine and Journal of Science*, *41*, 237–276.

Assmann, E. (1961). *Waldertragskunde: Organische Produktion, Struktur, Zuwachs und Ertrag von Waldbeständen*. BLV Verlagsgesellschaft. https://books.google.se/books?id=ukJXAAAAMAAJ

Assmann, E. (1970). *Principles of Forest Yield Study: Studies in the Organic Production, Structure, Increment and Yield of Forest Stands* (P. W. Davis, Ed.; S. H. Gardiner, Trans.). Pergamon Press.

Assmann, E., & Franz, F. (1963). *Vorläufige Fichten-Ertragstafel für Bayern*. Inst. f. Ertragskunde der forstliche forschungsanstalt München. https://www.waldwachstum.wzw.tum.de/fileadmin/publications/Assmann_1963_Franz_Fi-Ertragstafel.pdf

Assmann, E., & Franz, F. (1965). Vorläufige Fichten-Ertragstafel für Bayern. *Forstwissenschaftliges Centralblatt*, *84*(1/2), 13–43.

Axelsson, A., Lindberg, E., Reese, H., & Olsson, H. (2021). Tree species classification using Sentinel-2 imagery and Bayesian inference. *International Journal of Applied Earth Observation and Geoinformation*, *100*, 102318. https://doi.org/10.1016/j.jag.2021.102318

Bates, D., Mächler, M., Bolker, B., & Walker, S. (2015). Fitting Linear Mixed-Effects Models Using **lme4**. *Journal of Statistical Software*, *67*(1), Article 1. https://doi.org/10.18637/jss.v067.i01

Baule, B. (1917). Zu Mitscherlichs Gesetz der physiologischen Beziehungen. *Landwirtschaftliche Jahrbücher*, *51*, 363–385.

Bergh, J., Linder, S., Lundmark, T., & Elfving, B. (1999). The effect of water and nutrient availability on the productivity of Norway spruce in

northern and southern Sweden. *Forest Ecology and Management*, *119*(1–3), Article 1–3. https://doi.org/10.1016/s0378-1127(98)00509-x

Bertalanffy, L. von. (1938). A quantitative theory of organic growth (Inquiries on Growth Laws II). *Human Biology*, *10*(2), 181–213.

Beven, K. J., & Kirkby, M. J. (1979). A physically based, variable contributing area model of basin hydrology / Un modèle à base physique de zone d'appel variable de l'hydrologie du bassin versant. *Hydrological Sciences Bulletin*, *24*(1), 43–69. https://doi.org/10.1080/02626667909491834

Bi, D., Dix, M., Marsland, S., O'Farrell, S., Rashid, H., Uotila, P., Hirst, A., Kowalczyk, E., Golebiewski, M., Sullivan, A., Yan, H., Hannah, N., Franklin, C., Sun, Z., Vohralik, P., Watterson, I., Zhou, X., Fiedler, R., Collier, M., … Puri, K. (2013). The ACCESS coupled model: Description, control climate and evaluation. *Australian Meteorological and Oceanographic Journal*, *63*(1), 41–64. https://doi.org/10.22499/2.6301.004

Bitterlich, W. (1984). *The Relascope idea: Relative measurements in forestry*. Commonwealth Agricultural Bureaux.

Bohlin, I., Maltamo, M., Hedenås, H., Lämås, T., Dahlgren, J., & Mehtätalo, L. (2021). Predicting bilberry and cowberry yields using airborne laser scanning and other auxiliary data combined with National

Forest Inventory field plot data. *Forest Ecology and Management*, *502*, 119737. https://doi.org/10.1016/j.foreco.2021.119737

Bontemps, J. D., & Bouriaud, O. (2014). Predictive approaches to forest site productivity: Recent trends, challenges and future perspectives. *Forestry*, *87*(1), Article 1. https://doi.org/10.1093/forestry/cpt034

Brandel, G. (1994). *Nya volymfunction för tall, gran och björk* (11; Skogsfakta, p. 10). Forest Faculty. https://www.slu.se/contentassets/3eb2b64ac79f4bd4b9b9d331d233bcae/brandel.pdf

Broman, N., & Christoffersson, J. (1999). *Mätfel i provträdsvariabler och dess inverkan på precision och noggrannhet i volymskattningar: En jämförelse mellan Näslunds och Brandels volymfunktioner, baserad på Riksskogstaxeringens provträdsdata 1988-1992* (61; Arbetsrapport). Sveriges Lantbruksuniversitet. Inst. f. skoglig resurshushållning och geomatik.

Burkhart, H. E., & Tomé, M. (2014). *Modeling forest trees and stands*. Springer.

C3S/ECMWF. (2024). *Monthly means and monthly anomalies for surface air temperature from ERA5 averaged over the global domain (0–360°E, 90°S–90°N) from 1940 to 2024* [Dataset]. https://sites.ecmwf.int/data/c3sci/bulletin/202406/press_release/tim

eseries_era5_monthly_2t_global_allmonths_up_to_june_2024.csv?utm_source=press&utm_medium=referral&utm_id=cb-june-24

Cajander, A. K. (1909). *Ueber Waldtypen*. J. Simelii Arfvingars Boktryckeriaktiebolag.

Cajanus, W. (1914). Ueber die entwicklung gleichaltriger waldbestände: Eine statistische studie I. *Acta Forestalia Fennica*, *3*, 134.

Cao, Q. V., & Dean, T. J. (2015). *Using nonlinear quantile regression to estimate the self-thinning boundary curve* (Proceedings of the 17th Biennial Southern Silvicultural Research Conference. e-Gen. Tech. Rep. SRS-203., p. 3) [General Technical Report]. U.S. Dept. of Agriculture, Forest Service, Southern Research Station. https://www.srs.fs.usda.gov/pubs/gtr/gtr_srs203/gtr_srs203-073.pdf

Cieszewski, C. J. (2005). *New flexible GADA based dynamic site equation with polymorphism and variable asymptotes* (2005–2; PMRC Technical Report, Issues 2005–2). Daniel B. Warnell School of Forest Resources, University of Georgia. https://www.researchgate.net/publication/261833993

Clark, J. S. (1990). Integration of Ecological Levels: Individual Plant Growth, Population Mortality and Ecosystem Processes. *The Journal of Ecology*, *78*(2), 275. https://doi.org/10.2307/2261112

Coops, N. (1999). Improvement in Predicting Stand Growth of Pinus radiata (D. Don) across landscapes using NOAA AVHRR and Landsat MSS

Imagery Combined with a Forest Growth Process Model (3-PGS). *Photogrammetric Engineering & Remote Sensing*, *65*(10), 1149–1156.

Copernicus Climate Change Service (C3S). (2024). *European State of the Climate 2023*. Copernicus Climate Change Service (C3S). https://doi.org/10.24381/BS9V-8C66

Crawley, M. (2007). Plant population dynamics. In R. M. May & A. R. McLean (Eds.), *Theoretical ecology: Principles and applications* (Third Edition, p. 63). Oxford University Press.

Dalponte, M., & Coomes, D. A. (2016). Tree-centric mapping of forest carbon density from airborne laser scanning and hyperspectral data. *Methods in Ecology and Evolution*, *7*(10), 1236–1245. https://doi.org/10.1111/2041-210X.12575

Eichhorn, F. (1904). Beziehungen zwischen Bestandeshöhe und Bestandesmasse. *Allgemeine Forst Und Jagdzeitung*, *80*, 45–49.

Eide, E., & Langsaeter, A. (1941). Produksjonsundersøkelser i granskog. *Meddelser Fra Det Norske Skogforsøksvesen*, *26 Bind VII, hefte 3.*, Article 26 Bind VII, hefte 3.

Ekö, P.-M. (1985). *En produktionsmodell för skog i Sverige, baserad på bestånd från riksskogstaxeringens provytor: A growth simulator for Swedish forests, based on data from the national forest survey.*

Ekö, P.-M., Johansson, U., Petersson, N., Bergqvist, J., Elfving, B., & Frisk, J. (2008). Current growth differences of Norway spruce (*Picea abies*), Scots pine (*Pinus sylvestris*) and birch (*Betula pendula* and *Betula pubescens*) in different regions in Sweden. *Scandinavian Journal of Forest Research*, *23*(4), 307–318. https://doi.org/10.1080/02827580802249126

Elfving, B. (2003). *Övre höjdens utveckling i granplanteringar* (185; Arbetsrapporter). Department of Silviculture, Swedish University of Agricultural Sciences.

Elfving, B., & Kiviste, A. (1997). Construction of site index equations for Pinus sylvestris L. using permanent plot data in Sweden. *Forest Ecology and Management*, *98*(2), Article 2. https://doi.org/10.1016/s0378-1127(97)00077-7

Engel, M., Vospernik, S., Toïgo, M., Morin, X., Tomao, A., Trotta, C., Steckel, M., Barbati, A., Nothdurft, A., Pretzsch, H., Del Rio, M., Skrzyszewski, J., Ponette, Q., Löf, M., Jansons, Ā., & Brazaitis, G. (2021). Simulating the effects of thinning and species mixing on stands of oak (Quercus petraea (Matt.) Liebl./Quercus robur L.) and pine (Pinus sylvestris L.) across Europe. *Ecological Modelling*, *442*, 109406. https://doi.org/10.1016/j.ecolmodel.2020.109406

Eriksson, H., Johansson, U., & Kiviste, A. (1997). A site-index model for pure and mixed stands of *Betula pendula* and *Betula pubescens* in

Sweden. *Scandinavian Journal of Forest Research*, *12*(2), 149–156. https://doi.org/10.1080/02827589709355396

Fassnacht, F. E., White, J. C., Wulder, M. A., & Næsset, E. (2024). Remote sensing in forestry: Current challenges, considerations and directions. *Forestry: An International Journal of Forest Research*, *97*(1), 11–37. https://doi.org/10.1093/forestry/cpad024

Forest sector contribution to national economies 2015. (2022). FAO. https://doi.org/10.4060/cc2387en

Fridman, J., & Danell, K. (Eds.). (2023). *Sveriges skogar under 100 år: Riksskogstaxeringen 1923-2023*. Gidlunds förlag.

Friedlingstein, P., O'Sullivan, M., Jones, M. W., Andrew, R. M., Bakker, D. C. E., Hauck, J., Landschützer, P., Le Quéré, C., Luijkx, I. T., Peters, G. P., Peters, W., Pongratz, J., Schwingshackl, C., Sitch, S., Canadell, J. G., Ciais, P., Jackson, R. B., Alin, S. R., Anthoni, P., … Zheng, B. (2023). Global Carbon Budget 2023. *Earth System Science Data*, *15*(12), 5301–5369. https://doi.org/10.5194/essd-15-5301-2023

Furnival, G. M., & Wilson, R. W. Jr. (1976). Systems of equations for predicting forest growth and yield. In G. P. Patil (Ed.), *Many species populations, ecosytems, and systems analysis: Based on the proc. Of the Intern. Symposium on Statistical Ecology, New Haven, Conn., Aug., 1969* (2. print, pp. 43–57). International Symposium on

Statistical Ecology, University Park, Pa. Pennsylvania State Univ. Pr.

Gavilán-Acuña, G., Coops, N. C., Tompalski, P., & Mena-Quijada, P. (2022). Estimating potential tree height in *Pinus radiata* plantations using airborne laser scanning data. *Canadian Journal of Forest Research*, *52*(10), 1353–1366. https://doi.org/10.1139/cjfr-2022-0121

Gerhardt, E. (1923). *Ertragstafeln für Eiche, Buche, Tanne, Fichte und Kiefer*. Berlag v. Julius Springer.

Giesler, R., Högberg, M., & Högberg, P. (1998). Soil chemistry and plants in Fennoscandian boreal forest as exemplified by a local gradient. *Ecology*, *79*(1), 119–137.

Gingrich, S. F., & Meyer, H. A. (1955). Construction of an aerial stand volume table for Upland Oak. *Forest Science*, *1*(2), 140–147.

Gompertz, B. (1825). XXIV. On the nature of the function expressive of the law of human mortality, and on a new mode of determining the value of life contingencies. In a letter to Francis Baily, Esq. F. R. S. &c. *Philosophical Transactions of the Royal Society of London*, *115*, 513–583. https://doi.org/10.1098/rstl.1825.0026

Goward, S. N., Rocchio, L. E. P., Williams, D. L., Arvidson, T., Irons, J. R., Russell, C. A., & Johnston, S. S. (2017). *Landsat's Enduring*

Legacy: Pioneering Global Land Observations from Space. ASPRS. https://doi.org/10.14358/ASPRS.1.57083.101.7

Hägglund, B. (1972). *Om övre höjdens utveckling för gran i norra Sverige: Site index curves for Norway spruce in northern Sweden.* Royal College of Forestry.

Hägglund, B. (1973). *Om övre höjdens utveckling för gran i södra Sverige: Site index curves for Norway Spruce in southern Sweden.* Royal College of Forestry.

Hägglund, B. (1974). *Övre höjdens utveckling i tallbestånd: Site index curves for Scots pine in Sweden*. Royal College of Forestry.

Hägglund, B. (1979). *Ett system för bonitering av skogsmark—Analys, kontroll och diskussion inför praktiskt tillämpning* (14; Projekt HUGIN, Issue 14, p. 188). Skogsvetenskapliga fakulteten, Sveriges Lantbruksuniversitet.

Hägglund, B., & Lundmark, J.-E. (1977). *Site index estimation by means of site properties Scots pine and Norway Spruce in Sweden*. LiberFörlag/Allmänna Förlaget.

Haman, J., & Avery, M. (2017, August 8). *Introducing ciTools*. The Comprehensive R Archive Network. https://cran.r-project.org/web/packages/ciTools/vignettes/ciTools-demo.html

Hart, A. (2001). Mann-Whitney test is not just a test of medians: Differences in spread can be important. *BMJ*, *323*(7309), 391–393. https://doi.org/10.1136/bmj.323.7309.391

Hasenauer, H. (1999). Höhenzuwachsmodelle für die wichtigsten Baumarten Österreichs. *Forstwissenschaftliches Centralblatt*, *118*(1–6), 14–23. https://doi.org/10.1007/BF02768970

Hasenauer, H., & Monserud, R. A. (1996). A crown ratio model for Austrian forests. *Forest Ecology and Management*, *84*(1–3), 49–60. https://doi.org/10.1016/0378-1127(96)03768-1

Hember, R. A., Kurz, W. A., Metsaranta, J. M., Black, T. A., Guy, R. D., & Coops, N. C. (2012). Accelerating regrowth of temperate-maritime forests due to environmental change. *Global Change Biology*, *18*(6), 2026–2040. https://doi.org/10.1111/j.1365-2486.2012.02669.x

Hinze, J., Albrecht, A., & Michiels, H.-G. (2023). Climate-Adapted Potential Vegetation—A European Multiclass Model Estimating the Future Potential of Natural Vegetation. *Forests*, *14*(2), 239. https://doi.org/10.3390/f14020239

Hjerdt, K. N., McDonnell, J. J., Seibert, J., & Rodhe, A. (2004). A new topographic index to quantify downslope controls on local drainage. *Water Resources Research*, *40*(5), 2004WR003130. https://doi.org/10.1029/2004WR003130

Holopainen, M., Vastaranta, M., Haapanen, R., Yu, X., Hyyppä, J., Kaartinen, H., Viitala, R., & Hyyppä, H. (2010). Site-type estimation using airborne laser scanning and stand register data. *Photogrammetric Journal of Finland*, *22*(1), 16–32.

Huang, H., Ullah, F., Zhou, D.-X., Yi, M., & Zhao, Y. (2019). Mechanisms of ROS Regulation of Plant Development and Stress Responses. *Frontiers in Plant Science*, *10*, 800. https://doi.org/10.3389/fpls.2019.00800

Huuva, I., Wallerman, J., Fransson, J. E. S., & Persson, H. J. (2023). Prediction of Site Index and Age Using Time Series of TanDEM-X Phase Heights. *Remote Sensing*, *15*(17), 4195. https://doi.org/10.3390/rs15174195

Ilvessalo, Y. (1920). Tutkimuksia metsätyyppien taksatoorisesta merkityksestä nojautuen etupäässä kotimaiseen kasvutaulujen laatimistyöhön. *Acta Forestalia Fennica*, *15*(3), 157.

Kahn, M. (1994). *Modellierung der höhenentwicklung ausgewählter Baumarten in Abhängigkeit vom Standort* (141; Forstliche Forschungsberichte München).

Kardell, Ö. (2016). Swedish Forestry, Forest Pasture Grazing by Livestock, and Game Browsing Pressure Since 1900. *Environment and History*, *22*(4), 561–587.

Kneeling, A. (1994). *Methodischer beitrag zur auswertung der Österreichischen Forstinventur nach 1980.* [Diss.]. Univ. für Bodenkultur.

Knoke, T., Ammer, C., Stimm, B., & Mosandl, R. (2008). Admixing broadleaved to coniferous tree species: A review on yield, ecological stability and economics. *European Journal of Forest Research*, *127*(2), 89–101. https://doi.org/10.1007/s10342-007-0186-2

Kolmogorov, A. (1956). On the representation of continuous functions of several variables by superpositions of continuous functions of a smaller number of variables. *Proceedings of the USSR Academy of Sciences*, *108*, 179–182.

Kopezky, R. (1899). Neue verfahren der bestandesmassen-ermittlung. *Centrallblatt fur das gesamte Forstwesen*, 471–485.

Korf, V. (1939). A mathematical definition of stand volume growth law. *Lesnická Práce*, *18*, 337–339.

Kruskal, W. H., & Wallis, W. A. (1952). Use of Ranks in One-Criterion Variance Analysis. *Journal of the American Statistical Association*, *47*(260), 583–621. https://doi.org/10.1080/01621459.1952.10483441

Lacis, A. A., Schmidt, G. A., Rind, D., & Ruedy, R. A. (2010). Atmospheric CO_2: Principal Control Knob Governing Earth's Temperature.

Science, *330*(6002), 356–359. https://doi.org/10.1126/science.1190653

Larson, J., Vigren, C., Wallerman, J., Ågren, A. M., Appiah Mensah, A., & Laudon, H. (2024). Tree growth potential and its relationship with soil moisture conditions across a heterogeneous boreal forest landscape. *Scientific Reports*, *14*(1), 10611.

Ledermann, T. (2002). Ein Einwuchsmodell aus den Daten der österreichischen Waldinventur 1981-1996. *Centrallblatt Für Das Gesamte Forstwesen*, *119*, 40–76.

Ledermann, T. (2006). Description of PrognAus for Windows 2.2. In H. Hasenauer (Ed.), *Sustainable Forest Management* (pp. 71–78). Springer-Verlag. https://doi.org/10.1007/3-540-31304-4_6

Leijon, B. (1979). *Tallen och Granens produktion på lika ståndort. Redovisning till SJFR. Internal report.* (p. 100). Inst. f. skogsskötsel. Swedish University of Agricultural Sciences.

Li, W., Guo, Q., Jakubowski, M. K., & Kelly, M. (2012). A New Method for Segmenting Individual Trees from the Lidar Point Cloud. *Photogrammetric Engineering & Remote Sensing*, *78*(1), 75–84. https://doi.org/10.14358/PERS.78.1.75

Lidberg, W., Nilsson, M., & Ågren, A. (2020). Using machine learning to generate high-resolution wet area maps for planning forest

management: A study in a boreal forest landscape. *Ambio*, *49*(2), Article 2. https://doi.org/10.1007/s13280-019-01196-9

Lin, J., Gamarra, J. G. P., Drake, J. E., Cuchietti, A., & Yanai, R. D. (2023). Scaling up uncertainties in allometric models: How to see the forest, not the trees. *Forest Ecology and Management*, *537*, 120943. https://doi.org/10.1016/j.foreco.2023.120943

Lindsay, K., Bonan, G. B., Doney, S. C., Hoffman, F. M., Lawrence, D. M., Long, M. C., Mahowald, N. M., Keith Moore, J., Randerson, J. T., & Thornton, P. E. (2014). Preindustrial-Control and Twentieth-Century Carbon Cycle Experiments with the Earth System Model CESM1(BGC). *Journal of Climate*, *27*(24), 8981–9005. https://doi.org/10.1175/JCLI-D-12-00565.1

Lorimer, C. G. (1983). Tests of age-independent competition indices for individual trees in natural hardwood stands. *Forest Ecology and Management*, *6*(4), 343–360. https://doi.org/10.1016/0378-1127(83)90042-7

Lundmark, J.-E. (1974). *Ståndortsegenskaperna som bonitetsindikatorer i bestånd med tall och gran; Use of site properties for assessing site index in stands of Scots pine and Norway spruce* (16; Rapporter och Uppsatser / Research Notes, p. 298). Department of Forest Ecology and Forest Soils.

Lundqvist, B. (1957). Om höjdutvecklingen i kulturbestånd av tall och gran i Norrland: On the height growth of cultivated stands of pine and spruce in Northern Sweden. *Meddelanden Från Statens Skogsforskningsinstitut*, *47*(2), 64.

Mahony, C. R., Cannon, A. J., Wang, T., & Aitken, S. N. (2017). A closer look at novel climates: New methods and insights at continental to landscape scales. *Global Change Biology*, *23*(9), 3934–3955. https://doi.org/10.1111/gcb.13645

Mantova, M., Herbette, S., Cochard, H., & Torres-Ruiz, J. M. (2022). Hydraulic failure and tree mortality: From correlation to causation. *Trends in Plant Science*, *27*(4), 335–345. https://doi.org/10.1016/j.tplants.2021.10.003

Matsushita, M., Takata, K., Hitsuma, G., Yagihashi, T., Noguchi, M., Shibata, M., & Masaki, T. (2015). A novel growth model evaluating age–size effect on long-term trends in tree growth. *Functional Ecology*, *29*(10), 1250–1259. https://doi.org/10.1111/1365-2435.12416

Mensah, A. A., Holmström, E., Nyström, K., & Nilsson, U. (2022). Modelling potential yield capacity in conifers using Swedish long-term experiments. *Forest Ecology and Management*, *512*, 120162. https://doi.org/10.1016/j.foreco.2022.120162

Mitscherlich, E. A. (1909). Das gesetz des minimums und das gesetz des abnehmenden bodenertrages. *Landwirtsch Jahrbuch*, *38*, 537–552.

Monserud, R. A., & Sterba, H. (1996). A basal area increment model for individual trees growing in even- and uneven-aged forest stands in Austria. *Forest Ecology and Management*, *80*(1–3), 57–80. https://doi.org/10.1016/0378-1127(95)03638-5

Monserud, R. A., & Sterba, H. (1999). Modeling individual tree mortality for Austrian forest species. *Forest Ecology and Management*, *113*(2–3), 109–123. https://doi.org/10.1016/S0378-1127(98)00419-8

Murphy, P. N. C., Ogilvie, J., Castonguay, M., Zhang, C., Meng, F.-R., & Arp, P. A. (2008). Improving forest operations planning through high-resolution flow-channel and wet-areas mapping. *The Forestry Chronicle*, *84*(4), 568–574. https://doi.org/10.5558/tfc84568-4

Nachtmann, G. (2005). *Der Höhenzuwachs österreichischer Baumarten in Abhängigkeit von Standort und Konkurrenz* [PhD Thesis]. BOKU.

Næsset, E. (1997). Estimating timber volume of forest stands using airborne laser scanner data. *Remote Sensing of Environment*, *61*(2), 246–253. https://doi.org/10.1016/S0034-4257(97)00041-2

Näslund, M. (1936). *Skogsförsöksanstaltens gallringsförsök i tallskog primärbearbetning \ Die durchforstungsversuche der forstlichen versuchsanstalt Schwedens in kiefernwald primärbearbeitung* (29;

Meddelanden Från Statens Skogsförsöksanstalt \ Mitteilungen Aus Der Forstlichen Versuchsanstalt Schwedens, Issue 29, p. 43).

Nemani, R. R., Keeling, C. D., Hashimoto, H., Jolly, W. M., Piper, S. C., Tucker, C. J., Myneni, R. B., & Running, S. W. (2003). Climate-Driven Increases in Global Terrestrial Net Primary Production from 1982 to 1999. *Science*, *300*(5625), 1560–1563. https://doi.org/10.1126/science.1082750

Newnham, R. M. (1964). *The development of a stand model for Douglas fir* (Version 1) [Diss., University of British Columbia]. https://doi.library.ubc.ca/10.14288/1.0105410

Nilsson, M., Nordkvist, K., Jonzen, J., Lindgren, N., Axensten, P., Wallerman, J., Egberth, M., Larsson, S., Nilsson, L., Eriksson, J., & Olsson, H. (2017). A nationwide forest attribute map of Sweden predicted using airborne laser scanning data and field data from the National Forest Inventory. *Remote Sensing of Environment*, *194*, 447–454. https://doi.org/10.1016/j.rse.2016.10.022

NOAA. (2024). *No sign of greenhouse gases increases slowing in 2023*. NOAA. https://research.noaa.gov/2024/04/05/no-sign-of-greenhouse-gases-increases-slowing-in-2023/

Noordermeer, L., Gobakken, T., Næsset, E., & Bollandsås, O. M. (2020). Predicting and mapping site index in operational forest inventories using bitemporal airborne laser scanner data. *Forest Ecology and*

Management, *457*, 117768. https://doi.org/10.1016/j.foreco.2019.117768

Nord-Larsen, T., & Johannsen, V. K. (2007). A state-space approach to stand growth modelling of European beech. *Annals of Forest Science*, *64*(4), 365–374. https://doi.org/10.1051/forest:2007013

Nyström, M., Lindgren, N., Wallerman, J., Grafström, A., Muszta, A., Nyström, K., Bohlin, J., Willén, E., Fransson, J., Ehlers, S., Olsson, H., & Ståhl, G. (2015). Data Assimilation in Forest Inventory: First Empirical Results. *Forests*, *6*(12), 4540–4557. https://doi.org/10.3390/f6124384

Obeng, E. A., & Aguilar, F. X. (2018). Value orientation and payment for ecosystem services: Perceived detrimental consequences lead to willingness-to-pay for ecosystem services. *Journal of Environmental Management*, *206*, 458–471. https://doi.org/10.1016/j.jenvman.2017.10.059

Paterson, S. (1956). The forest area of the world and its potential productivity. *Medd. Göteborgs Univ. Geografiska Inst.*, *51*.

Peterson, B., Dubayah, R., Hyde, P., Hofton, M., Blair, J. B., & Fites-Kaufman, J. (2007). Use of LIDAR for forest inventory and forest management application. *In: McRoberts, Ronald E.; Reams, Gregory A.; Van Deusen, Paul C.; McWilliams, William H., Eds. Proceedings of the Seventh Annual Forest Inventory and Analysis*

Symposium; October 3-6, 2005; Portland, ME. Gen. Tech. Rep. WO-77. Washington, DC: US Department of Agriculture, Forest Service: 193-202., *77*.

Phillips, J. M., Liu, R., & Tomasi, C. (2006). *Outlier Robust ICP for Minimizing Fractional RMSD* (Version 1). arXiv. https://doi.org/10.48550/ARXIV.CS/0606098

Pretzsch, H., & Biber, P. (2005). A Re-Evaluation of Reineke's Rule and Stand Density Index. *Forest Science*, *51*(4), 304–320. https://doi.org/10.1093/forestscience/51.4.304

Pretzsch, H., Del Río, M., Arcangeli, C., Bielak, K., Dudzinska, M., Forrester, D. I., Klädtke, J., Kohnle, U., Ledermann, T., Matthews, R., Nagel, J., Nagel, R., Ningre, F., Nord-Larsen, T., & Biber, P. (2023). Forest growth in Europe shows diverging large regional trends. *Scientific Reports*, *13*(1), 15373. https://doi.org/10.1038/s41598-023-41077-6

Pretzsch, H., Steckel, M., Heym, M., Biber, P., Ammer, C., Ehbrecht, M., Bielak, K., Bravo, F., Ordóñez, C., Collet, C., Vast, F., Drössler, L., Brazaitis, G., Godvod, K., Jansons, A., de-Dios-García, J., Löf, M., Aldea, J., Korboulewsky, N., … del Río, M. (2020). Stand growth and structure of mixed-species and monospecific stands of Scots pine (Pinus sylvestris L.) and oak (Q. robur L., Quercus petraea (Matt.) Liebl.) analysed along a productivity gradient through

Europe. *European Journal of Forest Research*, *139*(3), 349–367. https://doi.org/10.1007/s10342-019-01233-y

Prodan, M. (1965). *Holzmesslehre*. J.D. Sauerländer.

Reineke, L. (1933). Perfecting a stand-density index for even-aged forests. *Journal of Agricultural Research*, *46*(7), 627–638.

Renner-Martin, K., Brunner, N., Kühleitner, M., Nowak, W. G., & Scheicher, K. (2018). On the exponent in the Von Bertalanffy growth model. *PeerJ*, *6*, e4205. https://doi.org/10.7717/peerj.4205

Rennolls, K. (1995). Forest height growth modelling. *Forest Ecology and Management*, *71*(3), Article 3. https://doi.org/10.1016/0378-1127(94)06102-O

Reyer, C. P. O. (2015). Forest Productivity Under Environmental Change-a Review of Stand-Scale Modeling Studies. *Current Forestry Reports*, *1*(2), Article 2. https://doi.org/10.1007/s40725-015-0009-5

Reyer, C. P. O., Bathgate, S., Blennow, K., Borges, J. G., Bugmann, H., Delzon, S., Faias, S. P., Garcia-Gonzalo, J., Gardiner, B., Gonzalez-Olabarria, J. R., Gracia, C., Hernandez, J. G., Kellomaki, S., Kramer, K., Lexer, M. J., Lindner, M., van der Maaten, E., Maroschek, M., Muys, B., … Hanewinkel, M. (2017). Are forest disturbances amplifying or canceling out climate change-induced productivity changes in European forests? *Environmental Research Letters*, *12*(3), Article 3. https://doi.org/10.1088/1748-9326/aa5ef1

Richards, F. J. (1959). A Flexible Growth Function for Empirical Use. *Journal of Experimental Botany*, *10*(2), 290–301. https://doi.org/10.1093/jxb/10.2.290

Riofrío, J., White, J. C., Tompalski, P., Coops, N. C., & Wulder, M. A. (2023). Modelling height growth of temperate mixedwood forests using an age-independent approach and multi-temporal airborne laser scanning data. *Forest Ecology and Management*, *543*, 121137. https://doi.org/10.1016/j.foreco.2023.121137

Ritchie, H., Rosado, P., & Samborska, V. (2024). *NOAA Global Monitoring Laboratory—Trends in Atmospheric Carbon Dioxide (2024); EPA based on various sources (2022) – with major processing by Our World in Data. "Carbon dioxide concentrations in the atmosphere" [dataset]. NOAA Global Monitoring Laboratory, "Trends in Atmospheric Carbon Dioxide"; United States Environmental Protection Agency, "Climate Change Indicators: Atmospheric Concentrations of Greenhouse Gases" [original data].* [Dataset]. https://ourworldindata.org/grapher/co2-long-term-concentration

Roussel, J.-R., & Auty, D. (2024). *Airborne LiDAR Data Manipulation and Visualization for Forestry Applications*. https://cran.r-project.org/package=lidR

Roussel, J.-R., Auty, D., Coops, N. C., Tompalski, P., Goodbody, T. R. H., Meador, A. S., Bourdon, J.-F., Boissieu, F. de, & Achim, A. (2020).

lidR: An R package for analysis of Airborne Laser Scanning (ALS) data. *Remote Sensing of Environment*, *251*, 112061. https://doi.org/10.1016/j.rse.2020.112061

Saarela, S., Wästlund, A., Holmström, E., Mensah, A. A., Holm, S., Nilsson, M., Fridman, J., & Ståhl, G. (2020). Mapping aboveground biomass and its prediction uncertainty using LiDAR and field data, accounting for tree-level allometric and LiDAR model errors. *Forest Ecosystems*, *7*(1), 43. https://doi.org/10.1186/s40663-020-00245-0

Salas-Eljatib, C. (2020). Height growth–rate at a given height: A mathematical perspective for forest productivity. *Ecological Modelling*, *431*, 109198. https://doi.org/10.1016/j.ecolmodel.2020.109198

Schieler, K. (1997). *Methode der zuwachsberechnung der Österreichischen Waldinventur* [Diss.]. Univ. für Bodenkultur.

Scoccimarro, E., Gualdi, S., Bellucci, A., Sanna, A., Giuseppe Fogli, P., Manzini, E., Vichi, M., Oddo, P., & Navarra, A. (2011). Effects of Tropical Cyclones on Ocean Heat Transport in a High-Resolution Coupled General Circulation Model. *Journal of Climate*, *24*(16), 4368–4384. https://doi.org/10.1175/2011JCLI4104.1

Seidl, R., Spies, T. A., Peterson, D. L., Stephens, S. L., & Hicke, J. A. (2016). REVIEW: Searching for resilience: addressing the impacts of changing disturbance regimes on forest ecosystem services. *Journal*

of Applied Ecology, *53*(1), 120–129. https://doi.org/10.1111/1365-2664.12511

Seidl, R., Thom, D., Kautz, M., Martin-Benito, D., Peltoniemi, M., Vacchiano, G., Wild, J., Ascoli, D., Petr, M., Honkaniemi, J., Lexer, M. J., Trotsiuk, V., Mairota, P., Svoboda, M., Fabrika, M., Nagel, T. A., & Reyer, C. P. O. (2017). Forest disturbances under climate change. *Nature Climate Change*, *7*(6), Article 6. https://doi.org/10.1038/nclimate3303

Serreze, M. C., & Barry, R. G. (2011). Processes and impacts of Arctic amplification: A research synthesis. *Global and Planetary Change*, *77*(1–2), Article 1–2. https://doi.org/10.1016/j.gloplacha.2011.03.004

Siipilehto, J., Allen, M., Nilsson, U., Brunner, A., Huuskonen, S., Haikarainen, S., Subramanian, N., Antón-Fernández, C., Holmström, E., Andreassen, K., & Hynynen, J. (2020). Stand-level mortality models for Nordic boreal forests. *Silva Fennica*, *54*(5). https://doi.org/10.14214/sf.10414

Skovsgaard, J. P., & Vanclay, J. K. (2008). Forest site productivity: A review of the evolution of dendrometric concepts for even-aged stands. *Forestry*, *81*(1), 13–31. https://doi.org/10.1093/forestry/cpm041

Skovsgaard, J. P., & Vanclay, J. K. (2013). Forest site productivity: A review of spatial and temporal variability in natural site conditions. *Forestry*, *86*(3), Article 3. https://doi.org/10.1093/forestry/cpt010

Slatkin, M., & Anderson, D. J. (1984). A Model of Competition for Space. *Ecology*, *65*(6), 1840–1845. https://doi.org/10.2307/1937781

Socha, J., Hawryło, P., Stereńczak, K., Miścicki, S., Tymińska-Czabańska, L., Młocek, W., & Gruba, P. (2020). Assessing the sensitivity of site index models developed using bi-temporal airborne laser scanning data to different top height estimates and grid cell sizes. *International Journal of Applied Earth Observation and Geoinformation*, *91*, 102129. https://doi.org/10.1016/j.jag.2020.102129

Socha, J., Pierzchalski, M., Bałazy, R., & Ciesielski, M. (2017). Modelling top height growth and site index using repeated laser scanning data. *Forest Ecology and Management*, *406*, 307–317. https://doi.org/10.1016/j.foreco.2017.09.039

Spiecker, H., Mielikäinen, K., Köhl, M., & Skovsgaard, J. P. (1996). *Growth Trends in European Forests: Studies from 12 Countries* (Vol. 5). Springer-Verlag Berlin Heidelberg.

Sprengel, C. (1828). Von den Substanzen der Ackerkrume und des Untergrundes. *Journal für Technische und Ökonomische Chemie*, *2*, Article 2.

Steckel, M., del Río, M., Heym, M., Aldea, J., Bielak, K., Brazaitis, G., Černý, J., Coll, L., Collet, C., Ehbrecht, M., Jansons, A., Nothdurft, A., Pach, M., Pardos, M., Ponette, Q., Reventlow, D. O. J., Sitko, R., Svoboda, M., Vallet, P., … Pretzsch, H. (2020). Species mixing reduces drought susceptibility of Scots pine (Pinus sylvestris L.) and oak (Quercus robur L., Quercus petraea (Matt.) Liebl.) – Site water supply and fertility modify the mixing effect. *Forest Ecology and Management*, *461*, 117908. https://doi.org/10.1016/j.foreco.2020.117908

Sterba, H., & Monserud, R. A. (1996). Validation of the single tree stand growth simulator PROGNAUS with permanent plot data. In M. Köhl & G. Z. Gertner (Eds.), *Statistics, mathematics and computers: Caring for the forest: Research in a changing world* (pp. 36–49). Swiss Federal Institute for Forest, Snow and Landscape Research, WSL/FNP. https://www.dora.lib4ri.ch/wsl/islandora/object/wsl%3A10453/datastream/PDF/K%C3%B6hl-1996-Caring_for_the_forest-%28published_version%29.pdf

Stereńczak, K., Mielcarek, M., Wertz, B., Bronisz, K., Zajączkowski, G., Jagodziński, A. M., Ochał, W., & Skorupski, M. (2019). Factors influencing the accuracy of ground-based tree-height measurements for major European tree species. *Journal of Environmental*

Management, *231*, 1284–1292. https://doi.org/10.1016/j.jenvman.2018.09.100

Swappach, A. (1912). *Ertragstafeln der wichtigeren Holzarten in tabellarischer und graphischer Form*. Verlag v. J. Neumann.

Tegnhammar, L. (1992). *On the estimation of site index for Norway Spruce*. Dept. of Forest Survey.

The World Bank Group. (2024). *GDP (constant 2015 US$)* [Dataset]. https://data.worldbank.org/indicator/NY.GDP.MKTP.KD

Tian, A., Wang, Y., Webb, A. A., Yu, P., Wang, X., & Liu, Z. (2023). Modelling the response of larch growth to age, density, and elevation and the implications for multifunctional management in northwest China. *Journal of Forestry Research*, *34*(5), 1423–1436. https://doi.org/10.1007/s11676-022-01539-5

Tomé, J., Tomé, M., Barreiro, S., & Paulo, J. A. (2006). Age-independent difference equations for modelling tree and stand growth. *Canadian Journal of Forest Research*, *36*(7), 1621–1630. https://doi.org/10.1139/x06-065

Tompalski, P., Coops, N. C., White, J. C., & Wulder, M. A. (2015). Augmenting Site Index Estimation with Airborne Laser Scanning Data. *Forest Science*, *61*(5), 861–873. https://doi.org/10.5849/forsci.14-175

Tomppo, E., Gschwantner, T., Lawrence, M., McRoberts, R. E., & SpringerLink (Online service). (2010). *National Forest Inventories: Pathways for Common Reporting*. Springer Netherlands,.

Tüxen, R. (1956). *Die heutige potentielle natürliche Vegetation als Gegenstand der Vegetationskartierung* (Vol. 13). Zentralstelle für Vegetationskartierung.

Tymińska-Czabańska, L., Socha, J., Hawryło, P., Bałazy, R., Ciesielski, M., Grabska-Szwagrzyk, E., & Netzel, P. (2021). Weather-sensitive height growth modelling of Norway spruce using repeated airborne laser scanning data. *Agricultural and Forest Meteorology*, *308–309*, 108568. https://doi.org/10.1016/j.agrformet.2021.108568

Tyndall, J. (1861). On the Absorption and Radiation of Heat by Gases and Vapours, and on the Physical Connexion of Radiation, Absorption, and Conduction. *Philosophical Transactions of the Royal Society of London*, *151*, 1–36.

Ulrich, B. (1990). Waldsterben: Forest decline in West Germany. *Environmental Science & Technology*, *24*(4), 436–441.

UNFCCC. (1997). *7. A). Kyoto Protocol to the United Nations Framework Convention on Climate Change.* (p. 194). https://treaties.un.org/doc/Treaties/1998/09/19980921%2004-41%20PM/Ch_XXVII_07_ap.pdf

v. Liebig, J. (1840). *Die organische Chemie in ihrer unwendung auf Agricultur und Physiologie*. Berlag v. Friedrich Viewig und Sohn. https://books.google.se/books?hl=en&lr=&id=kFEIb7WlzGkC&oi=fnd&pg=PA1&ots=Rs8YiJJJuh&sig=hEqOyIgPuXhMqmAlzav2vIpxUSM&redir_esc=y#v=onepage&q&f=false

Valmari, J. (1921). Beiträge zur chemischen Bodenanalyse. *Acta Forestalia Fennica*, *20*(4). https://doi.org/10.14214/aff.7064

Vospernik, S. (2021). Basal area increment models accounting for climate and mixture for Austrian tree species. *Forest Ecology and Management*, *480*, 118725. https://doi.org/10.1016/j.foreco.2020.118725

Vospernik, S., Heym, M., Pretzsch, H., Pach, M., Steckel, M., Aldea, J., Brazaitis, G., Bravo-Oviedo, A., Del Rio, M., Löf, M., Pardos, M., Bielak, K., Bravo, F., Coll, L., Černý, J., Droessler, L., Ehbrecht, M., Jansons, A., Korboulewsky, N., … Wolff, B. (2023). Tree species growth response to climate in mixtures of Quercus robur/Quercus petraea and Pinus sylvestris across Europe—A dynamic, sensitive equilibrium. *Forest Ecology and Management*, *530*, 120753. https://doi.org/10.1016/j.foreco.2022.120753

Vospernik, S., Monserud, R. A., & Sterba, H. (2015). Comparing individual-tree growth models using principles of stand growth for Norway spruce, Scots pine, and European beech. *Canadian Journal of Forest*

Research, *45*(8), 1006–1018. https://doi.org/10.1139/cjfr-2014-0394

Vospernik, S., & Sterba, H. (2015). Do competition-density rule and self-thinning rule agree? *Annals of Forest Science*, *72*(3), 379–390. https://doi.org/10.1007/s13595-014-0433-x

Wallentin, C., & Nilsson, U. (2014). Storm and snow damage in a Norway spruce thinning experiment in southern Sweden. *Forestry*, *87*(2), 229–238. https://doi.org/10.1093/forestry/cpt046

Walters, D. K., Gregoire, T. G., & Burkhart, H. E. (1989). Consistent Estimation of Site Index Curves Fitted to Temporary Plot Data. *Biometrics*, *45*(1), 23. https://doi.org/10.2307/2532032

Watanabe, M., Suzuki, T., O'ishi, R., Komuro, Y., Watanabe, S., Emori, S., Takemura, T., Chikira, M., Ogura, T., Sekiguchi, M., Takata, K., Yamazaki, D., Yokohata, T., Nozawa, T., Hasumi, H., Tatebe, H., & Kimoto, M. (2010). Improved Climate Simulation by MIROC5: Mean States, Variability, and Climate Sensitivity. *Journal of Climate*, *23*(23), 6312–6335. https://doi.org/10.1175/2010JCLI3679.1

Weller, D. E. (1990). Will the Real Self-Thinning Rule Please Stand Up?--A Reply to Osawa and Sugita. *Ecology*, *71*(3), 1204–1207. https://doi.org/10.2307/1937389

Westoby, M. (1984). The Self-Thinning Rule. In *Advances in Ecological Research* (Vol. 14, pp. 167–225). Elsevier. https://doi.org/10.1016/S0065-2504(08)60171-3

Wiedemann, E. (1923). *Zuwachsrückgang und Wuchsstockungen der Fichte in den mittleren und unteren Höhenlagen der sächsischen Staatsforsten* (p. 180). Sachsen Finanzministerium, Sächsische Forstliche Versuchsanstalt Abteilung für Standortslehre.

Wiedemann, E. (1937). Die Fichte 1936. *Mitteilungen Aus Forstwirtschaft Und Forstwissenschaft. Hannover.*

Wiedemann, E., & Schober, R. (1957). *Ertragstafeln* (2nd ed.). Verlag M. u. H. Schaper, Hannover.

Wielgosz, M., Puliti, S., Xiang, B., Schindler, K., & Astrup, R. (2024). SegmentAnyTree: A sensor and platform agnostic deep learning model for tree segmentation using laser scanning data. *Remote Sensing of Environment*, *313*, 114367. https://doi.org/10.1016/j.rse.2024.114367

WMO. (2024). *WMO Global Annual to Decadal Climate Update: Target years: 2024 and 2024-2028* (p. 27). https://library.wmo.int/idurl/4/68910

Wood, S. N. (2011). Fast stable restricted maximum likelihood and marginal likelihood estimation of semiparametric generalized linear models: Estimation of Semiparametric Generalized Linear Models. *Journal*

of the Royal Statistical Society: Series B (Statistical Methodology), *73*(1), Article 1. https://doi.org/10.1111/j.1467-9868.2010.00749.x

Wykoff, W. R., Crookston, N. L., & Stage, A. R. (1982). *User's Guide to the Stand Prognosis Model* (INT-GTR-133; p. INT-GTR-133). U.S. Department of Agriculture, Forest Service, Intermountain Forest and Range Experiment Station. https://doi.org/10.2737/INT-GTR-133

Yoda, K., Kira, T., Ogawa, H., & Hozumi, K. (1963). Self-Thinning in Overcrowded Pure Stands under Cultivated and Natural Conditions. *Journal of Biology*, *14*, 107–129.

Yue, C. F., Kahle, H.-P., Klädtke, J., & Kohnle, U. (2023). Forest stand-by-environment interaction invalidates the use of space-for-time substitution for site index modeling under climate change. *Forest Ecology and Management*, *527*, 120621. https://doi.org/10.1016/j.foreco.2022.120621

Zeide, B. (1993). Analysis of Growth Equations. *Forest Science*, *39*(3), 594–616. https://doi.org/10.1093/forestscience/39.3.594

Zhou, W., Chen, F., Meng, Y., Chandrasekaran, U., Luo, X., Yang, W., & Shu, K. (2020). Plant waterlogging/flooding stress responses: From seed germination to maturation. *Plant Physiology and Biochemistry*, *148*, 228–236. https://doi.org/10.1016/j.plaphy.2020.01.020

Zimová, S., Dobor, L., Hlásny, T., Rammer, W., & Seidl, R. (2020). Reducing rotation age to address increasing disturbances in Central

Europe: Potential and limitations. *Forest Ecology and Management*, *475*, 118408. https://doi.org/10.1016/j.foreco.2020.118408

Popular science summary

Forest modelling can be seen as two schools: one claiming we must mimic how trees work, and one claiming it is enough to mimic how trees behave. Papers I and II took tree-level models describing tree behaviour and modified some aspects such that they accounted for local weather. We inventoried forests with Scots Pine and Oak across Europe and forecast them with different climate models and future scenarios. We then created a simplified forest-level model so that we could run our tree-level model across Europe. Particularly across southern Europe, Scots Pine will produce less marketable wood under the future scenarios we investigated than it has done in the recent past. Oak stands may react negatively in many parts of Europe, but positively in some. Papers I and II recommend that future studies develop models that also consider how forest health and mortality is affected by changing climate and investigate how these models suggest management might affect forest growth in future climates. The third paper of this thesis explores a new technique where we have connected an indicator of forest growth based on tree heights measured at two times by laser scanning over 68 square kilometres and connected it to an indicator of soil moisture. We found that in northern forests forest productivity might not be very strongly affected by soil moisture alone, but productivity decreased on very wet sites. The last paper explores if information about single trees from very dense laser scanning could be used to complement ground-based inventories.

Populärvetenskaplig sammanfattning

Skogsmodellering kan ses som uppdelad i två skolor: en som hävdar att vi måste efterlikna hur träd fungerar, och en som hävdar att det räcker att efterlikna hur träd beter sig. Artiklarna I och II tog modeller på trädnivå som beskriver träds beteende och modifierade dom så att de inkluderar lokalt väder. Vi inventerade tall och ekbestånd igenom Europa och framskred dessa sedan med olika klimatmodeller och framtidsscenarier. Vi skapade sedan en förenklad modell på beståndsnivå så att vi kunde köra vår komplexa modell över hela Europa. Särskilt i södra Europa kommer vanlig tall att producera mindre säljbart virke under de framtidsscenarier som vi undersökte än vad det gjort på senare tid. Ekbestånd kan reagera negativt i många delar av Europa, men positivt i somliga. Artiklarna I och II rekommenderar att framtida studier utvecklar modeller som också tar hänsyn till hur skogarnas hälsa och dödlighet påverkas av förändrat klimat och undersöker hur dessa modeller tyder på att skötseln kan påverka skogens tillväxt i framtida klimat. Den tredje uppsatsen i avhandlingen utforskar en ny teknik där vi kopplat en indikator för skogstillväxt, baserad på trädhöjder över 68 kvadratkilometer som uppmätts vid två tillfällen genom laserskanning, till en indikator för markfuktighet. Vi fann att i nordliga skogar kanske inte skogsproduktiviteten påverkas särskilt starkt av enbart markfuktigheten, men produktiviteten minskade på mycket blöta platser. Den sista artikeln undersöker om information om enskilda träd från mycket tät laserskanning skulle kunna användas för att komplettera markbaserade inventeringar.

Acknowledgements

‘*I’m not sure this is for you, but since you’re so darned persistent…’*

- Anon.

First and foremost, a great deal of thanks to my supervisors, Göran Ståhl, Jörgen Wallerman, Tomas Lundmark and Anneli Ågren. If it is any consolation, on my parents’ bookshelf is placed a book: ‘the strong-willed child’. *Göran*: *Thank you* for supporting me in the second half of my Ph.D. You have contributed greatly with your support and discussions. *Jörgen*: This entire endeavour would have derailed years before I was employed if it had not been for your efforts. You have been a trusted advisor since day one. I hope they fix the ventilation in your office soon. *Anneli*: Thank you for having spearheaded our approaches with statistical learning. With at least moderate success, you have reminded me trees are actually rooted. *Tomas*: I am immensely grateful for your trust in that I would get something done, despite only one of our original projects making it to publication, and my Ph.D. thesis largely constituting a side-effort next to my work figuring out how growth models work. I hope our weekend projects have been as helpful to you as they have me. *Sonja*: A great deal of what I consider my best work has come to fruition thanks to you. I’m very glad I decided to send off an e-mail to you asking you to explain just *exactly how PrognAus* worked. *Lina*: Thank you for being *you*. *Simon:* Thank you for being a great friend! *Perry & Emmelie*: It’s a joy to follow you two. Thank you for putting up with me and subscribing to my foreign affairs podcast. *Anton, Gustav & Robin*: You guys are the best. *Alexandra & Erik*: Thank you for bringing my dog Alvin into my life and supporting me. *Arvin & Julia:* Guacamole is always free at my house. *Alex:* Thank you for sticking up for me with the modelling! *Logan & München team:* Thanks for helping me scour your library from afar!

Heureka Team: “I’ll be back”.

To Mom, Dad and my sister Sophie:
This is all thanks to you.

7. Appendix I

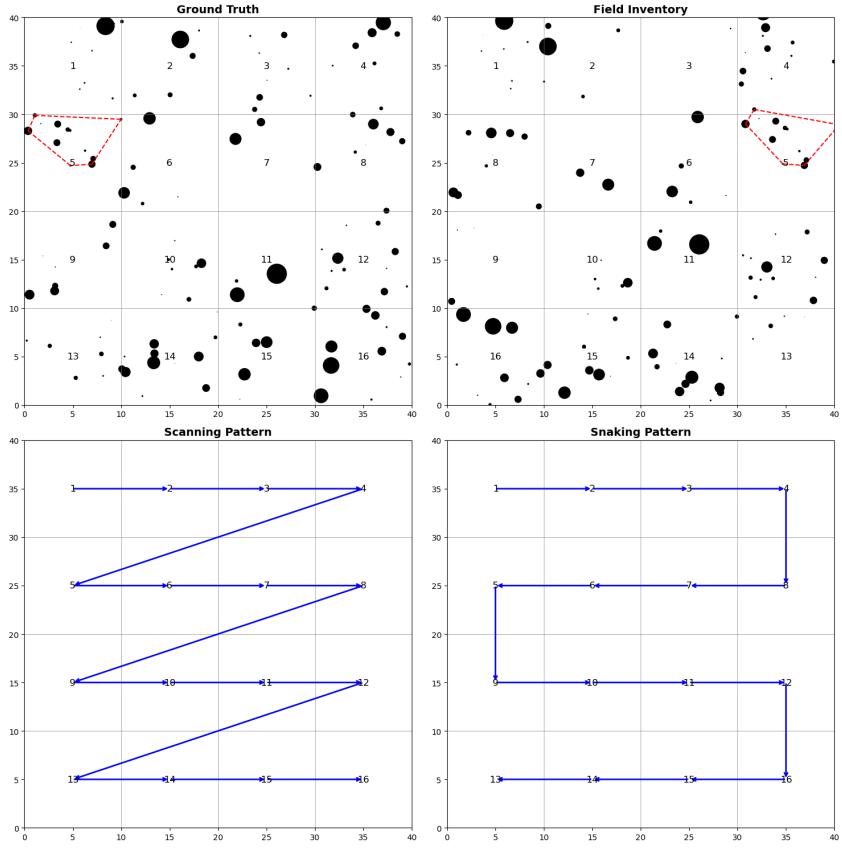

Figure 18. The tree co-registration problem.

> A 40x40 *m* square plot has been completely inventoried in 16 10x10 m subplots for each tree's diameter, species. Sample trees have been measured for height. Trees are provided with a local cartesian coordinate from fixed GPS points at subplot centres but are not provided with constant identities. Duplicate measurements of the same tree from several adjacent plots may exist. Due to human error, the plot identities are scrambled, and in some cases trees in more than one plot have been measured from a single plot centre. Align the individual trees into a coherent coordinate system based on recovered tree objects from ALS data, and then create growth series for single tree identities from subsequent field inventories not accompanied by ALS. The only allowed manipulations are rotation, translation, and mirroring in the XY plane.

Some complications compound the issue:

i) The trees are planted and thus interspersed with some spatial regularity and are relatively close in diameter, height attributes.
ii) Only some trees have height measurements which can be linked to ALS object estimates.
iii) The plots undergo active management, e.g. thinning, by which trees legitimately disappear. However, trees can illegitimately disappear due to human error or because of edge-proximity.

Iterative Closest Point (ICP) solutions:

Previous work at the institution for Forest Resource Management has been done by *Kenneth Olofsson* (unpubl.). Olofssons algorithm finds semi-global optimum positioning by brute-force using random-instantiations to perform a grid-search of the space before selecting the optimal positioning. However, this resulted in several notable errors which will impact the creation of growth-series: (weighted-) 2D ICP will consider the optimal position to minimize to total error of the subgroup – commonly resulting in solutions with moderate offsets for all points when there are some members with large errors or no correspondence in the target point cloud (missing trees). Secondly, the routine frequently found solutions in the buffer zone outside of the field-inventoried plot, or strong overlap between inventoried plots.

To recover growth series for individual trees, it was thus necessary to develop a novel approach, using the *Fractional ICP* approach, which has not

to the authors knowledge previously been applied to the tree co-registration problem.

Fractional ICP

Phillips *et al.* (2006) avoid the skewed alignment of point sets resulting from outliers where the transform was computed from ICP by making outlier detection part of the problem formulation to be solved.

Phillips *et al.* (ibid.), define a novel distance metric between two point-sets (D, M): the fractional root mean squared distance (FRMSD). The FRMSD regards the weighted distance of a specific fraction *f* of the best matches in a considered mapping between single points *p* in set D in the dictionary μ: $D \rightarrow M$.

$$FRMSD(D, M, f, \mu) = \frac{1}{f^{\lambda}} \sqrt{\frac{1}{|D_f|} \sum_{p \in D_f} \|p - \mu(p)\|^2}$$

Where f is bounded [0,1], and corresponds to the cardinality of the chosen fraction of *D: D_f*. Obviously, there is a fixed number of fractions to consider. λ serves to identify a critical distance at which a point is considered an outlier. Phillips *et al.* (2011) recommend λ first be set to a large (λ = 3) value to find similar solutions, before refining the estimate by setting λ=1.3 for 2D, λ=0.95 for 3D problems.

The problem thus becomes to find the transform *T* and fraction of outliers *f* which minimizes the expression $FRMSD(D, M, f, \mu)$. This can be shown to converge to a local minimum.

A program to handle individual trees, subplots, and plots, diameter to height mapping, saving transforms from subsets *d* of *D* to *M* in an interactive context has been developed and provided with a graphical user interface (GUI). The GUI facilitates manual adjustment of initial positioning and transform of the subplots *d*, binary decisions of points in target point set *M*, fitting of a diameter-height equation from sample trees, and more.

Our application applies an improvement threshold for the FICP algorithm of 1E-6 meters, or 1’000 iterations, before switching to the more aggressive λ. We apply a nonlinear scaling of diameters to imputed heights from the species-agnostic diameter-height function. As mentioned earlier, we compute the full 4x4 transformation matrix but apply only the 2D rotation, translation.

The open-source implementation will be continued to be developed and is expected to feature in at least 3 upcoming articles (including article IV).

8. Appendix II – Dominant height growth for article III

For this initial case, the species-specific fractions of trees on each plot which had attained a height of at least 70% of the single tallest tree on the plot were taken to be co-/dominants. The mean of the dominant tree heights plus two standard deviations was thus taken to best resemble the upper edge. The dominant age was calculated likewise.

We parametrised the expression presented by Cieszewski (2005) against this data:

$$H_2 = \frac{\left(\frac{t_2}{t_1}\right)^j H_1(b+R) - t^j}{H_1 a\left(1-\left(\frac{t_2}{t_1}\right)^j\right) + B + R}$$

Where $R = \sqrt{B^2 - 2a\left(c + t_1^j\right)}$ and $B = b - \frac{t_1^j}{H_1}$.

H_2 being the model estimate for the height at age t_2, the height-age pair H_1 and t_1 identifying the trajectory, and a, b, c, j being parameters to estimate.

Where the error model accounts for increasing possibility of disturbance, errors with the time between the measurement points (Rennolls, 1995).

$$Var\left(H_2 - E(H_2)\right) = \sigma^2(t_2 - t_1)$$

$$\epsilon = H_2 - E(H_2) \sim \mathcal{N}\left(0, \sigma^2(t_2 - t_1)\right)$$

To fit the data, we minimize the negative log-likelihood:

$$-\left(ln(L)\right) = (N/2)ln(2\pi\sigma^2) + (1/2)\sum ln(t_2 - t_1) + (1/2\sigma^2)\sum\{\epsilon^2/(t_2 - t_1)\}$$

Where N is the total number of paired observations (H_1,t_1), (H_2,t_2) and the sum being taken over all pairs. Results (fig. 19, *Norway Spruce*) were in very good agreement with the site-index curves currently in use in Sweden for Norway Spruce (Elfving, 2003) and Scots Pine (Elfving & Kiviste, 1997), but the dearth of inventory data for young stands of Birch resulted in slow trajectories compared to (Eriksson *et al.*, 1997).

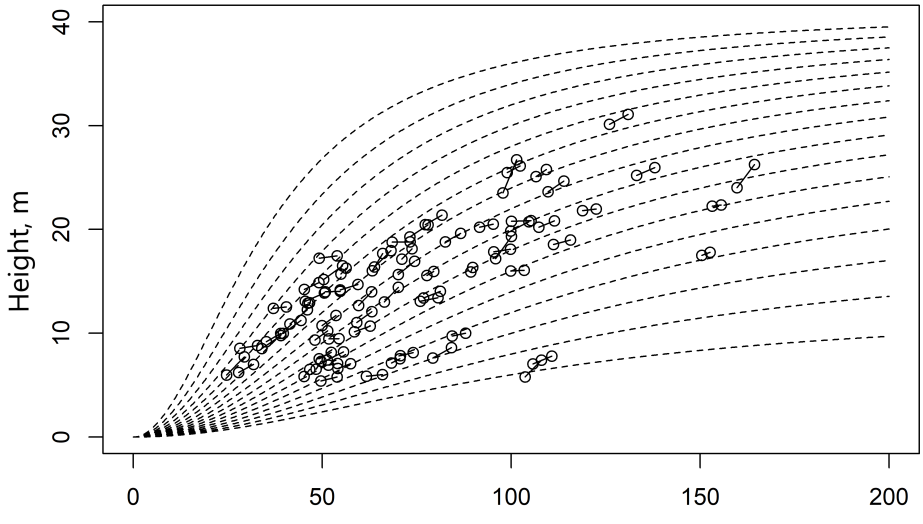

Figure 19. Model fit to data, height over age for Norway Spruce (*P. abies* (L.) H. Karst.).

I

Science of the Total Environment 942 (2024) 173342

Contents lists available at ScienceDirect

Science of the Total Environment

journal homepage: www.elsevier.com/locate/scitotenv

Can mixing *Quercus robur* and *Quercus petraea* with *Pinus sylvestris* compensate for productivity losses due to climate change?

Sonja Vospernik [a,*], Carl Vigren [b], Xavier Morin [c], Maude Toïgo [c], Kamil Bielak [d], Gediminas Brazaitis [e], Felipe Bravo [f], Michael Heym [g], Miren del Río [h], Aris Jansons [i], Magnus Löf [j], Arne Nothdurft [a], Marta Pardos [h], Maciej Pach [k], Quentin Ponette [l], Hans Pretzsch [m]

[a] Department of Forest- and Soil Sciences, Institute of Forest Growth, BOKU, University of Natural Resources and Life Sciences Vienna, Peter-Jordan-Str. 82, A-1190 Vienna, Austria
[b] Department of Forest Resource Management, Swedish University of Agricultural Sciences, Skogsmarksgränd 17, 907 36 Umeå, Sweden
[c] Centre d'Ecologie Fonctionnelle et Evolutive, UMR 5175 CNRS, Univ. Montpellier, EPHE, IRD, 1919 route de Mende, 34293 Montpellier Cedex 5, France
[d] Department of Silviculture, Institute of Forest Sciences, Warsaw University of Life Sciences, Nowoursynowska 159/34, 02776 Warsaw, Poland
[e] Vytautas Magnus University, Department of Forest Science, Studentu 11, Akademija LT-53361, Kaunas dist, Lithuania
[f] Instituto de Investigación en Gestión Forestal Sostenible (iuFOR), Unidad Asociada de I+D+i al CSIC, ETS de Ingenierías Agrarias, Universidad de Valladolid, Avda. De Madrid 44, 34004 Palencia, Spain
[g] Bavarian State Institute of Forestry (LWF), Department Silviculture and Mountain Forest, Germany
[h] Instituto de Ciencias Forestales (ICIFOR- INIA), CSIC, Ctra. A Coruña km 7.5, 28040 Madrid, Spain
[i] Latvian State Forest Research Institute Silava, Rigas 111, Salaspils. Latvia
[j] Swedish University of Agricultural Sciences, Southern Swedish Forest Research Centre, Box 190, 23422 Lomma, Sweden
[k] Department of Ecology and Silviculture, Faculty of Forestry, University of Agriculture in Krakow, al. 29-Listopada, 46 31-425 Kraków, Poland
[l] UCLouvain - Université catholique de Louvain, Earth & Life Institute, Croix du Sud 2 box L7.05.09, 1348 Louvain-la-Neuve, Belgium
[m] Chair of Forest Growth and Yield Science, Department of Life Science Systems, TUM School of Life Sciences, Technical University of Munich, Hans-Carl-Von-Carlowitz-Platz 2, 85354 Freising. Germany

HIGHLIGHTS

- Productivity losses increase with increasing severity of climatic scenario.
- Productivity decreases by 7.7 % and 11.6 % for *Q.* spp. and *P. sylvestris* for RCP 8.5.
- Climate change will shift the competitive advantage from *P. sylvestris* to *Q.* spp.
- Productivity losses can be mitigated but not compensated by the use of mixtures.
- Productivity losses at low latitudes are more severe than at high latitudes.

GRAPHICAL ABSTRACT

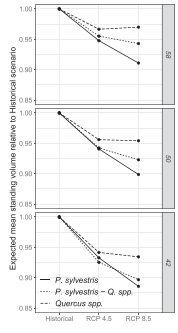

* Corresponding author.
E-mail address: Sonja.Vospernik@boku.ac.at (S. Vospernik).

https://doi.org/10.1016/j.scitotenv.2024.173342
Received 17 February 2024; Received in revised form 7 May 2024; Accepted 16 May 2024
Available online 5 June 2024
0048-9697/

ARTICLE INFO

Editor: Manuel Esteban Lucas-Borja

Keywords:
Mixture
Climate change
Individual tree growth simulation
Adaption
Oak
Pine

ABSTRACT

The climate change scenarios RCP 4.5 and RCP 8.5, with a representative concentration pathway for stabilization of radiative forcing of 4.5 W m^{-2} and 8.5 W m^{-2} by 2100, respectively, predict an increase in temperature of 1–4.5° Celsius for Europe and a simultaneous shift in precipitation patterns leading to increased drought frequency and severity. The negative consequences of such changes on tree growth on dry sites or at the dry end of a tree species distribution are well-known, but rarely quantified across large gradients. In this study, the growth of *Quercus robur* and *Quercus petraea* (*Q.* spp.) and *Pinus sylvestris* in pure and mixed stands was predicted for a historical scenario and the two climate change scenarios RCP 4.5 and RCP 8.5 using the individual tree growth model PrognAus. Predictions were made along an ecological gradient ranging from current mean annual temperatures of 5.5–11.4 °C and with mean annual precipitation sums of 586–929 mm. Initial data for the simulation consisted of 23 triplets established in pure and mixed stands of *Q.* spp. and *P. sylvestris*. After doing the simulations until 2100, we fitted a linear mixed model using the predicted volume in the year 2100 as response variable to describe the general trends in the simulation results. Productivity decreased for both *Q.* spp. and *P. sylvestris* with increasing temperature, and more so, for the warmer sites of the gradient. *P. sylvestris* is the more productive tree species in the current climate scenario, but the competitive advantage shifts to *Q.* spp., which is capable to endure very high negative water potentials, for the more severe climate change scenario. The *Q.* spp.-*P. sylvestris* mixture presents an intermediate resilience to increased scenario severity. Enrichment of *P. sylvestris* stands by creating mixtures with *Q.* spp., but not the opposite, might be a right silvicultural adaptive strategy, especially at lower latitudes. Tree species mixing can only partly compensate productivity losses due to climate change. This may, however, be possible in combination with other silvicultural adaptation strategies, such as thinning and uneven-aged management.

1. Introduction

Recent climate scenarios for Europe predict an average rise in temperature for the medium and extreme emission scenario in the range of 1–4.5 °C for the RCP 4.5, and 2.5–5.5 C for the RCP 8.5 greenhouse gas emission scenarios (Jacob et al., 2014). The climate change scenarios represent concentration pathways for stabilization of radiative forcing of 4.5 and 8.5 W m^{-2} by 2100, respectively (Jacob et al., 2014). The large scale spatial patterns in high resolution climate ensemble models are similar for both scenarios and the predicted increase in temperature across Europe is particularly pronounced in Southern Europe (Jacob et al., 2014). Associated with rises in temperature are changes in precipitation patterns, predicting a decrease in Southern Europe and an increase in precipitation in Central and Northern Europe and a seasonal shift in precipitation (Jacob et al., 2014).

As a consequence, we would expect to observe an earlier occurrence of phenophases (Körner and Basler, 2010; Puchałka et al., 2017; Menzel et al., 2020; Puchałka et al., 2024), a northward migration of tree species (Ozolinčius et al., 2014; Giesecke et al., 2017) similar to the one observed in earlier warming phases (Giesecke et al., 2017), growth depression (Eilmann et al., 2006; Pardos et al., 2021; Salomón et al., 2022) due to an earlier cessation of growth (Strieder and Vospernik, 2021; Puchałka et al., 2024) due to a premature cessation of the cambial activity (Puchałka et al., 2024), increased tree mortality due to hydraulic failure or carbon starvation (Benito Garzón et al., 2018; Choat et al., 2018; Arend et al., 2021; Mantova et al., 2022; Hartmann et al., 2022; Hammond et al., 2022) reinforced by an increased risk of insect pests and tree pathogens (Venäläinen et al., 2020) and an increase of natural hazards and abiotic disturbances (Dupuy et al., 2020; Maurer and Heinimann, 2020; Romeiro et al., 2022). Recent climate warming has pushed many ecosystems to the margins of their ecological niche (Bebi et al., 2001; Camarero et al., 2021) and further rising global temperatures will continue to exacerbate the situation.

Oak (*Quercus* spp. (*Quercus robur* L. and *Quercus petraea* (Matt.) Liebl.)) – Scots pine (*Pinus sylvestris* L.) mixed species forests are a plant association found on xeric, acidophilous sites (Müller, 1992) which are thought to be resistant and resilient to climatic warming (Pretzsch et al., 2020) since both tree genera are well adapted to drought.

Quercus spp. have deep penetrating tap roots and leaves with a thick-walled epidermis (Gil-Pelegrín et al., 2017). *Quercus* spp. can endure an extremely high negative water potential of −4 MPa and can withdraw considerable amounts of stored water from its stem and crown (Zweifel et al., 2009; Peters et al., 2023). As aniso-hydric tree species, they display very little climate sensitivity and quickly recover from summer drought, usually within 1–2 years (Gillner et al., 2013; Haerdtle et al., 2013; Vitasse et al., 2019). *Quercus* spp. are adopted to be productive even under high vapor pressure deficits, but extreme drought can move them to their physiological limit leading to premature leaf cessation (Zweifel et al., 2006).

P. sylvestris is a widely distributed tree species (Brus et al., 2012) that is also drought tolerant with its thick walled epidermis and inset stomata, which protect it from water loss (Zweifel et al., 2009). *P. sylvestris*, however, maintains a significantly higher water potential than do *Quercus* spp., not dropping below −1.5 and −2.5 MPa in leaves (Irvine et al., 1998; Zweifel et al., 2009) and it stores smaller amounts of water in its leaves and crown (Zweifel et al., 2007). The isohydric behavior and tighter stomatal control result in greater limitations of carbon assimilation than is observed for *Q.* spp. (Zweifel et al., 2009) resulting in more pronounced and longer lasting growth response to drought for *P. sylvestris* than for *Q.* spp. (Zweifel et al., 2009) and post-drought growth depression for *P. sylvestris* can last for up to 5 years (Galiano et al., 2011). Thus, while *P. sylvestris* is drought tolerant, it is better adapted to wet and cool conditions in dry environments, where it opens its stomata more widely than *Q.* spp. and then has a higher photosynthetic capacity (Zweifel et al., 2009; Peters et al., 2023).

Both *Q.* spp. and *P. sylvestris* are of high commercial importance (Durrant et al., 2016; Eaton et al., 2016) and many studies have investigated their productivity. At the same site *Q.* spp. were reported to maintain lower tree densities in terms of stem number, basal area and volume, but higher biomass productivity (Yuste et al., 2005), because of their higher wood density. Lower basal area for *Q.* spp. is also reflected by considerably lower maximum basal area per hectare attainable by this species in comparison to *P. sylvestris* (Vospernik and Sterba, 2015). Management concepts and commercial use for the two tree species differ considerably: *P. sylvestris* constitutes 20 % of the standing timber volume in Europe and has an easily workable wood for construction, furniture pulp and paper (Durrant et al., 2016), and can be more easily managed than *Q.* spp. In contrast, *Q.* spp. provides high quality hardwood, appreciated for its durability and hardness. The most valuable oak wood has narrow rings with long economic rotations and frequent management interventions (Eaton et al., 2016).

The increasing frequency of drought extremes associated with climate change is a key challenge to forest ecosystems. Consequently, the quantification of drought effects on tree growth and mortality is of

the highest concern for forest management and forest science (Bhuyan et al., 2017). Selection of drought tolerant tree species (Thurm et al., 2018; Vospernik, 2021), managing tree species mixture (Steckel et al., 2020), climate adapted forest management and selection of suitable provenances (Taeger et al., 2013; Karrer et al., 2022) are all important strategies to mitigate climate change impacts. In particular, mixing tree species has been proposed as one of the solutions to promote adaptive forest management because mixed stands are supposed to be, on average, more productive, more resistant and resilient to drought (Pretzsch et al., 2020; Steckel et al., 2020; Pardos et al., 2021), herbivores and pathogens (Jactel et al., 2017, 2019) than pure stands – although the strength of the mixture effects may strongly vary with species and site conditions (Pardos et al., 2021; Strieder and Vospernik, 2021).

While mixing tree species is beneficial, growth depressions follow drought. These are well documented (*Quercus*: Toïgo et al., 2015; Prokop et al., 2016; Roibu et al., 2020; Vospernik et al., 2023; *Pinus*: Rigling et al., 2002; Toïgo et al., 2015; Treml et al., 2022), since both tree species are well-represented in dendro-ecological studies. In general, *Q.* spp. tree ring chronologies correlate positively with precipitation in spring and early summer while during late-wood formation climate response is unstable and varying in sign from site to site (Prokop et al., 2016; Roibu et al., 2020; Vospernik et al., 2023). High autumn temperatures positively affect carbohydrate reserves and thus are positively associated with ring width for *Q.* spp. of the next year (Prokop et al., 2016; Roibu et al., 2020; Vospernik et al., 2023). Likewise, spring and early summer precipitation positively affect the growth of *P. sylvestris* on xeric sites (Rigling et al., 2002; Treml et al., 2022). Unlike *Q.* spp., *P. sylvestris* ring growth was reported to be positively affected by winter precipitation, which is important for successful shoot and root growth but *P. sylvestris* is negatively affected by high summer temperatures (Rigling et al., 2002; Treml et al., 2022). Fluctuations in the ring width of *P. sylvestris* are reported to be higher than that of *Q.* spp. because of its iso-hydric nature (Zweifel et al., 2009).

In Europe, additional growth depressions in future scenarios are thought to be most pronounced in Mediterranean areas (Aldea et al., 2018; Martínez-Sancho et al., 2021). Here, temperature rise is predicted to be highest (Jacob et al., 2014), and these sites are currently already particularly dry sites, with low water availability during summer (Aldea et al., 2018; Martínez-Sancho et al., 2021) with stressful site conditions. At these sites plant species are, however, genetically and phenologically adapted to low water availability (Martínez-Sancho et al., 2021), and trees at temperate or boreal sites with currently sufficient water availability and with currently larger absolute and relative growth rates, might be affected more by climatic warming, and decrease more in growth, while being still higher than in Mediterranean areas. At the north-eastern range limit, despite predicted maintaining their climatic niche, growth of *Q. robur* decreased in dry years (Puchałka et al., 2024), possibly because this widely distributed species has different ecotypes, which are only adapted to a proportion of the niche occupied by the species as a whole (Sáenz-Romero et al., 2019; Puchałka et al., 2024).

In order to supply decision makers, researchers and stakeholders with an in-depth information and quantification of the consequences of climate growth, it is imperative to integrate climate change scenarios with forest growth models. This can be done by using climate and mixture sensitive individual tree (*e.g.* Vospernik, 2021), gap (*e.g.* Morin et al., 2021) or process-based models (*e.g.* Gupta and Sharma, 2019; Bouwman et al., 2021). The first type of model predicts growth and mortality of individual trees, the second type uses a similar approach but focuses on grid cells and the latter focus on tree physiological processes such as photosynthesis, respiration, stomatal conductance or carbon allocation (Weiskittel et al., 2011). Individual tree growth models most easily integrate empirical research on tree rings and dendrometers and forest management scenarios because of the shared focus on the individual tree. Also, they are less computationally expensive than process based models assuring reasonable prediction times and the detailed output provided by these models is often not required. Therefore, they are the preferred means for simulating forest productivity (Weiskittel et al., 2011), but predictions of tree growth with climate change remain scarce (Bombi et al., 2017; Dyderski et al., 2018; Girardin et al., 2008; Bayat et al., 2022; De Wergifosse et al., 2022) and are still lacking for mixed *Q.* spp. and *P. sylvestris* stands.

Growth reactions for different climate scenarios have not yet been studied in detail for *Q.* spp.-*P. sylvestris* pure and mixed forests. In this study, we quantify growth reactions for *Quercus* and *Pinus* on different sites across Europe under different climate scenarios and compare pure and mixed species stand with respect to climatic resistance and resilience and productivity response.

1.1. Hypothesis

We hypothesize that:

1. The expected standing volume in 2100, decreases on average for all species with increased severity of the scenario (Historical ≪ RCP 4.5 ≪ RCP 8.5).
2. If hypothesis 1 holds, *Q.* spp. will be better able to buffer these changes than *P. sylvestris* (experience less of a decline with increased severity of scenario).
3. Additionally, we hypothesize that the mixed species stands will show less response in productivity than the single species stands do.
4. We expect that, in line with our current understanding of the species' climatic distribution, the volume fall-off with increased scenario severity will be stronger for lower-latitude plots, which are closer to their species distributional xeric limit.

2. Data

2.1. Tree data

Initial data for the simulation was data from *Q.* spp. – *P. sylvestris* triplets established as part of the ERA-Net SUMFOREST project REFORM ("REsilience of FORest Mixtures", reform-mixing.eu) across Europe. This is described in detail in previous studies focusing on stand productivity and tree drought resilience (Pretzsch et al., 2020; Steckel et al., 2020; Vospernik et al., 2023) and tree growth simulation under current climatic conditions (Engel et al., 2021). The dataset encompassed 23 triplets. By design, each triplet contains three plots, whereof two are single-species stands of *Q.* spp. and *P. sylvestris*, and one is a mixed stand of *Q.* spp. - *P. sylvestris*. The triplet data covered large geographic (Fig. 1) and environmental (Fig. 2) gradients across Europe. Mean annual temperatures at the sites varied between 5.5 °C and 11.4 °C and precipitation is 586–929 mm. Plots were established in mature stands with an interquartile age range of 55–91.5 years and an interquartile stand volume of 317–613 m^3ha^{-1} (Table 1) with median stand characteristics being comparable in both the pure and mixed stands. Even though there is variation between different triplets, the pure and mixed plots within each triplet show extremely little variation in stand characteristics, showing the plots were carefully established (Appendix: Table 1).

2.2. Climate scenarios

Historical and future climate time series were acquired from CHELSA (High Resolution Climatologies for Earth's Land Surface; https://chelsa-climate.org/), a high-resolution (30 arc *sec*) climate repository for the land surface (Karger et al., 2017). We accounted for existing variability in climate projections by simulating the data over the period 2006–2100 under four non-intercorrelated global circulation models (ACCESS1-3, CESM1-BGC, MIROC5, CMCC-CM) and two climate scenarios (RCP 4.5; RCP 8.5) following the recommendation of Sanderson et al. (2015). We retrieved time series for monthly minimum

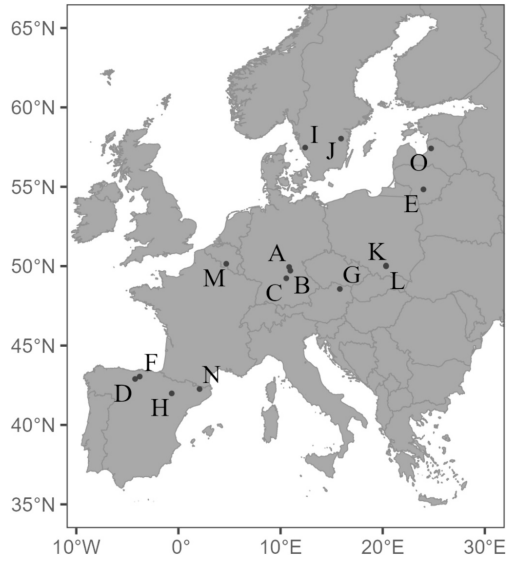

Fig. 1. Location of the study sites. Letters indicating the study site are also used in Fig. 2 and in the appendix.

temperature, monthly maximum temperature and monthly precipitation sum (Karger et al., 2020). We calculated the time series of mean temperature by averaging the minimum and maximum monthly temperature. We compared the results obtained in the context of climate change with those of a null scenario obtained from eight randomized historical climate time series (1979–2013) provided by CHELSA to determine the effects of climate change on tree growth. The time series of future climates provided by CHELSA showed stable precipitation regimes over the 21th century; For some regions an increase of precipitation was predicted, while for others there was no trend or an opposite trend. In contrast to past intra-annual precipitations recorded, the predicted precipitation sums, showed hardly any variation in precipitation sums between years. To overcome this short-coming, we replaced the precipitation forecasts with time series of randomized historical precipitation given by CHELSA. Finally, we calculated average climatic conditions per site to keep climatic conditions constant between plots of the same triplet. The climate conditions simulated in each scenario are illustrated in Fig. 2. While current mean annual temperatures varied between 5.5 °C and 11.4 °C (Appendix T1) and remain at this level in the historical scenarios, with some precipitation shifts, the scenario RCP 4.5 showed an increase in temperature up to mean annual temperatures of 12.5 °C during the study period and up to 14 °C in the RCP 8.5 scenario and little change in precipitation for the *Q.* spp. and *P. sylvestris* triplet plots.

3. Methods

3.1. Individual tree growth simulations

Simulations were carried out with the individual tree growth simulator PrognAus. The simulator consists of a basal area increment (Vospernik, 2021), a height increment (Nachtmann, 2006), a crown ratio (Hasenauer and Monserud, 1996), mortality (Monserud and Sterba, 1999) and an ingrowth model (Ledermann, 2002). The basal area increment model encompasses 22 species, which are modeled based

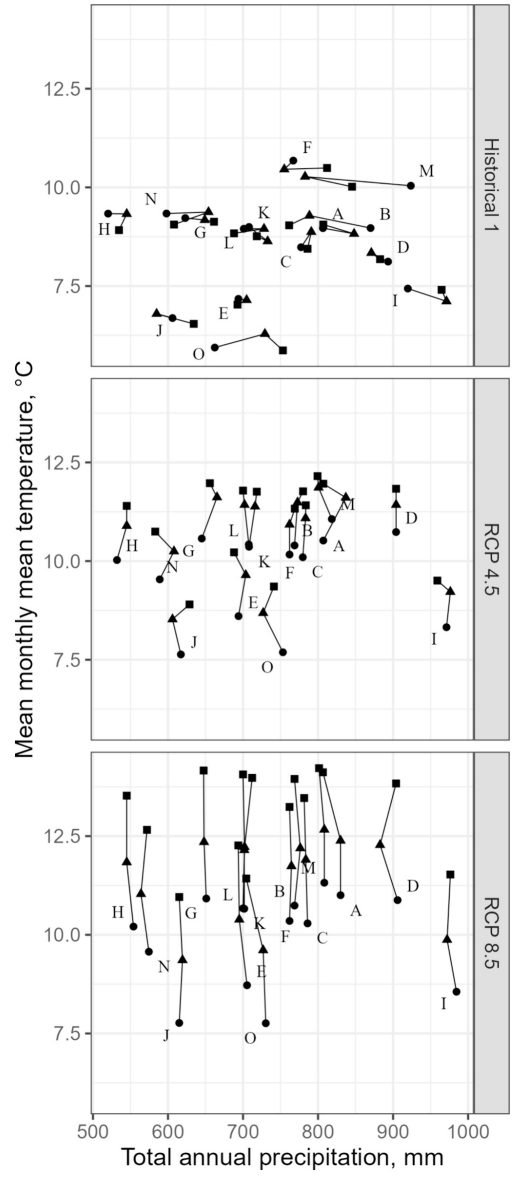

Fig. 2. Median of the mean monthly mean temperature °C and total annual precipitation (mm) during 3 periods of the simulation: 2017–2044 (circle); 2045–2072 (triangle); 2073–2100 (square). Trajectories with a shared letter denote the same site in different simulations.

on tree size, density and competition, climate, soil variables, harvesting and disturbances and mixture. The competition indices used are non-spatial and climate is modeled by separating climatic site effects from weather conditions by including long-term mean temperature, long-term mean precipitation and the yearly deviations thereof as input

Table 1
Summary (Q1: 25 % quantile, Q2: median, Q3: 75 % quantile) of mixture-wise initial stand conditions. Plot size (hectare), age (yrs), trees (ha^{-1}), basal area ($m^2\ ha^{-1}$), volume ($m^3\ ha^{-1}$).

	Q. spp.			Q. spp.-*P. sylv.*			*P. sylv.*		
	Q1	Q2	Q3	Q1	Q2	Q3	Q1	Q2	Q3
Plot size	0.06	0.11	0.16	0.15	0.19	0.29	0.07	0.11	0.12
Age	55	75	87	54	65.5	83	48	66	92
Trees	447	649	1493	553	779	1073	623	885	1196
Basal area	34.2	44.0	48.5	41.3	45.3	52.1	47.3	52.1	60.9
Volume	317	366	540	397	515	564	421	510	613
Basal area per species									
Q. spp.	87	93	97	35	45	48	0	3	6
P. sylvestris	0	0	3	42	52	55	86	92	97
Other	2	4	13	1	4	12	0	3	8

parameters. Mixture effects for many different species are represented by including the basal area proportion of them in the model. While the basal area increment model is climate and mixture sensitive (Vospernik, 2021), these effects are not explicitly included in the other Prognaus models (height increment: Nachtmann, 2006; crown ratio: Hasenauer and Monserud, 1996; mortality: Monserud and Sterba, 1999; or ingrowth: Ledermann, 2002) even though such effects might be implicitly reflected by the site factors used in the models (*e.g.* elevation) and stand variables (*e.g.* dominant height). All sub-models were developed based on the data of the Austrian National Forest Inventory. The data cover a large environmental gradient in temperature and precipitation (Vospernik, 2021) which because of Austria's large altitudinal (colline zone to timberline) extent and thus encompassing many climatic conditions encountered in Europe, but may not be representative for very dry Mediterranean sites. Nevertheless, the data encompass the climatic conditions encountered on triplet plots. Measurements taken on the triplet plots and climate scenarios were used as input for the individual tree growth simulations. Simulations were done at a yearly time step, without any silvicultural intervention or treatment applied during the simulation period from 2017 to 2100 and not taking into account ingrowth, thus focusing on the development of the current stand on the plots. An example of the simulation for an individual plot of a triplet is shown in Fig. 3.

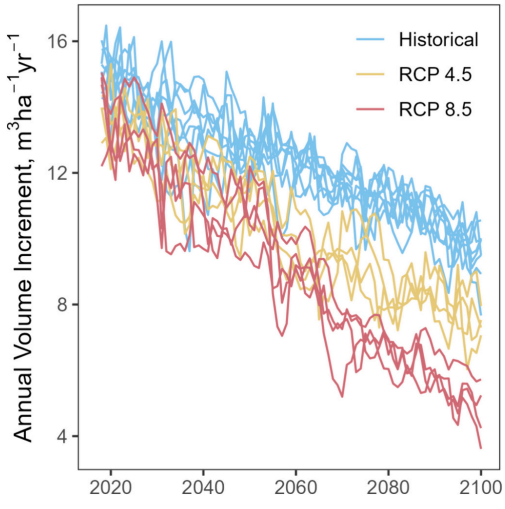

Fig. 3. Example of simulated trajectories for the German stand C-1, *P. sylvestris* (Initial conditions: volume 441 m^3ha^{-1}, basal area 50.6 m^2ha^{-1} (92.7 % *P. sylvestris*), number of trees 1750 ha^{-1}, 45 years of age). Annual volume increment decreases with age – but more rapidly so during more severe climatic scenarios.

3.2. Generalization of the model output to a stand-level model

Raw simulation results were generalized using a linear mixed model. Since the mortality model is not climate sensitive, and we do not have any information on the mortality prior to our inventory of the plots, analysis focused on the standing living volume (as opposed to the total production) at the end of the simulation (year 2100) given only information on the climatic scenario and the initial state of the stand in question. For this reason, we postulate that this relationship can be accurately assessed with a linear mixed model with readily accessible summary input terms from a forest stand.

Linear Mixed Models (LMM's) can be generally expressed as:

$$y = X\beta + Zu + \epsilon \quad (1)$$

where X is a matrix of the predictor variables, β are the fixed-effect coefficients, Z is a design matrix of the random effects, u are the random effects and ε the residuals.

To test our hypotheses H1 through H4, we designed a full best subset search (respecting the principle of marginality) of a global maximum model to select a LMM which accounts for potential differences in the scenario increments as the result of differing starting conditions in terms of standing volume and age, and any site-specific reaction. The best subset search was performed with MuMIn::dredge (v. 1.47.5, Bartoń, 2023), given a number of potential inputs (see supplementary code). All subset models included a plot-wise random effect and were fitted by maximum likelihood, ML (Laplace approximation) with `lme4::lme` (v. 1.1.33, Bates et al., 2015). The final model was that which resulted in the best (lowest) marginal Akaike's Criterion. The marginal AIC as a model selection criterion can be shown to be asymptotically related to a Leave-One-Cluster-Out Cross-Validation, which significantly cuts down on computational expense (Greven and Kneib, 2010; Fang, 2021). This is particularly suited for instances where the main interest is the prediction of previously unobserved levels.

The final model was then refitted by REML, Restricted Maximum Likelihood, to avoid the bias associated with the shrinkage property from ML estimation of random effect estimates. As the random effect estimates are then the empirical best linear unbiased predictors, which result in the minimum mean squared error given the variance components, this is particularly suitable for models mainly interested in prediction (Welham et al., 2014, p. 436). Since the (biased) estimator for the residual variance from ML is $\hat{\sigma}^2$, and the unbiased REML estimator is $\frac{n}{(n-p)}\hat{\sigma}^2$, the bias for our final model with 37 fixed-effect parameters and 648 observations would amount to $\frac{n}{(n-p)} = \frac{648}{(648-37)} = 1.06$.

Our final model with fixed-effect parameters is detailed below (Table 3). Random-effects values for the 72 plots are not presented.

The marginal mean estimates and corresponding confidence

Table 2
Simulation results for the different stand types. Volume (m^3ha^{-1}) and its standard deviation and cumulative mortality till the end of the simulation period (m^3ha^{-1}) and the standard deviation thereof.

Mixture	Climate	Volume 2100		Cumulative mortality 2100	
		Mean	SD	Mean	SD
		m^3ha^{-1}	m^3ha^{-1}	m^3ha^{-1}	m^3ha^{-1}
Oak	Historic	748.7	±61.2	420.1	±145.7
Oak	RCP 4.5	733.6	±64.8	357.3	±134.0
Oak	RCP 8.5	734.6	±66.5	370.6	±140.5
Oak-Pine	Historic	774.1	±79.7	363.1	±123.8
Oak-Pine	RCP 4.5	744.9	±85.9	315.4	±115.8
Oak-Pine	RCP 8.5	731.4	±87.7	307.2	±114.6
Pine	Historic	861.2	±101.1	374.4	±127.8
Pine	RCP 4.5	825.6	±101.7	342.4	±116.2
Pine	RCP 8.5	790.9	±100.9	324.6	±108.6

intervals for a new unobserved level were calculated with covariates set at their mixture-wise averages, longitude set at the mean of all plots, and latitude set as the median or one of the extreme values.

In order to assess the likelihood of any of the marginal estimates achieving at least the mean of another marginal estimate, confidence and prediction intervals for the 27 (3 climate scenarios, 3 latitudes, 3 stand species mixtures) marginal estimates were calculated by a bootstrapping routine (10'000 simulations), simulating the conditional distribution of the predictions, and considering the variance of the random effects. From this, comparisons of the response probabilities could be presented (Tables 4, 5 & 6). Where the tabulated values are the likelihood that a random unobserved datum from one of the marginal estimates will fall above the mean of any other marginal estimate. In text, we use the term degree of dominance (henceforth dominance) of the best performing species to signify this likelihood, *e.g.* If 78 % of *P. sylvestris* stands under a certain climate and at a certain latitude would be expected to achieve at least the mean of that of a *Q.* spp. stand, *P. sylvestris* displays a strong dominance over *Q.* spp.

4. Results

At the end of the simulation period (2100) the standing volume was highest in the historic scenario (Table 2). In this scenario also the density dependent cumulative mortality during the simulation period was highest resulting in the highest total productivity (2100).

4.1. Linear mixed model

A more detailed analysis of simulation results with the LMM gave the following results: climate (historical and future scenarios), geographical position and stand level (age, volume, stem number and mixture) variables were significant, at least when considering their interactions with other variables (Table 3, random effects not presented). In total, some 6.9 % of variance was explained by the model, whereof 79.5 % by the fixed effects, and some 17.3 % by the random-effects (Nakagawa and Schielzeth, 2013).

Where mixture (*Q.* spp., *Q.* spp. – *P. sylvestris* or *P. sylvestris*) is the species mix as a categorical variable; climate (Historical 1, RCP 4.5, RCP 8.5) is the simulated scenario; Age_{2017}, $Volume_{2017}$, $Stems_{2017}$ express

Table 3
Parameterised linear mixed model. Independent variable: 'Standing volume 2100'. *t*-Tests with Satterthwaite's method. Level of significance: ' ' 0.1, '.' 0.05, '*' 0.01, '**' 0.001, '***' 0.

Variable	Estimate	Std. error	Pr (>|t|)	
(Intercept)	8.126E+01	1.217E+02	0.507235	
Climate RCP 4.5	3.694E+01	2.268E+01	0.103829	
Climate RCP 8.5	2.829E+01	2.268E+01	0.212649	
Latitude	1.087E+01	2.823E+00	0.000304	***
Longitude	5.377E+00	6.423E+00	0.406091	
Mixture *Q.* spp. - *P. sylvestris*	2.272E+01	1.110E+02	0.838550	
Mixture *P. sylvestris*	−1.774E+02	1.126E+02	0.120639	
$Stems_{2017}$	6.779E−02	1.560E−02	5.92E−05	***
Age_{2017}	−9.396E−01	2.905E−01	0.002047	**
$Volume_{2017}$	3.474E−01	4.262E−02	4.96E−11	***
Climate RCP 4.5:Latitude	−1.367E+00	5.393E−01	0.011498	*
Climate RCP 8.5:Latitude	−1.555E+00	5.393E−01	0.004088	**
Climate RCP 4.5:Longitude	−5.784E+00	1.301E+00	1.07E−05	***
Climate RCP 8.5:Longitude	−8.659E+00	1.301E+00	6.86E−11	***
Climate RCP 4.5:Mixture *Q.* spp. - *P. sylvestris*	1.468E+00	2.923E+00	0.615741	
Climate RCP 8.5:Mixture *Q.* spp. - *P. sylvestris*	−1.193E+00	2.923E+00	0.683373	
Climate RCP 4.5:Mixture *P. sylvestris*	−1.655E+00	3.162E+00	0.600842	
Climate RCP 8.5:Mixture *P. sylvestris*	−1.068E+00	3.162E+00	0.735665	
Climate RCP 4.5:$Stems_{2017}$	8.408E−03	2.888E−03	0.003739	**
Climate RCP 8.5:$Stems_{2017}$	−3.968E−03	2.888E−03	0.169985	
Climate RCP 4.5:Age_{2017}	1.529E−01	5.607E−02	0.006606	**
Climate RCP 8.5:Age_{2017}	2.940E−01	5.607E−02	2.23E−07	***
Latitude:Mixture *Q.* spp. - *P. sylvestris*	2.238E+00	2.610E+00	0.394880	
Latitude:Mixture *P. sylvestris*	4.534E+00	2.596E+00	0.086333	.
Longitude:Mixture *Q.* spp. - *P. sylvestris*	−2.076E+00	1.388E+00	0.140418	
Longitude:Mixture *P. sylvestris*	−9.662E−01	1.323E+00	0.468259	
Mixture *Q.* spp. - *P. sylvestris*:$Stems_{2017}$	−6.888E−02	1.951E−02	0.000842	***
Mixture *P. sylvestris*:$Stems_{2017}$	−2.991E−02	2.086E−02	0.157294	
Mixture *Q.* spp. - *P. sylvestris*:Age_{2017}	−7.891E−01	3.778E−01	0.041375	*
Mixture *P. sylvestris*:Age_{2017}	−4.248E−01	3.596E−01	0.242611	
Climate RCP 4.5:Latitude:Longitude	1.958E−02	1.364E−01	0.886372	
Climate RCP 8.5:Latitude:Longitude	7.896E−02	1.364E−01	0.564897	
Historical:Latitude:Longitude	−4.069E−01	1.443E−01	0.006197	**
Climate RCP 4.5:Mixture *QP*[a]:$Stems_{2017}$	−4.834E−03	2.736E−03	0.077812	.
Climate RCP 8.5:Mixture *QP*[a]:$Stems_{2017}$	1.557E−02	2.736E−03	2.06E−08	***
Climate RCP 4.5:Mixture *P. sylvestris*:$Stems_{2017}$	7.689E−04	3.111E−03	0.804886	
Climate RCP 8.5:Mixture *P. sylvestris*:$Stems_{2017}$	2.672E−03	3.111E−03	0.390802	

[a] QP: Quercus spp. – *P. sylvestris*.

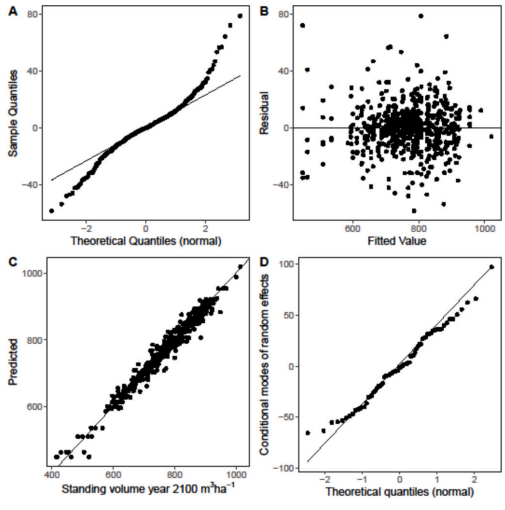

Fig. 4. Diagnostic plots of the LMM. Subplot A. QQ-plot of model residuals. Subplot B. Residuals *versus* fitted. Subplot C. Predicted *versus* actual values. Subplot D. Conditional modes *versus* normal quantiles.

the initial state of the plot in 2017 (in years, cubic meters, and stems per hectare, respectively); latitude and longitude express the location of each plot in decimal degrees. Colon (':') signifies interaction terms.

Model diagnostics (Fig. 4A) indicate model residuals are under-dispersed compared to that expected from $\mathcal{N}(0,1)$ and largely homoscedastic (Fig. 4B). As can be seen in the plot of the observed *versus* predicted (Fig. 4C) overall fit is satisfactory (mean absolute percentage error: 1.49 %). The mixed model conditional modes (random effects) are close to normal (Fig. 4D).

Dimension size adjusted Generalized Variance Inflation Factor (GVIF1/(2*df)) for the different variables was, as could be expected, moderately high to high as a result of the low number of factor levels and many interactions (see supplementary documentation) and inclusion of square terms (volume). This is not perceived to be problematic in terms of prediction, given that such data could be assumed to have the same multicollinearity.

Marginal mean estimates for the mixture-wise means of the covariates at the minimum, median and maximum latitude are presented in Fig. 5. For *P. sylvestris*, an almost linear decreasing trend with increasing scenario severity is shown, with a stronger slope at low latitudes. Both the species mixture (*Q.* spp. – *P. sylvestris*) and *Q.* spp. show a demonstrable stronger decrease in volume from the historical scenario to RCP 4.5 than a subsequent shift to RCP 8.5, where reactions are more diverse. *Q.* spp. in particular, shows a maintained mean value under RCP 8.5 compared to RCP 4.5 at the highest latitude, with slightly lower values for the median and lowest latitude. *Q.* spp. – *P. sylvestris* does show a continued decrease relative to the historic scenario when moving from the RCP 4.5 to the RCP 8.5 scenario, although not as strong as the jump

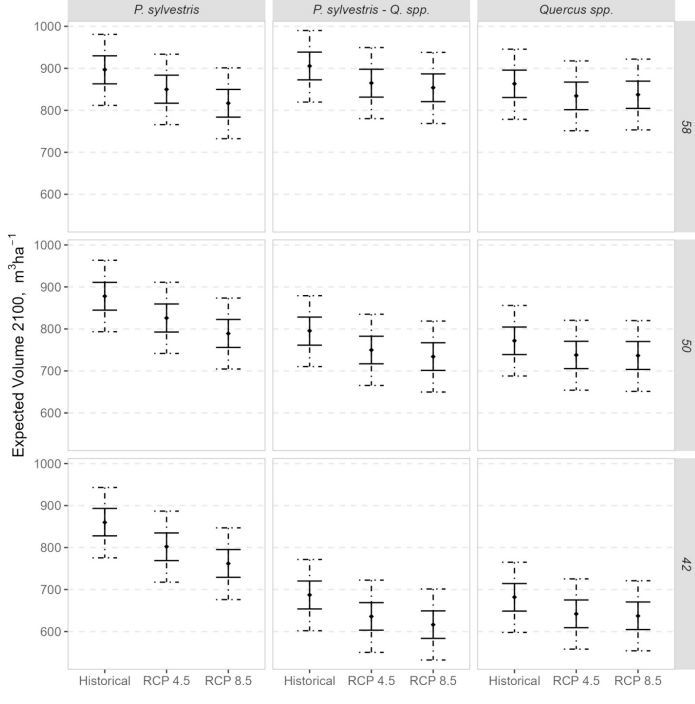

Fig. 5. Estimated marginal means (the predicted means of the response for each level, *ceteris paribus*) from the LMM. Points are the mean estimate. Solid error-bars represent the confidence interval of the estimate. Dashed error-bars represent the prediction interval of the estimate. Numbers in the panel strip text on the right refer to latitude in decimal degrees.

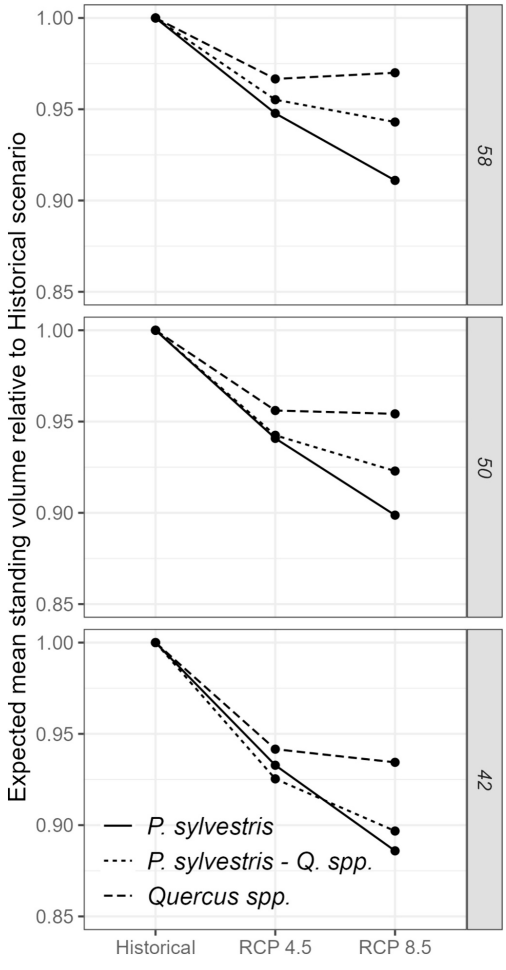

Fig. 6. Marginal mean estimates by stand composition and minimum, median and maximum latitude (values rounded in the figure only) expressed in terms of the historical scenario. Numbers in the panel strip text on the right refer to latitude in decimal degrees.

from the historic scenario to RCP 4.5 (Fig. 6).

At the three latitudes examined (58°N, 50°N, 42°N), *P. sylvestris* shows an almost linear decrease expressed relative to the historic scenario, in which the RCP 8.5 entails almost a repeat loss of standing volume (from high to low latitude, RCP 4.5: −5.2 %, −5.9 %, −6.7 %; RCP 8.5: −8.9 %, −10.1 %, −11.5 %). Q. spp. proves to be considerably more resilient than *P. sylvestris* in the RCP 4.5 – RCP 8.5 scenario comparison, where the rate of decrease observed in the Historical – RCP 4.5 shift has been stemmed completely, reversed, or only slightly continuing (RCP 4.5–3.3 %, −4.4 %, −5.8 %; RCP 8.5: −3.0 %, −4.6 %, −6.5 %). The Q. spp. – *P. sylvestris* mixture presents an intermediate resilience to increased scenario severity (RCP 4.5: −4.4 %, −5.8 %, −7.4 %; RCP 8.5: −5.7 %, −7.7 %, −10.3 %). Moving from the higher latitude towards the lower latitudes, the standing volume relative to the historical scenario rapidly encroaches on the losses experienced by the *P. sylvestris* stands, and at the lowest latitude under the RCP 4.5 scenario demonstrates an even inferior resilience.

4.2. Response probability tables

The effect of such a decrease in the mean estimate of standing volume 2100 is better expressed in terms of the response probabilities (Tables 4, 5, 6). It becomes then clear (as can also be seen from Fig. 5), that although *P. sylvestris* experiences the species-wise largest relative decrease relative to the historical scenario, the terms of its dominance (the likelihood that a given species could be expected to achieve at least the mean of a second species) is strongly related to the latitude examined. The dominance of *P. sylvestris* to *Q.* spp. under the same scenario decreases with increasing latitude and severity of the scenario. At 42°N, this dominance is close to absolute. At 50°N, this dominance has decreased to 99 %, 98 % and 89 % under the historical, RCP 4.5 and RCP 8.5 scenario, respectively. At 58°N, only 78 %, 64 % and 32 % of *P. sylvestris* stands are expected to achieve at least the mean standing volume of that of *Q.* spp. under the examined scenarios. The dominance of *Q.* spp. to the *Q.* spp. - *P. sylvestris* mixture increases with scenario severity, but *Q.* spp. - *P. sylvestris* is more strongly favored at higher latitudes. The dominance of *P. sylvestris* relative to the *Q.* spp. - *P. sylvestris* mixture decreases with latitude and scenario severity. In Tables 4, 5 and 6, bold values indicate series of scenario severities where the direction of the dominance switches. At 42°N, the relatively weak dominance of the *Q.* spp. - *P. sylvestris* mixture to *Q.* spp. is rapidly lost, such that under RCP 4.5 the dominance enjoyed by the *Q.* spp. - *P. sylvestris* mixture under the historical scenario is reversed and of the same strength. Under RCP 8.5 this dominance by *Q.* spp. has increased to almost 70 %. At the intermediate examined latitude, 50°N, a strong dominance (~71 %) of the *Q.* spp. - *P. sylvestris* mixture to *Q.* spp. is rapidly dismantled, and under the most severe scenario, RCP 8.5, switches direction, albeit very weakly. At the highest examined latitude, 58°N, a very strong dominance of *P. sylvestris* to *Q.* spp. of c. 78 % is reversed to a dominance of *Q.* spp. to *P. sylvestris* at 68 % under RCP 8.5.

Table 4
Response probabilities (probability of a new observation achieving at least the mean of the contestant) for 42°N. Read row to column. Scenario severity series (on the diagonals of the submatrices) are printed in bold if they demonstrate a directional change in dominance.

Latitude	42	*Q.* spp.			*Q.* spp. - *P. sylvestris*			*P. sylvestris*		
	%	Historical	RCP 4.5	RCP 8.5	Historical	RCP 4.5	RCP 8.5	Historical	RCP 4.5	RCP 8.5
Q. spp.	Historical	49.89	82.33	85.09	**44.91**	84.76	93.18	0.00	0.26	3.29
	RCP 4.5	17.80	49.69	54.22	14.55	**55.17**	72.10	0.00	0.01	0.30
	RCP 8.5	14.84	45.40	49.67	12.09	50.72	**68.46**	0.00	0.01	0.18
Q. spp.- *P. sylvestris*	Historical	**55.14**	85.67	88	49.79	88.02	94.82	0.00	0.37	4.40
	RCP 4.5	14.44	**44.68**	49.00	11.70	50.12	67.79	0.00	0.01	0.18
	RCP 8.5	6.32	28.33	**31.70**	5.31	32.48	49.39	0.00	0.00	0.03
P. sylvestris	Historical	99.99	100	100	100	100	100	49.72	91.16	98.76
	RCP 4.5	99.76	99.99	99.98	99.53	99.97	100	9.13	49.81	82.93
	RCP 8.5	97.00	99.64	99.80	95.52	99.79	99.92	1.21	16.87	50.31

Table 5
Response probabilities (probability of a new observation achieving at least the mean of the contestant) for 50°N. Read row to column. Scenario severity series (on the diagonals of the submatrices) are printed in bold if they demonstrate a directional change in dominance.

Latitude	50	*Q.* spp.			*Q.* spp. - *P. sylvestris*			*P. sylvestris*		
	%	Historical	RCP 4.5	RCP 8.5	Historical	RCP 4.5	RCP 8.5	Historical	RCP 4.5	RCP 8.5
Q. spp.	Historical	50.11	78.88	79.76	**28.52**	69.18	80.46	0.55	10.41	34.55
	RCP 4.5	21.65	50.14	51.41	8.91	**38.02**	52.74	0.05	1.86	12.46
	RCP 8.5	21.02	49.05	50.32	8.47	37.07	**51.73**	0.04	1.73	11.79
Q. spp.- *P. sylvestris*	Historical	**71.42**	91.35	91.90	49.99	84.99	92.46	2.90	24.35	55.85
	RCP 4.5	31.27	**61.57**	62.89	14.44	49.87	64.52	0.14	3.94	18.97
	RCP 8.5	19.79	47.01	**48.42**	7.84	35.48	50.00	0.04	1.49	10.87
P. sylvestris	Historical	99.28	99.93	99.95	97.32	99.86	99.94	49.71	88.69	98.14
	RCP 4.5	89.75	98.08	98.22	75.41	96.21	98.35	11.56	49.8	80.23
	RCP 8.5	65.29	88.59	89.14	43.43	81.23	89.79	1.91	19.50	49.19

Table 6
Response probabilities (probability of a new observation achieving at least the mean of the contestant) for 58°N. Read row to column. Scenario severity series (on the diagonals of the submatrices) are printed in bold if they demonstrate a directional change in dominance.

Latitude	58	*Q.* spp.			*Q.* spp. - *P. sylvestris*			*P. sylvestris*		
	%	Historical	RCP 4.5	RCP 8.5	Historical	RCP 4.5	RCP 8.5	Historical	RCP 4.5	RCP 8.5
Q. spp.	Historical	50.22	74.69	72.85	16.22	47.81	58.74	**21.62**	62.23	85.69
	RCP 4.5	24.75	50.28	47.14	5.20	23.68	32.51	7.49	**35.85**	65.33
	RCP 8.5	27.02	53.12	50.03	6.02	26.09	35.18	8.47	38.51	**68.10**
Q. spp.- *P. sylvestris*	Historical	83.64	94.98	94.57	49.91	82.20	88.61	58.04	89.83	98.00
	RCP 4.5	52.40	76.45	74.54	17.55	50.00	60.87	23.46	64.11	87.01
	RCP 8.5	41.43	67.51	65.32	11.63	39.61	49.91	15.94	53.88	80.36
P. sylvestris	Historical	**78.13**	92.61	91.59	41.96	76.30	83.93	49.92	86.2	96.79
	RCP 4.5	37.97	**64.16**	61.67	9.99	36.16	46.03	13.98	49.68	77.53
	RCP 8.5	14.34	34.93	**31.92**	2.10	13.22	19.66	3.33	22.73	50.11

5. Discussion

Q. spp. are predicted to be a winners of climate change increasing their current range with increasing climate warming, while the current range of *P. sylvestris* is predicted to decrease (Bombi et al., 2017; Dyderski et al., 2018). In line with these species distribution predictions, our growth simulations suggest that with increasing climatic warming, the decrease in the growth of *Q.* spp. is predicted to remain weak, whereas larger differences were found for *P. sylvestris* so that *P. sylvestris* can only be considered moderately resistant to a warming climate. The between species differences are consistent with the respective autoecologies: *Q.* spp., with its deep root system and its ability to endure very negative water potentials, is well adapted to climatic warming (Zweifel et al., 2006) because it continues sequestering carbon under drought conditions, while *P. sylvestris* closes its stomata earlier, at the cost of photosynthesis. Empirical research also shows that *Q.* spp. show less variability in ring width in comparison to other tree species (Gillner et al., 2013; Vitasse et al., 2019).

Mixture is currently beneficial for productivity at the stand level but positive mixture effects on productivity for *Q.* spp. and *P. sylvestris* are minor and only partly compensate for the decrease in growth with increasing climatic warming and the advantage of mixture is reported to decrease with drought (Aldea et al., 2022). Minor gains in productivity were also reported in empirical studies quantifying the effect of mixing on *Q.* spp. and *P. sylvestris* and improved drought response in the mixture was reported in some studies (Steckel et al., 2020) and a greater temporal stability (del Río et al., 2022), while other studies were not able to confirm a beneficial effect of mixture on drought (Bonal et al., 2017). Gains in productivity reported for *Q.* spp. and *P. sylvestris* mixed stands were 7 % and 9 %, respectively (Steckel et al., 2020; Pretzsch et al., 2020) and are thus smaller than the 8.9–11.5 % productivity loss expected for the more productive *P. sylvestris* in the RCP 8.5 scenario. Although only partly compensating for productivity losses, the mixture has also a positive effect on many ecosystem services such as provision of habitats or biodiversity (Heinrichs et al., 2019; Felton et al., 2022), and spreads the risk associated with extreme events (*e.g.* Schwarz and Bauhus, 2019) and insect outbreaks and herbivory (*e.g.* Griess and Knoke, 2011; Jactel et al., 2017; Jactel et al., 2021).

Results obtained in this study are optimistic, in that climate effects were only considered in the basal area increment model, but not yet for the height increment or mortality model. The effect of climate on height increment is, however, reported to be minor. Empirical studies on height growth of *Q.* spp. (Stimm et al., 2021) and *P. sylvestris* (Taeger et al., 2013) found no effect or small effects (<5 %) on height growth and weaker correlations with climatic variables of the current year (Taeger et al., 2013). This is because height increment is formed during a very short period in spring, and therefore only influenced by the climate in this period (Taeger et al., 2013). Shoot formation itself is a two-year process, starting with bud formation during late summer of the first year and the actual expansion occurring during spring/early summer in the second year (Bréda et al., 2006). In addition to water availability, temperature during the phase of bud formation is regarded as a trigger for shoot length (Kozlowski et al., 1991; Salminen and Jalkanen, 2005). This explains the weaker relation of annual height growth to the moisture deficit of the current year.

Climate has an important impact on individual tree mortality. Large scale mortality due to drought was reported for *P. sylvestris* (Dobbertin et al., 2005; Bigler et al., 2006; Allen et al., 2010; Cailleret et al., 2017; Brandl et al., 2020; George et al., 2022) and *Q.* spp. (Cailleret et al., 2017; Brandl et al., 2020; George et al., 2022), yet such elevated mortality effects are not explicitly included in our modelling approach, with mortality models based on the empirical data of the Austrian National Forest Inventory. Mechanisms, that lead to drought induced elevated mortality are complex and include plant physiological response to climate, climate influences on insect and pests and pathogens and their interaction (Anderegg et al., 2015). Purely physiological causes for drought induced mortality are hydraulic failure or carbon starvation (McDowell, 2011; Mantova et al., 2022), but foundational evidence of the mechanistic link has not been identified yet (Mantova et al., 2022). Susceptibility to insects and pests is driven by drought, which stresses

trees but also by many characteristics of host trees, pathogens or insects (Anderegg et al., 2015), which make mortality factors difficult to disentangle. Cailleret et al. (2017), analysed radial growth patterns preceding mortality, and observed a radial growth decline in 84 % of the trees prior to mortality, but did not separate drought induced mortality from competition induced mortality. Competition induced mortality or natural thinning, results from the increasing space and resource requirement of trees with increasing size and occurs in high density stands (Pretzsch et al., 2023) and it is the mortality component most existing mortality models focus on. Climate-sensitive mortality models have been suggested by Brandl et al. (2020) who found an increased mortality risk for *Q.* spp. and *P. sylvestris* with increasing temperature but the models are not fully compatible with the PrognAus modelling framework since the study focused on dominant trees and did not include competition induced mortality. Mortality models, separating the influence of different stressors will improve climate sensitive tree growth simulation in the future. Moreover, mortality due to catastrophic events and disturbances, reported to increase with climate change (e,g, Romeiro et al., 2022) was not included in the simulations and therefore climate change will certainly cause larger economic losses than predicted by our approach. As can be seen already with other species, such as *Picea abies* in the Alps, salvaging operations constituted 39.41 % of the harvested timber volume (https://info.bml.gv.at/themen/wald/wald-in-oesterreich/wald-und-zahlen/holzeinschlagsmeldung-2022.html). In line with this, the potential range of *P. sylvestris* is predicted to decrease because of increase mortality at the dry edge of the distribution (Bombi et al., 2017; Dyderski et al., 2018).

This study shows that increasing climatic warming imposes ecological and economical threats even to relatively well drought-adapted tree species such as *Q.* spp. and *P. sylvestris* and that productivity losses for these species are higher at the dry end of the climatic gradient of their distribution. Results suggest a relative competitive advantage of *Q.* spp. over *P. sylvestris* with increasing drought frequency and severity.

Also, when analyzing growth reactions it is important to consider a different drought adaption of different provenances, as shown in the study of Taeger et al. (2013) and broadlydistributed species are optimally adapted only to a proportion of the climatic niche occupied by the species as a whole (Sáenz-Romero et al., 2019). Carefully selecting drought-resistant provenances can further mitigate climate-related risks. Stronger drought resistance of saplings is often found in saplings from drier locations (Cregg and Zhang, 2001).

In future research, the quantification of future productivity losses should be extended to other species; A limitation of this study is that it investigates the growth reactions of old stands, whereas those of younger stands may differ. More intensively investigating the more dynamic young stands is another key issue.

6. Conclusion

Climatic warming will result in severe productivity losses at dry sites or the dry end of distribution of the tree species studied here. This study suggests a competitive advantage and higher productivity of *P. sylvestris* under the current climate, the mixture of *Q.* spp. and *P. sylvestris* could be recommended with RCP 4.5, while for scenario RCP 8.5 there may be considerable loss in productivity for *P. sylvestris* and only *Q.* spp. can be recommended. Enrichment of *P. sylvestris* stands by creating mixtures with *Q.* spp., but not the opposite, might be a right silvicultural adaptive strategy, especially at lower latitudes. Tree species mixing can only partly compensate productivity losses due to climate change. This may, however, be possible in combination with other silvicultural adaptation strategies, such as thinning and uneven-aged management, which were not investigated in this study. Other options in RCP 8.5 could be assisted migration with more drought resistant species or the introduction with non-native species, although the collateral risk of such a strategy should not be minimized (Dimitrova et al., 2022).

To better understand the influence of climate on forest productivity, fitting climate and competition sensitive mortality models for a large range of species compatible with individual tree growth models is a field for future research and a next step in climate sensitive growth predictions. Equally important is the integration of the associated risk in growth predictions.

Further enhanced precipitation models in climatic predictions showing more variability would further be necessary, since predictions currently available showed too little variation in precipitation between by years. Annual precipitation, however, largely affects growth reactions.

Supplementary data to this article can be found online at https://doi.org/10.1016/j.scitotenv.2024.173342.

CRediT authorship contribution statement

Sonja Vospernik: Writing – review & editing, Writing – original draft, Visualization, Methodology, Funding acquisition, Formal analysis, Data curation, Conceptualization. **Carl Vigren:** Writing – review & editing, Writing – original draft, Visualization, Formal analysis. **Xavier Morin:** Writing – review & editing, Data curation, Conceptualization. **Maude Toïgo:** Writing – review & editing, Data curation, Conceptualization. **Kamil Bielak:** Writing – review & editing, Investigation. **Gediminas Brazaitis:** Writing – review & editing, Conceptualization. **Felipe Bravo:** Writing – review & editing, Conceptualization. **Michael Heym:** Writing – review & editing, Conceptualization. **Miren del Río:** Writing – review & editing, Project administration, Funding acquisition, Conceptualization. **Aris Jansons:** Writing – review & editing, Conceptualization. **Magnus Löf:** Writing – review & editing, Conceptualization. **Arne Nothdurft:** Writing – review & editing, Conceptualization. **Marta Pardos:** Writing – review & editing, Conceptualization. **Maciej Pach:** Writing – review & editing, Conceptualization. **Quentin Ponette:** Writing – review & editing, Conceptualization. **Hans Pretzsch:** Writing – review & editing, Conceptualization.

Declaration of competing interest

We have no conflicts of interest to disclose.

Data availability

Data will be made available on request.

Acknowledgements

The authors thank the European Union for funding the project “Mixed species forest management. Lowering risk, increasing resilience (REFORM)” under the framework of Sumforest ERA-NET. All contributors thank their national funding institutions to establish, measure and analyze data from the triplets. The Polish State Forests Enterprise also supported one of the Polish co-authors (Grant No: OR.271.3.15.2017). The Orléans site, OPTMix was installed thanks to ONF (National Forest Service, France), belongs to research infrastructure ANAEE-F; it is also included in the SOERE TEMPO, ZAL (LTSER Zone Atelier Loire) and the GIS oop network. FB and MdR thank the support by the Spanish Ministerio de Ciencia e Innovación (# PID2021-126275OB-C21/C22) and by the Junta de Castilla y Leon, Spain, and the European Union for funding the Projects VA183P20 (SMART—Bosques mixtos: Selvicultura, Mitigacion, Adaptacion, Resiliencia y Trade-offs) and CLU-2019-01—iuFOR Institute Unit of Excellence of the University of Valladolid through the ERDF “Europe drives our growth”. CV thanks the Knut and Alice Wallenberg Foundation for funding his phD project.

References

Aldea, J., Bravo, F., Vázquez-Piqué, J., Rubio-Cuadrado, A., Del Río, M., 2018. Species-specific weather response in the daily stem variation cycles of Mediterranean pine-

oak mixed stands. Agric. For. Meteorol. 256–257, 220–230. https://doi.org/10.1016/j.agrformet.2018.03.013.
Aldea, J., Ruíz-Peinado, R., Del Río, M., Pretzsch, H., Heym, M., Brazaitis, G., Jansons, A., Metslaid, M., Barbeito, I., Bielak, K., Hylen, G., Holm, S., Nothdurft, A., Sitko, R., Löf, M., 2022. Timing and duration of drought modulate tree growth response in pure and mixed stands of Scots pine and Norway spruce. J. Ecol. 110, 2673–2683. https://doi.org/10.1111/1365-2745.13978.
Allen, C.D., Macalady, A.K., Chenchouni, H., Bachelet, D., McDowell, N., Vennetier, M., Kitzberger, T., Rigling, A., Breshears, D.D., Hogg, E.H. (Ted), Gonzalez, P., Fensham, R., Zhang, Z., Castro, J., Demidova, N., Lim, J.-H., Allard, G., Running, S. W., Semerci, A., Cobb, N., 2010. A global overview of drought and heat-induced tree mortality reveals emerging climate change risks for forests. For. Ecol. Manag. 259 (4), 660–684. https://doi.org/10.1016/j.foreco.2009.09.001.
Anderegg, W.R.L., Hicke, J.A., Fisher, R.A., Allen, C.D., Aukema, J., Bentz, B., Hood, S., Lichstein, J.W., Macalady, A.K., McDowell, N., Pan, Y., Raffa, K., Sala, A., Shaw, J. D., Stephenson, N.L., Tague, C., Zeppel, M., 2015. Tree mortality from drought, insects, and their interactions in a changing climate. New Phytol. 208 (3), 674–683. https://doi.org/10.1111/nph.13477.
Arend, M., Link, R.M., Patthey, R., Hoch, G., Schuldt, B., Kahmen, A., 2021. Rapid hydraulic collapse as cause of drought-induced mortality in conifers. Proc. Natl. Acad. Sci. 118, e2025251118 https://doi.org/10.1073/pnas.2025251118.
Bartoń, K., 2023. MuMIn: multi-model inference. R package version 1.47.5 [WWW Document]. URL. https://CRAN.R-project.org/package=MuMIn.
Bates, D., Mächler, M., Bolker, B., Walker, S., 2015. Fitting linear mixed-effects models using **lme4**. J. Stat. Softw. 67 https://doi.org/10.18637/jss.v067.i01.
Bayat, M., Knoke, T., Heidari, S., Hamidi, S.K., Burkhart, H., Jaafari, A., 2022. Modeling tree growth responses to climate change: a case study in natural deciduous mountain forests. Forests 13, 1816. https://doi.org/10.3390/f13111816.
Bebi, P., Kienast, F., Schönenberger, W., 2001. Assessing structures in mountain forests as a basis for investigating the forests' dynamics and protective function. For. Ecol. Manag. 12.
Benito Garzón, M., González Muñoz, N., Wigneron, J.-P., Moisy, C., Fernández-Manjarrés, J., Delzon, S., 2018. The legacy of water deficit on populations having experienced negative hydraulic safety margin. Glob. Ecol. Biogeogr. 27, 346–356. https://doi.org/10.1111/geb.12701.
Bhuyan, U., Zang, C., Menzel, A., 2017. Different responses of multispecies tree ring growth to various drought indices across Europe. Dendrochronologia 44, 1–8. https://doi.org/10.1016/j.dendro.2017.02.002.
Bigler, C., Bräker, O.U., Bugmann, H., Dobbertin, M., Rigling, A., 2006. Drought as an inciting mortality factor in scots pine stands of the Valais, Switzerland. Ecosystems 9, 330–343. https://doi.org/10.1007/s10021-005-0126-2.
Bombi, P., D'Andrea, E., Rezaie, N., Cammarano, M., Matteucci, G., 2017. Which climate change path are we following? Bad news from Scots pine. PLoS One 12 (12), e0189468. https://doi.org/10.1371/journal.pone.0189468.
Bonal, D., Pau, M., Toigo, M., Granier, A., Perot, T., 2017. Mixing oak and pine trees does not improve the functional response to severe drought in central French forests. Ann. For. Sci. 74 (4), 72. https://doi.org/10.1007/s13595-017-0671-9.
Bouwman, M., Forrester, D.I., Den Ouden, J., Nabuurs, G.-J., Mohren, G.M.J., 2021. Species interactions under climate change in mixed stands of Scots pine and pedunculate oak. For. Ecol. Manag. 481, 118615 https://doi.org/10.1016/j.foreco.2020.118615.
Brandl, S., Paul, C., Knoke, T., Falk, W., 2020. The influence of climate and management on survival probability for Germany's most important tree species. For. Ecol. Manag. 458, 117652 https://doi.org/10.1016/j.foreco.2019.117652.
Bréda, N., Huc, R., Granier, A., Dreyer, E., 2006. Temperate forest trees and stands under severe drought: a review of ecophysiological responses, adaptation processes and long-term consequences. Ann. For. Sci. 63 (6), 625–644. https://doi.org/10.1051/forest:2006042.
Brus, D.J., Hengeveld, G.M., Walvoort, D.J.J., Goedhart, P.W., Heidema, A.H., Nabuurs, G.J., Gunia, K., 2012. Statistical mapping of tree species over Europe. Eur. J. Forest Res. 131 (1), 145–157. https://doi.org/10.1007/s10342-011-0513-5.
Cailleret, M., Jansen, S., Robert, E.M.R., Desoto, L., Aakala, T., Antos, J.A., Beikircher, B., Bigler, C., Bugmann, H., Caccianiga, M., Čada, V., Camarero, J.J., Cherubini, P., Cochard, H., Coyea, M.R., Čufar, K., Das, A.J., Davi, H., Delzon, S., Dorman, M., Gea-Izquierdo, G., Gillner, S., Haavik, L.J., Hartmann, H., Hereş, A., Hultine, K.R., Janda, P., Kane, J.M., Kharuk, V.I., Kitzberger, T., Klein, T., Kramer, K., Lens, F., Levanic, T., Linares Calderon, J.C., Lloret, F., Lobo-Do-Vale, R., Lombardi, F., López Rodríguez, R., Mäkinen, H., Mayr, S., Mészáros, I., Metsaranta, J.M., Minunno, F., Oberhuber, W., Papadopoulos, A., Peltoniemi, M., Petritan, A.M., Rohner, B., Sangüesa-Barreda, G., Sarris, D., Smith, J.M., Stan, A.B., Sterck, F., Stojanović, D.B., Suarez, M.L., Svoboda, M., Tognetti, R., Torres-Ruiz, J.M., Trotsiuk, V., Villalba, R., Vodde, F., Westwood, A.R., Wyckoff, P.H., Zafirov, N., Martínez-Vilalta, J., 2017. A synthesis of radial growth patterns preceding tree mortality. Glob. Chang. Biol. 23 (4), 1675–1690. https://doi.org/10.1111/gcb.13535.
Camarero, J.J., Gazol, A., Sangüesa-Barreda, G., Vergarechea, M., Alfaro-Sánchez, R., Cattaneo, N., Vicente-Serrano, S.M., 2021. Tree growth is more limited by drought in rear-edge forests most of the times. For. Ecosyst. 8, 25. https://doi.org/10.1186/s40663-021-00303-1.
Choat, B., Brodribb, T.J., Brodersen, C.R., Duursma, R.A., López, R., Medlyn, B.E., 2018. Triggers of tree mortality under drought. Nature 558, 531–539. https://doi.org/10.1038/s41586-018-0240-x.
Cregg, B.M., Zhang, J.W., 2001. Physiology and morphology of *Pinus sylvestris* seedlings from diverse sources under cyclic drought stress. For. Ecol. Manag. 154, 131–139. https://doi.org/10.1016/S0378-1127(00)00626-5.
De Wergifosse, Louis, André, F., Goosse, H., Boczon, A., Cecchini, S., Ciceu, A., Collalti, A., Cools, N., D'Andrea, E., De Vos, B., Hamdi, R., Ingerslev, M., Knudsen, M.A., Kowalska, A., Leca, S., Matteucci, G., Nord-Larsen, T., Sanders, T.G., Schmitz, A., Termonia, P., Vanguelova, E., Van Schaeybroeck, B., Verstraeten, A., Vesterdal, L., Jonard, M., 2022. Simulating tree growth response to climate change in structurally diverse oak and beech forests. Sci. Total Environ. 806, 150422 https://doi.org/10.1016/j.scitotenv.2021.150422.
del Río, M., Pretzsch, H., Ruiz-Peinado, R., Jactel, H., Coll, L., Löf, M., Aldea, J., Ammer, C., Avdagić, A., Barbeito, I., Bielak, K., Bravo, F., Brazaitis, G., Cerný, J., Collet, C., Condés, S., Drössler, L., Fabrika, M., Heym, M., Holm, S., Hylen, G., Jansons, A., Kurylyak, V., Lombardi, F., Matović, B., Metslaid, M., Motta, R., Nord-Larsen, T., Nothdurft, A., den Ouden, J., Pach, M., Pardos, M., Poeydebat, C., Ponette, Q., Pérot, T., Reventlow, D.O.J., Sitko, R., Sramek, V., Steckel, M., Svoboda, M., Verheyen, K., Vospernik, S., Wolff, B., Zlatanov, T., Bravo-Oviedo, A., 2022. Emerging stability of forest productivity by mixing two species buffers temperature destabilizing effect. J. Appl. Ecol. 1365–2664, 14267 https://doi.org/10.1111/1365-2664.14267.
Dimitrova, A., Csilléry, K., Klisz, M., Lévesque, M., Heinrichs, S., Cailleret, M., Andivia, E., Madsen, P., Böhenius, H., Cvjetkovic, B., De Cuyper, B., De Dato, G., Ferus, P., Heinze, B., Ivetić, V., Köbölkuti, Z., Lazarević, J., Lazdina, D., Maaten, T., Makovskis, K., Milovanović, J., Monteiro, A.T., Nonić, M., Place, S., Puchalka, R., Montagnoli, A., 2022. Risks, benefits, and knowledge gaps of non-native tree species in Europe. Front. Ecol. Evol. 10, 908464 https://doi.org/10.3389/fevo.2022.908464.
Dobbertin, M., Mayer, P., Wohlgemuth, T., Feldmeyer-Christe, E., Zimmermann, N.E., Rigling, A., 2005. The decline of *Pinus sylvestris* L. forests in the Swiss Rhone Valley - a result of drought stress? https://www7.nau.edu/mpcer/direnet/publications/publications_d/files/dobbertin_decline_pinus.pdf.
Dupuy, J.L., Fargeon, H., Martin-StPaul, N., et al., 2020. Climate change impact on future wildfire danger and activity in southern Europe: a review. Ann. For. Sci. 77, 35. https://doi.org/10.1007/s13595-020-00933.
Durrant, T.H., de Rigo, D., Caudullo, G., 2016. *Pinus sylvestris* in Europe: distribution, habitat usage and threats. In: San-Miguel-Ayanz, J., de Rigo, D., Caudullo, G., Houston Durrant, T., Mauri, A. (Eds.), European Atlas of Forest Tree Species. Publ. Off. EU. Luxembourg (e016b94++ pp.).
Dyderski, M.K., Paź, S., Frelich, L.E., Jagodziński, A.M., 2018. How much does climate change threaten European forest tree species distributions? Glob. Chang. Biol. 24 (3), 1150–1163. https://doi.org/10.1111/gcb.13925.
Eaton, E., Caudullo, G., Oliveira, S., de Rigo, D., 2016. *Quercus robur* and *Quercus petraea* in Europe: distribution, habitat, usage and threads. In: San-Miguel-Ayanz, J., de Rigo, D., Caudullo, G., Houston Durrant, T., Mauri, A. (Eds.), European Atlas of Forest Tree Species. Publ. Off. EU. Luxembourg (e01c6df+ pp.).
Eilmann, B., Weber, P., Rigling, A., Eckstein, D., 2006. Growth reactions of *Pinus sylvestris* L. and *Quercus pubescens* Willd. to drought years at a xeric site in Valais, Switzerland. Dendrochronologia 23 (3), 121–132. https://doi.org/10.1016/j.dendro.2005.10.002.
Engel, M., Vospernik, S., Toïgo, M., Morin, X., Tomao, A., Trotta, C., Steckel, M., Barbati, A., Nothdurft, A., Pretzsch, H., del Río, M., Skrzyszewski, J., Ponette, Q., Löf, M., Jansons, Ā., Brazaitis, G., 2021. Simulating the effects of thinning and species mixing on stands of oak (*Quercus petraea* (Matt.) Liebl./*Quercus robur* L.) and pine (*Pinus sylvestris* L.) across Europe. Ecol. Model. 442, 109406 https://doi.org/10.1016/j.ecolmodel.2020.109406.
Fang, Y., 2021. Asymptotic equivalence between cross-validations and Akaike information criteria in mixed-effects models. J. Data Sci. 15–21 https://doi.org/10.6339/JDS.201101_09(1).0002.
Felton, A., Felton, A.M., Wam, H.K., Witzell, J., Wallgren, M., Löf, M., Sonesson, J., Lindbladh, M., Björkman, C., Blennow, K., Cleary, M., Jonsell, M., Klapwijk, M.J., Niklasson, M., Petersson, L., Rönnberg, J., Sang, Å.O., Wrethling, F., Hedwall, P.-O., 2022. Forest biodiversity and ecosystem services from spruce-birch mixtures: the potential importance of tree spatial arrangement. Environ. Chall. 6, 100407 https://doi.org/10.1016/j.envc.2021.100407.
Galiano, L., Martínez-Vilalta, J., Lloret, F., 2011. Carbon reserves and canopy defoliation determine the recovery of Scots pine 4 yr after a drought episode. New Phytol. 190, 750–759. https://doi.org/10.1111/j.1469-8137.2010.03628.x.
George, J.-P., Bürkner, P.-C., Sanders, T.G.M., Neumann, M., Cammalleri, C., Vogt, J.V., Lang, M., 2022. Long-term forest monitoring reveals constant mortality rise in European forests. Plant Biol. J. 24 (7), 1108–1119. https://doi.org/10.1111/plb.13469.
Giesecke, T., Brewer, S., Finsinger, W., Leydet, M., Bradshaw, R.H.W., 2017. Patterns and dynamics of European vegetation change over the last 15,000 years. J. Biogeogr. 44, 1441–1456. https://doi.org/10.1111/jbi.12974.
Gillner, S., Vogt, J., Roloff, A., 2013. Climatic response and impacts of drought on oaks at urban and forest sites. Urban For. Urban Green. 12, 597–605. https://doi.org/10.1016/j.ufug.2013.05.003.
Gil-Pelegrín, E., Peguero-Pina, J.J., Sancho-Knapik, D. (Eds.), 2017. Oaks Physiological Ecology. Exploring the Functional Diversity of Genus *Quercus* L., Tree Physiology. Springer International Publishing, Cham. https://doi.org/10.1007/978-3-319-69099-5.
Girardin, M.P., Raulier, F., Bernier, P.Y., Tardif, J.C., 2008. Response of tree growth to a changing climate in boreal central Canada: a comparison of empirical, process-based, and hybrid modelling approaches. Ecol. Model. 213, 209–228. https://doi.org/10.1016/j.ecolmodel.2007.12.010.
Greven, S., Kneib, T., 2010. On the behaviour of marginal and conditional AIC in linear mixed models. Biometrika 97 (4), 773–789. https://doi.org/10.1093/biomet/asp042.
Griess, V.C., Knoke, T., 2011. Growth performance, windthrow, and insects: meta-analyses of parameters influencing performance of mixed-species stands in boreal

and northern temperate biomes. Can. J. For. Res. 41, 1141–1159. https://doi.org/10.1139/x11-042.
Gupta, R., Sharma, L.K., 2019. The process-based forest growth model 3-PG for use in forest management: a review. Ecol. Model. 397, 55–73. https://doi.org/10.1016/j.ecolmodel.2019.01.007.
Haerdtle, W., Niemayer, T., Assman, T., Aulinger, A., Fichtner, A., Lang, A., Leuschner, C., Neuwirth, B., Pfister, L., Quante, M., Ries, C., Schuldt, A., von Oheimb, G., 2013. Climatic responses of tree-ring width and δ13C signatures of sessile oak (*Quercus petraea* Liebl.) on soils. Plant Ecol. 214, 1147–1156. https://doi.org/10.1007/s11258-013-0239-1.
Hammond, W.M., Williams, A.P., Abatzoglou, J.T., Adams, H.D., Klein, T., López, R., Sáenz-Romero, C., Hartmann, H., Breshears, D.D., Allen, C.D., 2022. Global field observations of tree die-off reveal hotter-drought fingerprint for Earth's forests. Nat. Commun. 13 (1), 1761. https://doi.org/10.1038/s41467-022-29289-2.
Hartmann, H., Bastos, A., Das, A.J., Esquivel-Muelbert, A., Hammond, W.M., Martínez-Vilalta, J., McDowell, N.G., Powers, J.S., Pugh, T.A.M., Ruthrof, K.X., Allen, C.D., 2022. Climate change risks to global forest health: emergence of unexpected events of elevated tree mortality worldwide. Annu. Rev. Plant Biol. 73 (1), 673–702. https://doi.org/10.1146/annurev-arplant-102820-012804.
Hasenauer, H., Monserud, R.A., 1996. A crown ratio model for Austrian forests. For. Ecol. Manag. 84, 49–60. https://doi.org/10.1016/0378-1127(96)03768-1.
Heinrichs, S., Ammer, C., Mund, M., Boch, S., Budde, S., Fischer, M., Müller, J., Schöning, I., Schulze, E.-D., Schmidt, W., Weckesser, M., Schall, P., 2019. Landscape-scale mixtures of tree species are more effective than stand-scale mixtures for biodiversity of vascular plants, bryophytes and lichens. Forests 10, 73. https://doi.org/10.3390/f10010073.
Irvine, J., Perks, M.P., Magnani, F., Grace, J., 1998. The response of *Pinus sylvestris* to drought: stomatal control of transpiration and hydraulic conductance. Tree Physiol. 18 (6), 393–402. https://doi.org/10.1093/treephys/18.6.393.
Jacob, D., Petersen, J., Eggert, B., Alias, A., Christensen, O.B., Bouwer, L.M., Braun, A., Colette, A., Déqué, M., Georgievski, G., Georgopoulou, E., Gobiet, A., Menut, L., Nikulin, G., Haensler, A., Hempelmann, N., Jones, C., Keuler, K., Kovats, S., Kröner, N., Kotlarski, S., Kriegsmann, A., Martin, E., van Meijgaard, E., Moseley, C., Pfeifer, S., Preuschmann, S., Radermacher, C., Radtke, K., Rechid, D., Rounsevell, M., Samuelsson, P., Somot, S., Soussana, J.-F., Teichmann, C., Valentini, R., Vautard, R., Weber, B., Yiou, P., 2014. EURO-CORDEX: new high-resolution climate change projections for European impact research. Reg. Environ. Chang. 14, 563–578. https://doi.org/10.1007/s10113-013-0499-2.
Jactel, H., Bauhus, J., Boberg, J., Bonal, D., Castagneyrol, B., Gardiner, B., Gonzalez-Olabarria, J.R., Koricheva, J., Meurisse, N., Brockerhoff, E.G., 2017. Tree diversity drives forest stand resistance to natural disturbances. Curr. For. Rep. 3, 223–243. https://doi.org/10.1007/s40725-017-0064-1.
Jactel, H., Koricheva, J., Castagneyrol, B., 2019. Responses of forest insect pests to climate change: not so simple. Curr. Opin. Insect Sci. 35, 103–108. https://doi.org/10.1016/j.cois.2019.07.010.
Jactel, H., Moreira, X., Castagneyrol, B., 2021. Tree diversity and forest resistance to insect pests: patterns, mechanisms, and prospects. Annu. Rev. Entomol. 66, 277–296. https://doi.org/10.1146/annurev-ento-041720-075234.
Karger, D.N., Conrad, O., Böhner, J., Kawohl, T., Kreft, H., Soria-Auza, R.W., Zimmermann, N.E., Linder, H.P., Kessler, M., 2017. Climatologies at high resolution for the earth's land surface areas. Sci. Data 4, 170122. https://doi.org/10.1038/sdata.2017.122.
Karger, D.N., Schmatz, D.R., Dettling, G., Zimmermann, N.E., 2020. High-resolution monthly precipitation and temperature time series from 2006 to 2100. Sci. Data 7, 248. https://doi.org/10.1038/s41597-020-00587-y.
Karrer, G., Bassler-Binder, G., Willner, W., 2022. Assessment of drought-tolerant provenances of Austria's indigenous tree species. Sustainability 14, 2861. https://doi.org/10.3390/su14052861.
Körner, C., Basler, D., 2010. Phenology under global warming. Science 327, 1461–1462. https://doi.org/10.1126/science.1186473.
Kozlowski, T.T., Kramer, P.J., Pallardy, S.G., 1991. The physiological ecology of woody plants. Pallardy Academic Press, New York, Tokyo, London, Toronto, Sydney.
Ledermann, T., 2002. Ein Einwuchsmodell aus den Daten der österreichischen Waldinventur 1981–1996. Cent. Für Gesamte Forstwes. 119, 40–76.
Mantova, M., Herbette, S., Cochard, H., Torres-Ruiz, J.M., 2022. Hydraulic failure and tree mortality: from correlation to causation. Trends Plant Sci. 27 (4), 335–345. https://doi.org/10.1016/j.tplants.2021.10.003.
Martínez-Sancho, E., Gutiérrez, E., Valeriano, C., Ribas, M., Popkova, M.I., Shishov, V.V., Dorado-Liñán, I., 2021. Intra- and inter-annual growth patterns of a mixed pine-oak forest under Mediterranean climate. Forests 12, 1746. https://doi.org/10.3390/f12121746.
Maurer, S., Heinimann, H.R., 2020. Framework for assessing the windthrow risk to Norway spruce forests in Switzerland. Eur. J. Forest Res. 139 (2), 259–272. https://doi.org/10.1007/s10342-019-01251-w.
McDowell, N.G., 2011. Mechanisms linking drought, hydraulics, carbon metabolism, and vegetation mortality. Plant Physiol. 155 (3), 1051–1059. https://doi.org/10.1104/pp.110.170704.
Menzel, A., Yuan, Y., Matiu, M., Sparks, T., Scheifinger, H., Gehrig, R., Estrella, N., 2020. Climate change fingerprints in recent European plant phenology. Glob. Chang. Biol. 26, 2599–2612. https://doi.org/10.1111/gcb.15000.
Monserud, R.A., Sterba, H., 1999. Modeling individual tree mortality for Austrian forest species. For. Ecol. Manag. 113, 109–123. https://doi.org/10.1016/S0378-1127(98)00419-8.
Morin, X., Bugmann, H., Coligny, F., Martin-StPaul, N., Cailleret, M., Limousin, J., Ourcival, J., Prevosto, B., Simioni, G., Toigo, M., Vennetier, M., Catteau, E., Guillemot, J., 2021. Beyond forest succession: a gap model to study ecosystem functioning and tree community composition under climate change. Funct. Ecol. 35, 955–975. https://doi.org/10.1111/1365-2435.13760.
Müller, S., 1992. Natural acidophilous *Quercus* and *Pinus* forests in the northern Vosges, France, from a geographical perspective. J. Veg. Sci. 3, 631–636. https://doi.org/10.2307/3235830.
Nachtmann, G., 2006. Height increment models for individual trees in Austria depending on site and competition. Austrian J. For. Sci. 123, 199–222.
Nakagawa, S., Schielzeth, H., 2013. A general and simple method for obtaining R^2 from generalized linear mixed-effects models. Methods Ecol. Evol. 4 (2), 133–142. https://doi.org/10.1111/j.2041-210x.2012.00261.x.
Ozolinčius, R., Lekevičius, E., Stakėnas, V., Galvonaitė, A., Samas, A., Valiukas, D., 2014. Lithuanian forests and climate change: possible effects on tree species composition. Eur. J. For. Res. 133, 51–60. https://doi.org/10.1007/s10342-013-0735-9.
Pardos, M., Del Río, M., Pretzsch, H., Jactel, H., Bielak, K., Bravo, F., Brazaitis, G., Defossez, E., Engel, M., Godvod, K., Jacobs, K., Jansone, L., Jansons, A., Morin, X., Nothdurft, A., Oreti, L., Ponette, Q., Pach, M., Riofrío, J., Ruíz-Peinado, R., Tomao, A., Uhl, E., Calama, R., 2021. The greater resilience of mixed forests to drought mainly depends on their composition: analysis along a climate gradient across Europe. For. Ecol. Manag. 481, 118687 https://doi.org/10.1016/j.foreco.2020.118687.
Peters, R.L., Steppe, K., Pappas, C., Zweifel, R., Babst, F., Dietrich, L., Von Arx, G., Poyatos, R., Fonti, M., Fonti, P., Grossiord, C., Gharun, M., Buchmann, N., Steger, D. N., Kahmen, A., 2023. Daytime stomatal regulation in mature temperate trees prioritizes stem rehydration at night. New Phytol. 239, 533–546. https://doi.org/10.1111/nph.18964.
Pretzsch, H., Steckel, M., Heym, M., Biber, P., Ammer, C., Ehbrecht, M., Bielak, K., Bravo, F., Ordóñez, C., Collet, C., Vast, F., Drössler, L., Brazaitis, G., Godvod, K., Jansons, A., de-Dios-García, J., Löf, M., Aldea, J., Korboulewsky, N., Reventlow, D.O. J., Nothdurft, A., Engel, M., Pach, M., Skrzyszewski, J., Pardos, M., Ponette, Q., Sitko, R., Fabrika, M., Svoboda, M., Černý, J., Wolff, B., Ruíz-Peinado, R., del Río, M., 2020. Stand growth and structure of mixed-species and monospecific stands of Scots pine (*Pinus sylvestris* L.) and oak (*Quercus robur* L., *Quercus petraea* (Matt.) Liebl.) analysed along a productivity gradient through Europe. Eur. J. For. Res. 139, 349–367. https://doi.org/10.1007/s10342-019-01233-y.
Pretzsch, H., Del Río, M., Arcangeli, C., Bielak, K., Dudzinska, M., Ian Forrester, D., Kohnle, U., Ledermann, T., Matthews, R., Nagel, R., Ningre, F., Nord-Larsen, T., Szeligowski, H., Biber, P., 2023. Competition-based mortality and tree losses. An essential component of net primary productivity. For. Ecol. Manag. 544, 121204 https://doi.org/10.1016/j.foreco.2023.121204.
Prokop, O., Kolář, T., Büntgen, U., Kyncl, J., Kyncl, T., Bošeľa, M., Choma, M., Barta, P., Rybníček, M., 2016. On the palaeoclimatic potential of a millennium-long oak ring width chronology from Slovakia. Dendrochronologia 40, 93–101. https://doi.org/10.1016/j.dendro.2016.08.001.
Puchałka, R., Koprowski, M., Gričar, J., Przybylak, R., 2017. Does tree-ring formation follow leaf phenology in Pedunculate oak (*Quercus robur* L.)? Eur. J. Forest Res. 136 (2), 259–268. https://doi.org/10.1007/s10342-017-1026-7.
Puchałka, R., Prislan, P., Klisz, M., Koprowski, M., Gričar, J., 2024. Tree-ring formation dynamics in *Fagus sylvatica* and *Quercus petraea* in a dry and a wet year. Dendrobiology 91, 1–15. https://doi.org/10.12657/denbio.091.001.
Rigling, A., Bräker, O., Schneiter, G., Schweingruber, F., 2002. Intra-annual tree-ring parameters indicating differences in drought stress of *Pinus sylvestris* forests within the Erico-Pinion in the Valais (Switzerland). Plant Ecol. 163 (105–121), 2002.
Roibu, C.-C., Sfeclă, V., Mursa, A., Ionita, M., Nagavciuc, V., Chiriloaei, F., Leşan, I., Popa, I., 2020. The climatic response of tree ring width components of ash (*Fraxinus excelsior* L.) and common oak (*Quercus robur* L.) from Eastern Europe. Forests 11, 600. https://doi.org/10.3390/f11050600.
Romeiro, M.R.J., Eid, T., Antón-Fernández, C., Kangas, A., Trømborg, E., 2022. Natural disturbances risks in European Boreal and Temperate forests and their links to climate change – a review of modelling approaches. For. Ecol. Manag. 509, 120071 https://doi.org/10.1016/j.foreco.2022.120071.
Sáenz-Romero, C., Kremer, A., Nagy, L., Újvári-Jármay, É., Ducousso, A., Kóczán-Horváth, A., Hansen, J.K., Mátyás, C., 2019. Common garden comparisons confirm inherited differences in sensitivity to climate change between forest tree species. PeerJ 7, e6213. https://doi.org/10.7717/peerj.6213.
Salminen, H., Jalkanen, R., 2005. Modelling the effect of temperature on height increment of Scots pine at high latitudes. Silva Fenn. 39 (4), 497–508. https://doi.org/10.14214/sf.362.
Salomón, R.L., Peters, R.L., Zweifel, R., Sass-Klaassen, U.G.W., Stegehuis, A.I., Smiljanic, M., Poyatos, R., Babst, F., Cienciala, E., Fonti, P., Lerink, B.J.W., Lindner, M., Martinez-Vilalta, J., Mencuccini, M., Nabuurs, G.-J., van der Maaten, E., von Arx, G., Bär, A., Akhmetzyanov, L., Balanzategui, D., Bellan, M., Bendix, J., Berveiller, D., Blaženec, M., Čada, V., Carraro, V., Cecchini, S., Chan, T., Conedera, M., Delpierre, N., Delzon, S., Ditmarová, Ľ., Dolezal, J., Dufrêne, E., Edvardsson, J., Ehekircher, S., Forner, A., Frouz, J., Ganthaler, A., Gryc, V., Güney, A., Heinrich, I., Hentschel, R., Janda, P., Ježík, M., Kahle, H.-P., Knüsel, S., Krejza, J., Kuberski, Ł., Kučera, J., Lebourgeois, F., Mikoláš, M., Matula, R., Mayr, S., Oberhuber, W., Obojes, N., Osborne, B., Paljakka, T., Plichta, R., Rabbel, I., Rathgeber, C.B.K., Salmon, Y., Saunders, M., Scharnweber, T., Sitková, Z., Stangler, D.F., Stereńczak, K., Stojanović, M., Střelcová, K., Světlík, J., Svoboda, M., Tobin, B., Trotsiuk, V., Urban, J., Valladares, F., Vavrčík, H., Vejpustková, M., Walthert, L., Wilmking, M., Zin, E., Zou, J., Steppe, K., 2022. The 2018 European heatwave led to stem dehydration but not to consistent growth reductions in forests. Nat. Commun. 13, 28. https://doi.org/10.1038/s41467-021-27579-9.
Sanderson, B.M., Knutti, R., Caldwell, P., 2015. Addressing interdependency in a multimodel ensemble by interpolation of model properties. J. Clim. 28, 5150–5170. https://doi.org/10.1175/JCLI-D-14-00361.1.

Schwarz, J.A., Bauhus, J., 2019. Benefits of mixtures on growth performance of silver fir (*Abies alba*) and European beech (*Fagus sylvatica*) increase with tree size without reducing drought tolerance. Front. For. Glob. Change 2, 79. https://doi.org/10.3389/ffgc.2019.00079.

Steckel, M., del Río, M., Heym, M., Aldea, J., Bielak, K., Brazaitis, G., Černý, J., Coll, L., Collet, C., Ehbrecht, M., Jansons, A., Nothdurft, A., Pach, M., Pardos, M., Ponette, Q., Reventlow, D.O.J., Sitko, R., Svoboda, M., Vallet, P., Wolff, B., Pretzsch, H., 2020. Species mixing reduces drought susceptibility of Scots pine (*Pinus sylvestris* L.) and oak (*Quercus robur* L., *Quercus petraea* (Matt.) Liebl.) – site water supply and fertility modify the mixing effect. For. Ecol. Manag. 461, 117908 https://doi.org/10.1016/j.foreco.2020.117908.

Stimm, K., Heym, M., Uhl, E., Tretter, S., Pretzsch, H., 2021. Height growth-related competitiveness of oak (*Quercus petraea* (Matt.) Liebl. and *Quercus robur* L.) under climate change in Central Europe. Is silvicultural assistance still required in mixed-species stands? For. Ecol. Manag. 482, 118780 https://doi.org/10.1016/j.foreco.2020.118780.

Strieder, E., Vospernik, S., 2021. Intra-annual diameter growth variation of six common European tree species in pure and mixed stands. Silva Fenn. 55 https://doi.org/10.14214/sf.10449.

Taeger, S., Zang, C., Liesebach, M., Schneck, V., Menzel, A., 2013. Impact of climate and drought events on the growth of Scots pine (*Pinus sylvestris* L.) provenances. For. Ecol. Manag. 307, 30–42. https://doi.org/10.1016/j.foreco.2013.06.053.

Thurm, E.A., Hernandez, L., Baltensweiler, A., Ayan, S., Rasztovits, E., Bielak, K., Zlatanov, T.M., Hladnik, D., Balic, B., Freudenschuss, A., Büchsenmeister, R., Falk, W., 2018. Alternative tree species under climate warming in managed European forests. For. Ecol. Manag. 430, 485–497. https://doi.org/10.1016/j.foreco.2018.08.028.

Toïgo, M., Vallet, P., Tuilleras, V., Lebourgeois, F., Rozenberg, P., Perret, S., Courbaud, B., Perot, T., 2015. Species mixture increases the effect of drought on tree ring density, but not on ring width, in *Quercus petraea* - *Pinus sylvestris* stands. For. Ecol. Manag. 345, 73–82. https://doi.org/10.1016/j.foreco.2015.02.019.

Treml, V., Mašek, J., Tumajer, J., Rydval, M., Čada, V., Ledvinka, O., Svoboda, M., 2022. Trends in climatically driven extreme growth reductions of *Picea abies* and *Pinus sylvestris* in Central Europe. Glob. Chang. Biol. 28, 557–570. https://doi.org/10.1111/gcb.15922.

Venäläinen, A., Lehtonen, I., Laapas, M., Ruosteenoja, K., Tikkanen, O., Viiri, H., Ikonen, V., Peltola, H., 2020. Climate change induces multiple risks to boreal forests and forestry in Finland: a literature review. Glob. Chang. Biol. 26, 4178–4196. https://doi.org/10.1111/gcb.15183.

Vitasse, Y., Bottero, A., Cailleret, M., Bigler, C., Fonti, P., Gessler, A., Lévesque, M., Rohner, B., Weber, P., Rigling, A., Wohlgemuth, T., 2019. Contrasting resistance and resilience to extreme drought and late spring frost in five major European tree species. Glob. Chang. Biol. 25, 3781–3792. https://doi.org/10.1111/gcb.14803.

Vospernik, S., 2021. Basal area increment models accounting for climate and mixture for Austrian tree species. For. Ecol. Manag. 480, 118725 https://doi.org/10.1016/j.foreco.2020.118725.

Vospernik, S., Sterba, H., 2015. Do competition-density rule and self-thinning rule agree? Ann. For. Sci. 72, 379–390. https://doi.org/10.1007/s13595-014-0433-x.

Vospernik, S., Heym, M., Pretzsch, H., Pach, M., Steckel, M., Aldea, J., Brazaitis, G., Bravo-Oviedo, A., Del Rio, M., Löf, M., Pardos, M., Bielak, K., Bravo, F., Coll, L., Černý, J., Droessler, L., Ehbrecht, M., Jansons, A., Korboulewsky, N., Jourdan, M., Nord-Larsen, T., Nothdurft, A., Ruiz-Peinado, R., Ponette, Q., Sitko, R., Svoboda, M., Wolff, B., 2023. Tree species growth response to climate in mixtures of *Quercus robur*/*Quercus petraea* and *Pinus sylvestris* across Europe - a dynamic, sensitive equilibrium. For. Ecol. Manag. 530, 120753 https://doi.org/10.1016/j.foreco.2022.120753.

Weiskittel, A.R., Hann, D.W., Kershaw, J.A., Vanclay, J., 2011. Forest Growth and Yield Modeling. Wiley-Blackwell, John Wiley & Sons Ltd., Oxford.

Welham, S.J., Gezan, S.A., Clark, S.J., Mead, A., 2014. Statistical Methods in Biology - Design and Analysis of Experiments and Regression. Chapman and Hall/CRC, New York.

Yuste, J.C., Konopka, B., Janssens, I.A., Coenen, K., Xiao, C.W., Ceulemans, R., 2005. Contrasting net primary productivity and carbon distribution between neighboring stands of *Quercus robur* and *Pinus sylvestris*. Tree Physiol. 25, 701–712. https://doi.org/10.1093/treephys/25.6.701.

Zweifel, R., Zimmermann, L., Zeugin, F., Newbery, D.M., 2006. Intra-annual radial growth and water relations of trees: implications towards a growth mechanism. J. Exp. Bot. 57, 1445–1459. https://doi.org/10.1093/jxb/erj125.

Zweifel, R., Steppe, K., Sterck, F.J., 2007. Stomatal regulation by microclimate and tree water relations: interpreting ecophysiological field data with a hydraulic plant model 19. J. Exp. Bot. 58 (8), 2113–2131. https://doi.org/10.1093/jxb/erm050.

Zweifel, R., Rigling, A., Dobbertin, M., 2009. Species-specific stomatal response of trees to drought - a link to vegetation dynamics? J. Veg. Sci. 20, 442–454. https://doi.org/10.1111/j.1654-1103.2009.05701.x.

III

scientific reports

Check for updates

OPEN

Tree growth potential and its relationship with soil moisture conditions across a heterogeneous boreal forest landscape

Johannes Larson[1✉], Carl Vigren[2], Jörgen Wallerman[2], Anneli M. Ågren[1], Alex Appiah Mensah[2] & Hjalmar Laudon[1]

Forest growth varies across landscapes due to the intricate relationships between various environmental drivers and forest management. In this study, we analysed the variation of tree growth potential across a landscape scale and its relation to soil moisture. We hypothesised that soil moisture conditions drive landscape-level variation in site quality and that intermediate soil moisture conditions demonstrate the highest potential forest production. We used an age-independent difference model to estimate site quality in terms of maximum achievable tree height by measuring the relative change in Lorey's mean height for a five year period across 337 plots within a 68 km² boreal landscape. We achieved wall-to-wall estimates of site quality by extrapolating the modelled relationship using repeated airborne laser scanning data collected in connection to the field surveys. We found a clear decrease in site quality under the highest soil moisture conditions. However, intermediate soil moisture conditions did not demonstrate clear site quality differences; this is most likely a result of the nature of the modelled soil moisture conditions and limitations connected to the site quality estimation. There was considerable unexplained variation in the modelled site quality both on the plot and landscape levels. We successfully demonstrated that there is a significant relationship between soil moisture conditions and site quality despite limitations associated with a short study period in a low productive region and the precision of airborne laser scanning measurements of mean height.

Forest growth rate is a key aspect of forested ecosystems, and is influenced, among other things, by the complex and dynamic interactions among environmental factors that vary depending on local biotic and abiotic conditions. On both global and regional scales, climate and soil conditions represent some of the most influential factors that explain spatial variation in forest growth. Forest management adds further complexity to landscape variation of forest properties by altering important forest characteristics such as age, structure, and species distribution[1]. It is important to note that both unmanaged and managed forest areas are also affected by natural disturbances such as forest fires, windstorms, and insect outbreaks. As such, untangling the complex interactions between the environmental drivers that regulate forest growth constitutes a grand scientific challenge. This is particularly relevant for the managed boreal forests of northern Europe, where the expansive forested landscape has been managed for several hundred years; this has resulted in a patchwork of human-induced actions and natural disturbance that exert significant influences on the regulation of growth rate.

Within boreal landscapes, large variations in forest growth and carbon sequestration have been observed across short distances[2,3]. Furthermore, previous studies have identified topographic position as a key factor for the variation in soil moisture conditions, which regulate soil development, nutrient accumulation, and vegetation patterns[4–7]. Therefore, on the local landscape scale—where climate drivers such as temperature and precipitation can be considered constant—the topographic position at a specific location may largely affect the forest growth potential as a result of the differences in accumulated water surrounding areas[8].

Site quality is the combination of the physical and biological factors of a geographical location or site. Site quality is inherent to the site, but may be influenced by management or e.g. climate change[9]. Site quality can be used to describe tree growth potential at a specific site. The fraction of a site's growth potential that is realised by

[1]Department of Forest Ecology and Management, Swedish University of Agricultural Sciences, Skogsmarksgränd 17, 901 83 Umeå, Sweden. [2]Department of Forest Resource Management, Swedish University of Agricultural Sciences, Skogsmarksgränd 17, 901 83 Umeå, Sweden. ✉email: Johannes.Larson@slu.se

trees to produce a certain amount of volume is often quantitatively expressed as site productivity. This type of information is critical for forest management planning as it provides the context for projecting forest production over a certain period[10] and supports decision-making concerning both conservation and restoration efforts[11]. As such, landscape-scale information on the variation in forest site productivity can significantly improve forest management[12] and enhance understanding of which biotic factors influence forest growth within the landscape.

In even-age stands, the relationship between tree height and age of a given species is closely related to the capacity of the site to produce woody biomass[13]. Therefore, site index, which is defined as the expected height of the dominant trees at a reference age is a commonly used indicator for site productivity. In Sweden, site index is generally estimated using two main methods: (1) by height development curves and (2) by site factors. Method 1 uses the height and age of the dominant trees (i.e., the 100 largest trees in diameter per hectare) to estimate the expected height at a reference age (e.g. 100 years for Scots pine—*Pinus sylvestris* L. and Norway spruce—*Picea abies* (L.) H. Karst, and 50 years for birch—*Betula pendula* Roth. and *Betula pubescens* Ehrh.)[10,14,15]. This method of estimating site index is denoted as SIH. The requirement of information about dominant height and age means that the method cannot be applied to all forest lands in Sweden (e.g., after clear-cut or thinning from above). Therefore site index is often assessed using method 2, which is based on a combination of site factors including climate, field vegetation, location and soil properties[16]. This method of estimating site index is denoted as SIS. SIS, although age-independent, is in comparison to SIH found to be lower in accuracy (~ 4 m). Using the abovementioned methods for landscape-scale assessment of site quality poses several challenges because the methods require homogeneous stand conditions (i.e., the methods are age-and/or species-dependent), commonly not available on the landscape scale. Furthermore, a major limitation of both methods is that they are limited to fixed sample plots or field registers, which effectively constrains the potential landscape-wide extrapolation. Hence, an approach that is age-and species-independent has the potential to provide unbiased assessments of the variation in site productivity across a broader scale[17].

When two measurements in time are available, age-independent difference equations have satisfactorily been used to model site productivity. For example, Tomé et al.[17] developed age-independent difference equations for both dominant height (*Eucalyptus globulus* Labill.) and DBH (*Quercus suber* L.) growth in Portugal by reformulating well-established theoretical growth functions. This approach provides a possibility for assessing the variation in forest growth potential when age is unknown, in some cases even with higher accuracy in comparison to age-dependent methods[18]. Furthermore, this approach facilitates landscape scale assessment of the variation in forest productivity using remote sensing when two measurements in time are available.

Remote sensing, particularly airborne laser scanning (ALS), has rapidly advanced during the last decade. The use of ALS in resolving the three-dimensional properties of forest vegetation structure has shown great potential for measuring and estimating key attributes, such as forest growth and site productivity, at the landscape scale[19–22]. Furthermore, bi-temporal ALS data can be highly beneficial as this information can be used to reduce uncertainties related to disturbance from management (e.g., thinning, clear-cutting, etc.) and facilitates the precise estimation of site productivity through the added information of growth between periods[23]. In parallel with the developments of high resolution remote sensing for measuring forest attributes, ALS data has massively increased the resolution of topographical information and has become an essential tool for modelling soil moisture conditions on a landscape scale[24]. Landscape scale information of environmental factors such as soil moisture, provides large opportunities to study its effect on site quality. For example, Mohamedou et al.[25] demonstrated how modelling soil moisture conditions based on terrain indices can increase the accuracy of site productivity estimates in boreal forests.

At present, landscape assessments of the variation in site quality and its relation to environmental drivers are rare, in particular across small landscapes. Within smaller spatial scales, certain environmental factors, and the interactions among them, remain constant, allowing researchers to concentrate on a specific subset of environmental drivers. Studying how variation in soil moisture conditions influences site quality may provide important insights into how environmental drivers affect forest growth, as well as enhance our ability to predict where water availability will limit tree growth potential. This type of knowledge is highly relevant for the scaling of forest ecosystem processes and development of sustainable forest management approaches in the future. Unfortunately, datasets appropriate for site quality estimation across smaller landscapes are rare. In the present study, we bridge this gap by using high-resolution, bi-temporal forest growth data to assess site quality on a landscape scale, information which is then used to investigate how site quality is related to topography-derived soil moisture conditions.

The presented research was conducted to test the following hypotheses: (1) spatial variation in soil moisture drives landscape-level variation in site quality; and (2) areas with intermediate soil moisture conditions demonstrate the highest potential forest production. To test these hypotheses, we first developed an age-independent estimate of site quality based on repeated forest surveys (2014–2019) with a 5 year study period. In the second step, site quality was estimated by using bi-temporal ALS data from the previously fitted site quality model. Thereafter, site quality was evaluated on plot and landscape level under differing soil moisture conditions. Finally, we discuss how the obtained results provide evidence for the connection between soil moisture conditions and forest production in a managed, heterogeneous boreal landscape.

Methods

The study approach was generally centred on analysing the variation in site quality using soil moisture conditions. The estimation of site quality was based on the principle of age-independent difference equations using two measurements in time of Lorey's mean height. The approach for site quality estimation was carried out in three main steps: (1) global parameters were estimated using a difference equation adjusted for relative height from field measurements. In the second step (2) we reformulated the fitted equation to estimate plot specific

site quality estimates. In step (3), landscape estimation of site quality was made using the model from step (2) and repeated measurements from ALS as input data. Finally, the variation in estimated site quality for both on a plot and landscape scale was analysed in context of soil moisture conditions obtained from field survey and map predictions.

Site description

The study was carried out in the Krycklan Catchment Study[26] which is located in northern Sweden (64° 14′ N, 19° 46′ E) which covers a 68 km^2. The area consists of a managed forest landscape with a mosaic of wetlands and lakes, typical for the region. The mean annual temperature of the area is 2.4 °C, with a mean annual precipitation of 636 mm $year^{-1}$ based on 30 years of data (1991–2021). The catchment has a gently undulating terrain, with elevations ranging from 127 to 372 m above sea level. The upper parts of the catchment are dominated by unsorted sediments, while glaciofluvial sorted sediments are common in the lower parts. The forest soils are predominantly iron podzols. Forest cover 87% of the area and is dominated by Scots pine (*Pinus sylvestris*) (63%) and Norway spruce (*Picea abies*) (26%), with scattered occurrence of deciduous species consisting mainly of birch (*Betula pendula* and *Betula pubescens*). Since 1922, approximately 25% of the catchment has been set aside for forest research and 1% is protected as nature reserves. Ownership of the remaining area is divided among forest companies and private owners. Forests in non-protected areas are managed by conventional rotation forestry and are predominantly even-aged, artificially regenerated, and thinned. Therefore, the area has evolved into a mosaic of stands of different ages, basal area and stocks (Table 1). The field layer vegetation is dominated by ericaceous shrubs (*Vaccinium* spp.) such as bilberry and lingonberry on moss mats of splendid feather moss (*Hylocomium splendens*) and red-stemmed feather moss (*Pleurozium schreberi*).

Field data

In 2014, a survey grid covering the entire catchment area was established; this grid comprises of > 500 plots (radius: 10 m, area: 314.5 m^2) that are spaced 350 × 350 m apart (Fig. 1). The plot locations were allocated using a randomly chosen origin, which was oriented along the coordinate axis of the SWEREF 99 TM projection.

	Lorey's mean height (m)	Stand age[1]	Basal area (m^2)	Volume (m^3 ha^{-1})
Min	0	0	0	0
Median	13	64	19	129
Mean	12	69	18	139
Max	26	200	63	721

Table 1. Descriptive statistics of plot-level data from the Krycklan forest survey 2014 ($n = 484$). [1]Stand age (i.e., number of years since stand establishment) was determined for each sample plot as the basal area-weighted mean age obtained by coring 8–10 dominant trees outside each sample plot.

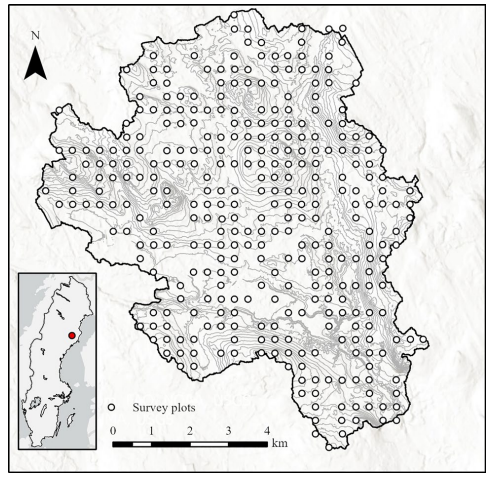

Figure 1. Map of the Krycklan catchment and the location of the 337 survey plots (350 × 350 m square grid). The map was created using ArcGIS Pro (version 3.0.2).

Accurate centre positions for each plot were determined using differentially-corrected GPS measurements, which were obtained with a Trimble GeoXTR receiver and the SWEPOS real-time differential correction service. A forest survey was conducted in the late fall and early spring of the 2014 and 2019 growing seasons. All trees with a diameter at breast height (DBH, 1.3 m) greater than 4 cm were measured at each plot. To reduce the labour necessary for surveying, the plot radius was reduced from 10 to 5 m for stands with a high stem density (e.g., regenerating or young forests). For all measured trees, DBH, species, and tree status (live or dead) was recorded. Tree height was measured for subjectively selected undamaged sub-samples of at least three trees of each species with a laser-guided hypsometer selected to capture tree size variation in DBH for each species. The selection of sample trees was made independently at each survey occasion. We fitted a mixed-effects model with plot-level random effects, where the dependent variable was the height of the measured trees and the independent variable was their DBH. We then estimated the height of the remaining trees using these models, followed by calculating the plot Lorey's mean height (basal area weighted mean height). Plots without measured trees such as clear-cut areas, treeless mires were removed. In addition plots with a decrease in Lorey's mean height between the two observations were excluded, which could be caused by management, natural disturbance or the independent selection of sample trees at each survey occasion . After this exclusion, our survey data encompassed a total of 337 survey plots, each with consecutive measurements of Lorey's mean height. In addition to the tree measurements, the plots were classified into soil moisture classes (dry, mesic, mesic-moist, moist, and wet) based on an estimation of each plot's average depth to groundwater level during the vegetation period; these estimates were based on the position of each plot in the landscape and vegetation patterns as per protocols of the Swedish National Forest Inventory[27]. The soil types for 315 of the survey plots were determined in a soil survey completed between 2019 and 2020[28] according to World Reference Base for Soil Resources (WRB) guidelines.

ALS data

Airborne Laser scanning (ALS) covering the entire study area was performed adjacent to both forest survey campaigns (Table 2.). In August 2015, the study area was scanned using an Optech Titan X sensor (flight height: 1000 m) to yield an average point density of 20 points per m^2. The sensor scanned the area using three specific wavelengths, e.g., 532 nm (green), 1064 (NIR), and 1550 nm (SWIR). At the end of June 2019, the area was scanned using a Riegl VQ-1560i-DW sensor at wavelengths of 532 nm (green) and 1064 (NIR); this yielded an average point density of 20 points per m^2[26].

The raw ALS point clouds were then processed by classifying point returns as ground, vegetation, unclassified, and noise. This enabled the generation of a Digital Elevation Model (DEM) to which all of the ALS points were normalised. The point returns were aggregated to 10×10 m metrics using CloudMetrics Fusion software[29]. Outlier assessments, carried out using bivariate scatterplots, were performed to examine the relationship between field measurements of Lorey's mean height and the 95th percentile height of laser returns (P95) from two scannings. Observations with a height difference > 5 m between the field measured Lorey's mean height and P95 were excluded because these observations were considered to represent instances in which silvicultural practices, such as thinning or clearcutting had been performed between the scanning and field measurements. The number of plots excluded due to this discrepancy was 38 in 2014 and 25 plots in 2019.

An area-based approach was used to obtain wall-to-wall coverage of Lorey's mean height across the entire study area[30]. In the first step, the observed Lorey's mean height from the geo-referenced survey plots at each survey occasion was regressed on the ALS metrics from the corresponding ALS scanning. In the second step, the models were applied over tessellations of individual grid cells to generate wall-to-wall estimates of Lorey's mean height at time of each survey occasion (2014 and 2019). We tested different predictive models using various combinations of commonly used ALS metrics related to height and density[23,31]. The final predictive model chosen for each year was formulated as a linear regression with the same independent variables which included P95 and the standard derivation of height (heightStdDev). Both models showed high accuracy, with the residual standard error (RSE) falling below 1.1 m for both the 2014 and 2019 (Table 3). The estimations of Lorey's mean height predicted from the individual models at each survey year, corresponded well to the field measurements ($n = 337$) (Fig. 2).

Site quality estimate

This study required an age-independent estimation of site quality to avoid the limitations of the commonly used 'site index', which requires inputs such as the ages and heights of dominant trees or, alternatively, vegetation type and site properties. A mean height growth model with a sigmoidal shape will involve an asymptote and a

	2015	2019
Time period	2015-08-23	2019-06-27
Season	Leaf on	Leaf on
Instrument	Optech Titan X	Riegl VQ-1560i-DW
Flying height	1000 m	1000 m
Measured wavelengths	532 nm (green), 1064 (NIR), and 1550 nm(SWIR)	532 nm (green), 1064 (NIR)
Point density	20 points/m^2	20 points/m^2

Table 2. ALS data specifications.

Year	Model	Adj R^2	RSE (m)
2014	Height = $\beta_0 + \beta_1$(P95) + β_2(heightStdDev) + β_3(P95 * heightStdDev)	0.96	1.05
2019	Height = $\beta_0 + \beta_1$(P95) + β_2(heightStdDev) + β_3(P95*heightStdDev)	0.95	1.03

Table 3. Results from linear regression predicting Lorey's mean height for 2014 and 2019 using the area-based method.

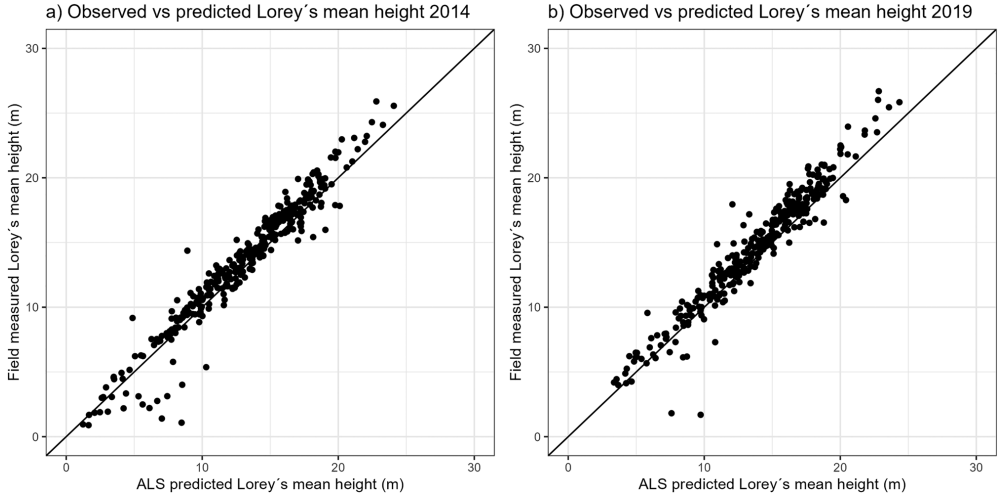

Figure 2. Plots illustrating the observed vs. predicted Lorey's mean tree heights from forest surveys conducted in 2014 (**a**) and 2019 (**b**).

shape parameter describing how the asymptote is reached; as such, an estimator of site quality can be deduced by expressing one of the parameters as a function of an un-observed site quality. The Richard's growth model is suitable for this purpose as it was empirically derived from tree physiology, has desirable properties, and has been widely used in forest growth analyses[32,33]. We focused on the age-independent difference formulation (Eq. 1) of the Richard's model[34] presented by Tomé et al.[17] to derive the site quality estimate:

$$Y_{i+a} = A\left\{1 - e^{-ka}\left[1 - \left(\frac{Y_i}{A}\right)^m\right]\right\}^{\frac{1}{m}} \quad (1)$$

where Y is Lorey's mean height in metres, A is the asymptote/maximum height (m) when time/age approaches infinity, k is a parameter related to the growth rate, m is a shape parameter related to the point of inflection, and a is the number of periods. The generalised model did not consider tree species. This age-independent difference formula can be used to model height growth for the estimation of site quality when two successive measurements are available; this includes the assumption that the growth function passes through the two height measurements in both survey periods. In Eq. 1, the parameter A is most often the parameter that is most strongly related to site quality[23], as well as easy to interpret because it is expressed in the same dimension as the response variable, height. The k parameter can also be expressed as a measure of relative height growth from the field mean height measurements at time i and $i + a$, and a global parameter b:

$$k = b * \left(\frac{Y_{i+a}}{Y_i}\right) \quad (2)$$

Equation (2) was substituted into Eq. (1) to obtain estimates of the global parameters m and b. The parameters were estimated using generalised nonlinear least squares in the R Environment[35]. To derive plot-specific site quality estimates (A_o), Eqs. (1) and (2) were algebraically reformulated (Eq. 3) as a function of the height measurements at times 1 and 2 (corresponding to the survey periods 2015 and 2019, respectively) and the global parameters m and b as:

$$A_o = \left(\frac{Y_{i+a}{}^m - e^{-ka} Y_i{}^m}{1 - e^{-ka}} \right)^{\frac{1}{m}} \quad (3)$$

Landscape site quality estimate

We used Eq. (3) to estimate the site quality parameter (A_o) to describe the expected maximum height over the entire study area based on the ALS data, more specifically, Lorey's mean heights from the bi-temporal ALS data. We masked roads, railroads, and powerlines to reduce noise. In addition, we masked clear-cuts from 2000 to 2020 based on data from the Swedish Forest Agency.

Auxiliary data

To investigate variation in site quality within the study area, environmental variables describing the site properties were obtained for the 337 plots and on the landscape level. Soil moisture conditions were extracted from the continuous SLU (Swedish University of Agricultural Science) soil moisture map that describes variation in soil moisture conditions across Sweden[24]. The map was produced using machine learning, more specifically, by combining geographically mapped information, e.g., various ALS-derived terrain indices, climate data, and quaternary deposit information. The most important predictors of the developed soil moisture model was the Depth to water index (DTW), the Topographic wetness index (TWI), and mapped information of wetlands. The training and validation data sets included almost 20,000 survey plots with soil moisture classifications across Sweden, and the final mapped information expresses the probability that a 2×2 m pixel is classified as wet (0–100%). Ågren et al.[24] previously used the survey plots included in this study as an independent validation dataset. For the present study, the 2×2 m resolution available in the SLU map was resampled to a 10×10 m grid using bilinear interpolation to match both the resolution of the field plots and the ALS metrics over the study area.

Statistical analyses

After assessing the spatial autocorrelation of plots using a semivariogram (Fig. S1), we concluded that each plot could be considered as an independent observation. To address the first hypothesis, i.e., that soil moisture drives variation in site quality at the landscape scale, we used second-order polynomial regression to examine the relationship between site quality and modelled soil moisture. To address the second hypothesis, we performed a non-parametric Kruskal–Wallis test[36], followed by a Dunn-Bonferoni test[37], to test for significant differences in estimated site quality between pairs with different soil moisture classifications, soil types and dominating species. The Kruskal–Wallis test was chosen because not all of the groups fulfilled the assumption of a normal distribution and the presence of differences in sample sizes[38]. All of the statistical analyses were conducted using R software[35].

Results

The growth in tree height between the two surveys for individual survey plots ranged from 0 to 4.8 m, with a mean of 0.8 m; the median relative height growth was 6%. We fitted the age-independent difference equation (Eq. 1) on the complete dataset ($n = 337$ field plots) using generalised nonlinear least squares to obtain estimates of the global parameters, denoted as m, b and A_{global} (Table 4). The overall model was significant and showed a good fit, with a residual standard error of 0.41 m. In addition, the model errors did not show any obvious signs of heteroscedasticity (Fig. 3).

The estimated global parameters m and b were used to estimate site quality (A_o, or the expected maximum height) for each survey plot using the algebraic solution for A_o (Eq. 3). The estimated site quality (A_o) had a mean of 25.9 m and ranged from 7.2 to 67.3 m (Fig. 4).

We found significant differences in site quality among plots with different classified soil moisture conditions (Kruskal–Wallis chi-squared = 24.633, df = 4, p-value < 0.001), with the highest potential forest production found in areas with intermediate soil moisture conditions (Fig. 5a). Moreover, mesic sites showed significantly higher site quality in comparison to moist and wet soil moisture classes. Significant differences in site quality were also observed for plots characterised by different soil types (Kruskal–Wallis chi-squared = 29.464, df = 5, p-value < 0.001), with histosols showing significantly lower site quality values in comparison to arenosols, podzols, and regosols in the post-hoc Dunn-Bonferoni test (Fig. 5b).

Equation (3), when applied to the landscape level, used bi-temporal ALS estimates of mean height to compute the expected site quality (i.e., maximum height) for each pixel (10×10 m spatial resolution). Estimated site quality using bi-temporal ALS data demonstrated a near-normal distribution that included a similar range as the estimated site quality using field data. The visual comparison of modelled soil moisture and site quality revealed

				Fit statistics			
Parameter	Estimate	Std. error	t-value	AIC	BIC	logLink	RMSE(m)
A_{global}	26.99	1.70	15.88	576.85	592.13	−284.43	0.41
b	0.021	0.00	6.24				
m	0.57	0.10	5.53				

Table 4. Estimated parameters of model 1, based on the field data.

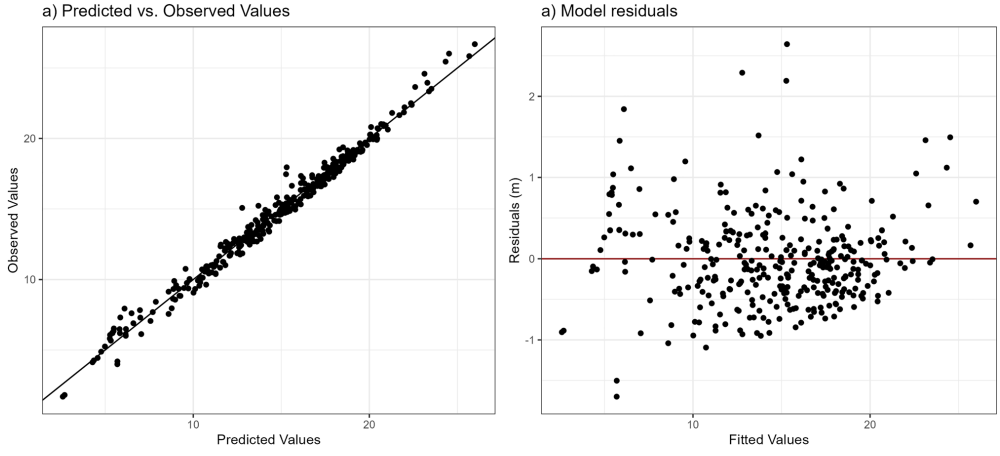

Figure 3. Plot of the predicted vs. observed Lorey's mean height values (**a**), and residuals from the predicted model in comparison to observed values (red line) (**b**).

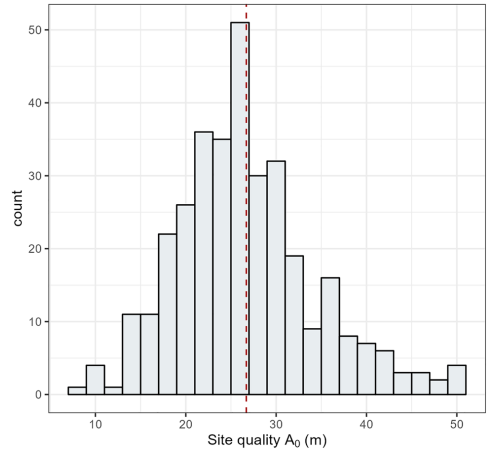

Figure 4. Histogram of estimated site quality (A_0). Note: all observations over 50 m were placed in the 48–50 m class.

noticeable patterns (Fig. 6). For example, areas with low site quality estimates generally showed rather wet soil moisture conditions, and thus, were located in areas dominated by peat soils. On the other hand, some areas showed higher site quality in comparison to neighbouring areas, in some cases likely associated with different dominating species. For example, clear differences in site quality could be observed within an experimental trial with blocks of different tree species (Fig. 6b). Stand edges could also be observed where younger stands showed higher site quality in comparison to mature stands. An effect of tree species was in line with the observations from field data plot scale, where plots dominated by *Pinus contorta* showed a significantly higher mean site quality than plots dominated by other tree species (Fig. S2).

At the landscape scale, the relationship between site quality and the modelled soil moisture conditions (the probability of a point being classified as wet) was described by a second-degree polynomial regression model ($R^2 = 0.11$, p-value < 0.001, F-stat $= 31{,}380$); indicating that site quality decreases as soil moisture increases. However, the estimated site quality showed large variation in relation to the predicted soil moisture condition (Fig. 7).

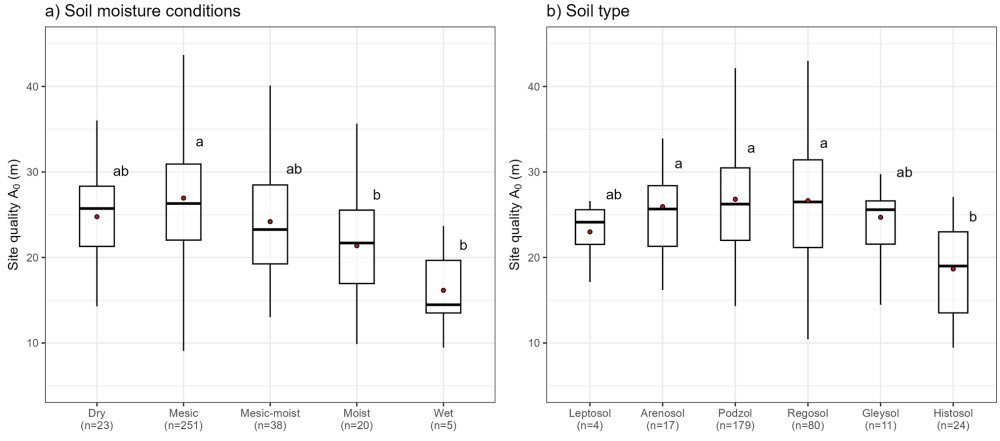

Figure 5. The relationship between site quality and (**a**) soil moisture conditions and (**b**) soil type. Lowercase letters show the results from the corresponding Dunn-Bonferoni test.

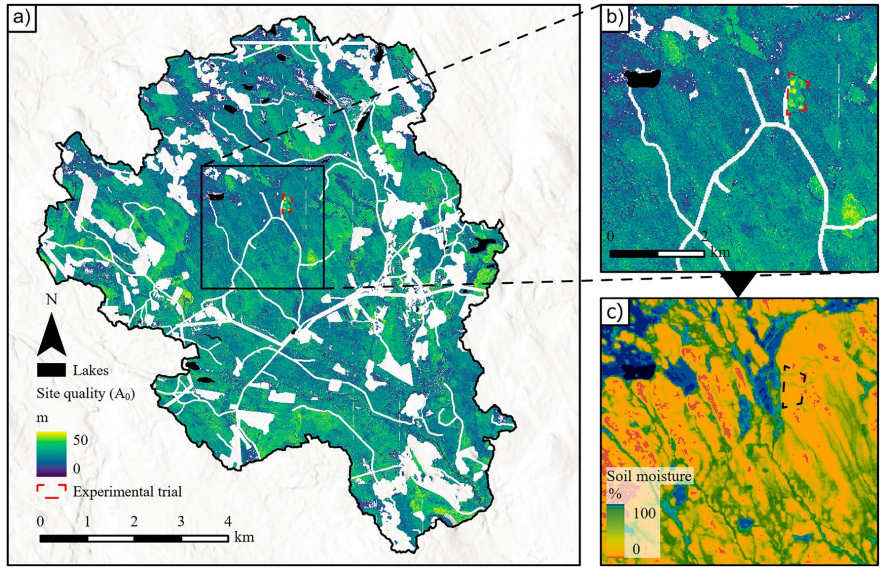

Figure 6. Predicted site quality across the Krycklan catchment, based on bi-temporal ALS data (**a**). Predictions of site quality in a smaller area (**b**), with the SLU soil moisture map over the same area (**c**). White areas are masked areas such as clear-cuts, roads. agricultural fields, or and power lines. An experimental trials of different tree species bordered with red (black in c). The map was created using ArcGIS Pro (version 3.0.2), https://www.esri.com/en-us/arcgis/products/arcgis-pro/overview.

Discussion

Understanding the factors that explain variations in site quality across a certain landscape is a tremendous scientific challenge due to the complex interactions between different environmental drivers varying in importance across scales. This study focused on a 68 km^2 meso-scale heterogeneous landscape, a decision which effectively controlled for dominant environmental drivers that are present on the national and regional levels, including climatic gradients. We estimated forest site quality across the Krycklan catchment by using an age-independent difference approach based on repeated and extensive field measurements of mean height. To estimate site quality

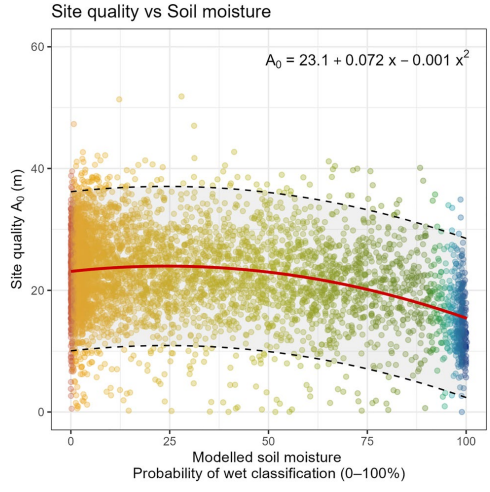

Figure 7. The modelled polynomial relationship between site quality (A_0) and soil moisture across the entire study area. The plot displays a random sample of 5000 (10%) raster cells, coloured corresponding to the SLU soil moisture map (Fig. 6c). The regression line is shown in red, with the dashed lines representing the 95% prediction intervals. The modelled soil moisture, shown as a percentage, denotes the probability of the point being predicted as wet rather than the volumetric soil water content.

over the entire landscape, we applied our age-independent model to the available bi-temporal ALS data, which had been obtained in close succession to the field plot surveys. The landscape estimates of site quality were compared to readily available auxiliary data to assess the effects of soil moisture conditions on forest production potential in the study area.

The use of bi-temporal ALS data to estimate forest growth and site quality has gained momentum in recent years, and has already proven successful in multiple previous studies using varying approaches[19,39,40]. Previous researchers have emphasised that age-independent models can rely on ALS data to yield landscape assessments of site quality across various time periods without the constraint of age-specific information for trees[22,23,39]. For instance, landscape estimates of site productivity, commonly presented using the site index, become challenging when information on forest age, species distribution, or top/dominant height or site properties is limited to field plots. Furthermore, the site index can only be directly estimated if the stand meets standard assumptions such as level of stocking, species composition, and that the stand history has not excessively affected the development of the dominant/co-dominant tree species.

The methodological differences between the present study and previous research mean that direct comparisons of our results to what has been reported in prior years are challenging. However, it is possible to compare the results obtained from our age-independent model for tree height, which was used to estimate the global parameters and derive the site-independent site quality estimates. The age independent height model predicting height at time two, showed satisfactory accuracy with a RMSE of 0.41 m (Table 4). This is in line with the model performance (RMSE value of 0.64 m) reported for an age-dependent Chapman-Richard function with RMSE of 0.64 m[41].

The site quality estimates reported in this study represent the site-specific maximum attainable Lorey's mean height when time/age approaches infinity. This theoretical value cannot be validated within the boundaries of this study and is limited to be used to compare differences in site quality between sites. At the same time, the site quality estimates showed a large range from 7 to > 50 m, where especially the values in the highest can be considered to be unreasonable. Furthermore, the current study was limited to information from only two field survey inventories that were separated by a period of 5 years. This can be considered as a short growth period, and the two measurements may not include all of the information necessary to explain the variation in site quality, especially if the measurements do not contain the empirical asymptote. The study period in the presented research is far from the period needed to begin reaching the asymptote, that is, the maximum value of the site quality parameter. It is also important to note that the use of tree height (ascertained through the height-age site index approach) does not fully explain between-site differences in productivity. In other words, even if we have a certain site index, there may be significant variation in the woody volume of the plot due to differences in carrying capacity, species composition, and site properties[10,13,42,43]. Thus, we postulate that additional information to height differences, such as species, basal area, or volume, may improve both site index or site quality estimates[13]. However, such information—especially volume—is not as readily available as tree height, which is available for the whole of Sweden due to enhanced forest inventories. Another advantage of using height is that this metric, in

comparison to basal area and volume, is not heavily affected by management and/or stand density. Nevertheless, a previous study based on bi-temporal ALS data reported stand density effects on *P. sylvestris* height growth in highly productive stands[44].

After the site quality model had been fitted to the data set describing the survey plots (Eq. 3), it was then applied to the bi-temporal ALS data to compute the expectedsite quality for 10×10 m raster cells of the study area. The different laser scanners used in the 2015 and 2019 surveys could have caused potential errors in the pixel-level estimations of site quality (Table 2). However, we would like to argue that this potential source of error is small due the two separate calibration for each scanning based on field measured Lorey's mean height. Other potential sources of errors in the site quality estimates include the unavailability of tree species information at the landscape level, along with the effects of forest management. The magnitude of the effects of these error sources warrants further investigation. Another source of uncertainty is associated to a short study period in combination with the low productive forests in the region, which may not have been sufficient to capture the variation in site quality. The average field measured Lorey's mean height difference was 0.8 m in the studied period. Ground-based tree-height measurements of pine and spruce involve a mean error of 0.3 and 0.1 m, respectively[45], which may limit the observation of between-site differences. Gathering landscape-level species information has the potential to improve site quality estimates, which was apparent in the higher estimates of site quality in an experimental tree species trial (Fig. 6a). Furthermore, the observed stand edges with higher site quality associated to younger stands may be an effect of a higher proportion of birch, which is a fast growing pioneer species[46]. Previous studies have found that dividing the study area into strata based on tree species improves prediction accuracy[47].

The reported results were consistent with our hypothesis in that site quality decrease in high soil moisture conditions. Histosols in this region are associated with saturated soil conditions and showed significantly lower site quality in comparison to other soil types. Similar findings for soil moisture conditions and soil types have been observed in studies of the relationship between normalised mean annual increment in relation to soil properties across Sweden[48]. Previous studies have also proven the utility of soil moisture maps in comparison to other terrain indices[49], as well as the ability to predicting thick organic soil layers based on soil moisture[50]. Lower site quality is expected in these areas because the saturated soil conditions decrease tree growth[48,51]. Notably, the modelled soil moisture was not able to explain the variation in soil quality among drier areas. We suspect several reasons for this. Firstly, the soil moisture map used in this study was create to differentiate between the soil moisture classes, e.g., dry (dry and mesic) and wet (mesic-moist, moist and wet); this may not adequately capture the variation within these groups observed on plot level (Fig. 5)[24]. The use of remote sensing technologies in combination with additional auxiliary data is not a new phenomenon. When site index was modelled for *Pinus pinaster* Ait. stands in Spain, climate-related factors such as potential evapotranspiration, mean minimum temperature, and mean precipitation were among the most important variables that explained variation in a site-specific quality parameter[21]. Using terrain indices to model soil moisture conditions has successfully improved predictions of forest growth in numerous studies[25,51].

The variation of site quality is not only driven by soil moisture conditions, but rather the effect of complex relationships between various environmental drivers. However, our study provides a unique insight into how soil moisture conditions drive site quality variation on a local landscape. To better understand the landscape-scale variation of site quality, the effects of additional biological and physical factors need to be studied. For example, soil physical and chemical properties have a large effect on site quality, however such information is challenging to extrapolate across a landscape scale.

Conclusion

This study presents a landscape scale perspective on the relationship between forest site quality and soil moisture conditions within a managed boreal forest landscape. We estimated site quality across the entire study area using an age-independent difference height growth model based on repeated forest surveys and ALS scanning. Evaluation of site quality estimates showed lowest site quality in areas with the highest soil moisture levels. Although substantial variation was observed for estimated site quality, there was no distinct trend that was indicative of increased site quality in areas with intermediate soil moisture conditions. Collectively, our results deepen our understanding of how certain soil moisture conditions relates to growth potential across a heterogeneous boreal landscape.

Data availability

The dataset generated during the current study is available from the corresponding author on reasonable request.

Received: 15 January 2024; Accepted: 30 April 2024
Published online: 09 May 2024

References

1. Gauthier, S. *et al.* Ecosystem Management of the Boreal Forest in the Era of Global Change. In *Boreal Forests in the Face of Climate Change: Sustainable Management* (eds Girona, M. M. *et al.*) 3–49 (Springer International Publishing, 2023). https://doi.org/10.1007/978-3-031-15988-6_1.
2. Giesler, R., Högberg, M. & Högberg, P. Soil chemistry and plants in fennoscandian boreal forests as exemplified by a local gradient. *Ecology* **79**, 119–137 (1998).
3. Peichl, M. *et al.* Landscape-variability of the carbon balance across managed boreal forests. *Glob. Change Biol.* **29**, 1119–1132 (2023).
4. Seibert, J., Stendahl, J. & Sørensen, R. Topographical influences on soil properties in boreal forests. *Geoderma* **141**, 139–148 (2007).
5. Li, X., McCarty, G. W., Du, L. & Lee, S. Use of topographic models for mapping soil properties and processes. *Soil Syst.* **4**, 32 (2020).

6. Jansson, R., Laudon, H., Johansson, E. & Augspurger, C. The importance of groundwater discharge for plant species number in riparian zones. *Ecology* **88**, 131–139 (2007).
7. Moeslund, J. E., Arge, L., Bøcher, P. K., Dalgaard, T. & Svenning, J.-C. Topography as a driver of local terrestrial vascular plant diversity patterns. *Nordic J. Bot.* **31**, 129–144 (2013).
8. Laudon, H. *et al.* The role of biogeochemical hotspots, landscape heterogeneity, and hydrological connectivity for minimizing forestry effects on water quality. *Ambio* **45**, 152–162 (2016).
9. Skovsgaard, J. & Vanclay, J. K. Forest site productivity: A review of the evolution of dendrometric concepts for even-aged stands. *Forestry* **81**, 13–31 (2008).
10. Appiah Mensah, A., Holmström, E., Nyström, K. & Nilsson, U. Modelling potential yield capacity in conifers using Swedish long-term experiments. *For. Ecol. Manag.* **512**, 120162 (2022).
11. Felton, A. *et al.* Projecting biodiversity and wood production in future forest landscapes: 15 key modeling considerations. *J. Environ. Manag.* **197**, 404–414 (2017).
12. Ulvdal, P., Öhman, K., Eriksson, L. O., Wästerlund, D. S. & Lämås, T. Handling uncertainties in forest information: The hierarchical forest planning process and its use of information at large forest companies. *Forestry* **96**, 62–75 (2023).
13. Assmann, E. *The Principles of Forest Yield Study: Studies in the Organic Production, Structure, Increment and Yield of Forest Stands* (Pergamon Press, 1970).
14. Hägglund, B. Evaluation of forest site productivity. *For. Abstr.* **42**, 515–527 (1981).
15. Eriksson, H., Johansson, U. & Kiviste, A. A site-index model for pure and mixed stands of *B. pendula* and *B. pubescens* in Sweden. *Scand. J. For. Res.* **12**, 149–156 (1997).
16. Hägglund, B. & Lundmark, J. E. Skattning av höjdboniteten med ståndortsfaktorer. *Tall Och Gran I Sverige* **28**, 1–240 (1977).
17. Tomé, J., Tomé, M., Barreiro, S. & Paulo, J. A. Age-independent difference equations for modelling tree and stand growth. *Can. J. For. Res.* **36**, 1621–1630 (2006).
18. Arias-Rodil, M., Crecente-Campo, F., Barrio-Anta, M. & Diéguez-Aranda, U. Evaluation of age-independent methods of estimating site index and predicting height growth: a case study for maritime pine in Asturias (NW Spain). *Eur. J. For. Res.* **134**, 223–233 (2015).
19. Noordermeer, L., Bollandsås, O. M., Gobakken, T. & Næsset, E. Direct and indirect site index determination for Norway spruce and Scots pine using bitemporal airborne laser scanner data. *For. Ecol. Manag.* **428**, 104–114 (2018).
20. Solberg, S., Kvaalen, H. & Puliti, S. Age-independent site index mapping with repeated single-tree airborne laser scanning. *Scand. J. For. Res.* **34**, 763–770 (2019).
21. Guerra-Hernández, J. *et al.* Developing a site index model for *P. Pinaster* stands in NW Spain by combining bi-temporal ALS data and environmental data. *For. Ecol. Manag.* **481**, 118690 (2021).
22. Tompalski, P. *et al.* Estimating changes in forest attributes and enhancing growth projections: A review of existing approaches and future directions using airborne 3D point cloud data. *Curr. For. Rep.* **7**, 1–24 (2021).
23. Appiah Mensah, A., Jonzén, J., Nyström, K., Wallerman, J. & Nilsson, M. Mapping site index in coniferous forests using bi-temporal airborne laser scanning data and field data from the Swedish national forest inventory. *For. Ecol. Manag.* **547**, 121395 (2023).
24. Ågren, A. M., Larson, J., Paul, S. S., Laudon, H. & Lidberg, W. Use of multiple LIDAR-derived digital terrain indices and machine learning for high-resolution national-scale soil moisture mapping of the Swedish forest landscape. *Geoderma* **404**, 115280 (2021).
25. Mohamedou, C., Tokola, T. & Eerikäinen, K. LiDAR-based TWI and terrain attributes in improving parametric predictor for tree growth in southeast Finland. *Int. J. Appl. Earth Obs. Geoinf.* **62**, 183–191 (2017).
26. Laudon, H. *et al.* Northern landscapes in transition: Evidence, approach and ways forward using the Krycklan Catchment Study. *Hydrol. Process.* **35**, e14170 (2021).
27. Fridman, J. *et al.* Adapting national forest inventories to changing requirements—The case of the Swedish National Forest Inventory at the turn of the 20th century. *Silva Fenn.* **48**, 1095 (2014).
28. IUSS Working Group WRB. *World Reference Base for Soil Resources 2014, Update 2015 International Soil Classification System for Naming Soils and Creating Legends for Soil Maps*. 978–92–5–108370–3 (2015).
29. McGaughey, R. J. FUSION/LDV: Software for LiDAR Data Analysis and Visualization. U.S.Department of Agriculture, Forest Service (2016).
30. Næsset, E. Predicting forest stand characteristics with airborne scanning laser using a practical two-stage procedure and field data. *Remote Sens. Environ.* **80**, 88–99 (2002).
31. Nilsson, M. *et al.* A nationwide forest attribute map of Sweden predicted using airborne laser scanning data and field data from the National Forest Inventory. *Remote Sens. Environ.* **194**, 447–454 (2017).
32. Zeide, B. Analysis of growth equations. *For. Sci.* **39**, 594–616 (1993).
33. Burkhart, H. E. & Tomé, M. *Modeling Forest Trees and Stands* (Springer, 2012).
34. Richards, F. J. A flexible growth function for empirical use. *J. Exp. Bot.* **10**, 290–301 (1959).
35. R Core Team. R: A language and environment for statistical computing. R Foundation for Statistical Computing (2020).
36. Kruskal, W. H. & Wallis, W. A. Use of ranks in one-criterion variance analysis. *J. Am. Stat. Assoc.* **47**, 583–621 (1952).
37. Dunn, O. J. Multiple comparisons using rank sums. *Technometrics* **6**, 241–252 (1964).
38. Hollander, M., Wolfe, D. A. & Chicken, E. *Nonparametric Statistical Methods* (Wiley, 2013).
39. Socha, J., Pierzchalski, M., Bałazy, R. & Ciesielski, M. Modelling top height growth and site index using repeated laser scanning data. *For. Ecol. Manag.* **406**, 307–317 (2017).
40. Tompalski, P. *et al.* Combining multi-date airborne laser scanning and digital aerial photogrammetric data for forest growth and yield modelling. *Remote Sens.* **10**, 347 (2018).
41. Appiah Mensah, A. *et al.* The millennium shift: Investigating the relationship between environment and growth trends of Norway spruce and Scots pine in northern Europe. *For. Ecol. Manag.* **481**, 118727 (2021).
42. Hasenauer, H., Burkhart, H. E. & Sterba, H. Variation in potential volume yield of loblolly pine plantations. *For. Sci.* **40**, 162–176 (1994).
43. Skovsgaard, J. P. *Management of Sitka Spruce without Thinnings. An Analysis of Stand Structure and Volume Production of Unthinned Stands of Sitka Spruce (Picea Sitchensis (Bong.) Carr.) in Denmark*. (1997).
44. Tymińska-Czabańska, L., Hawryło, P. & Socha, J. Assessment of the effect of stand density on the height growth of Scots pine using repeated ALS data. *Int. J. Appl. Earth Obs. Geoinf.* **108**, 102763 (2022).
45. Stereńczak, K. *et al.* Factors influencing the accuracy of ground-based tree-height measurements for major European tree species. *J. Environ. Manag.* **231**, 1284–1292 (2019).
46. Hynynen, J. *et al.* Silviculture of birch (*B. pendula* Roth and *B. pubescens* Ehrh.) in northern Europe. *For. Int. J. For. Res.* **83**, 103–119 (2010).
47. Hauglin, M., Rahlf, J., Schumacher, J., Astrup, R. & Breidenbach, J. Large scale mapping of forest attributes using heterogeneous sets of airborne laser scanning and National Forest Inventory data. *For. Ecosyst.* **8**, 65 (2021).
48. Van Sundert, K., Horemans, J. A., Stendahl, J. & Vicca, S. The influence of soil properties and nutrients on conifer forest growth in Sweden, and the first steps in developing a nutrient availability metric. *Biogeosciences* **15**, 3475–3496 (2018).
49. Larson, J., Lidberg, W., Ågren, A. M. & Laudon, H. Predicting soil moisture across a heterogeneous boreal catchment using terrain indices. *Hydrol. Earth Syst. Sci.* **26**, 4837–4851 (2022).

50. Ågren, A. M., Hasselquist, E. M., Stendahl, J., Nilsson, M. B. & Paul, S. S. Delineating the distribution of mineral and peat soils at the landscape scale in northern boreal regions. *Soil* **8**, 733–749 (2022).
51. Laamrani, A. *et al.* Effects of topography and thickness of organic layer on productivity of black spruce boreal forests of the Canadian Clay Belt region. *For. Ecol. Manag.* **330**, 144–157 (2014).

Acknowledgements
This work was supported by the Knut and Alice Wallenberg Foundation (2018.0259), VR (SITES), the Kempe Foundation, and the Swedish University of Agricultural Sciences (SLU). We also thank the staff at the Svartberget research station, SLU, for their valuable contributions.

Author contributions
J.L. and H.L. designed the study. J.L. was responsible for a major part of the data collection. J.L. conducted the modelling and statistical analysis in collaboration with A.A.M. and C.V. J.L. wrote the manuscript in collaboration with the co-authors.

Funding
Open access funding provided by Swedish University of Agricultural Sciences.

Competing interests
The authors declare no competing interests.

Additional information
Supplementary Information The online version contains supplementary material available at https://doi.org/10.1038/s41598-024-61098-z.

Correspondence and requests for materials should be addressed to J.L.

Reprints and permissions information is available at www.nature.com/reprints.

Publisher's note Springer Nature remains neutral with regard to jurisdictional claims in published maps and institutional affiliations.

Acta Universitatis Agriculturae Sueciae

Doctoral Thesis No. 2024:97

This thesis explores the application of a hybrid empirical growth model to predict potential future growth of Oak and Scots Pine stands and their mixture across Europe and presents high-resolution spatiotemporal results. Further, it relates a proxy for site productivity from bitemporal LiDAR scans to soil moisture. Preliminary results regarding the potential of high-density LiDAR to complement field inventories are presented.

Carl Vigren received his doctoral education at the Department of Forest Resource Management at the Swedish University of Agricultural Sciences (SLU), Umeå. In 2018 he was awarded his MSc degree in Forest Science from SLU, Umeå.

Acta Universitatis Agriculturae Sueciae presents doctoral theses from the Swedish University of Agricultural Sciences (SLU).

SLU generates knowledge for the sustainable use of biological natural resources. Research, education, extension, as well as environmental monitoring and assessment are used to achieve this goal.

ISSN 1652-6880
ISBN (print version) 978-91-8046-424-6
ISBN (electronic version) 978-91-8046-432-1